THE ASTROPHYSICAL JOURNAL

AN INTERNATIONAL REVIEW OF SPECTROSCOPY AND ASTRONOMICAL PHYSICS

VOLUME 90 NOVEMBER 1939 NUMBER 4

A SPECTROPHOTOMETRIC STUDY OF ALGOL

JOHN S. HALL

ABSTRACT

Photoelectric observations of Algol have been made in the visual region (5500 A) and in the infrared region (8660 A) near primary minimum at the Sproul Observatory. The infrared observations have been continued at other phases, first at Sproul and finally at the Amherst College Observatory.

The difference in magnitude (Algol *minus* β Tauri) has been observed in thirteen different spectral regions at Amherst when Algol was near quarter-phase.

The time of primary minimum determined from the observations at 5500 A is identical with that found from those at 8660 A, within the error of measurement. This is estimated to be three minutes.

The rectified depths of the primary and the secondary minima determined from the infrared light-curve are $0^m.761$ and $0^m.129$, respectively. The corresponding values found by Stebbins at 4500 A are $1^m.134$ and $0^m.042$. If the color temperature of the primary, a B8 star, is assumed to be 15,000°, that of the bright side of the eclipsing companion is near 5800°. Its dark side is about 200° cooler.

The discussion of data from several accurate photometric investigations of Algol in other spectral regions has been made in the same manner as the infrared data, in order that the results may be compared on a similar basis.

The values of the reflection and ellipticity coefficients, determined from the infrared light-curve, are found to be $+0.034 \pm .003$ and $+0.007 \pm .006$, respectively. A comparison of the reflection coefficients found for Algol in the different spectral regions, as well as those found by others in the visual and photographic regions for other stars, indicates that this coefficient increases with wave length. A comparison of the ellipticity coefficients found in the infrared and blue regions gives some indication that the equator of the eclipsing companion is more eccentric than that of the primary.

Although the photometric data can be satisfied if the third body, C, is assumed to be completely dark, such a solution is strongly contradicted by considerations of mass. First, the mass-luminosity relationship was applied to these data, and the mass ratio m_A/m_B was determined. This mass ratio was then combined with the mass functions determined from spectroscopic studies of the short- and long-period orbits, and the minimum mass of C was found to be comparable with that of A. This implies that A and C are comparable in bolometric magnitude. Such a solution is definitely denied by the photometric data. If B is assumed to be similar to the bright component of ζ Herculis, and therefore $1^m.5$ too bright for its mass, A is twice as massive as C and 3.3 times as massive as B, and the bolometric difference in magnitude $(C - A)$ is increased

from zero to $1^m.94$. This solution is compatible with the photometric data, provided C is of earlier spectral type than G. From what we know of the luminosities of the stars it is improbable that C is earlier than the primary, or earlier than B8; and if the parallax of Algol is correct, it would be an A-type star in order to be on the main sequence. When it is assumed that it is A5, the relative luminosities shown in Table 12 result.

The assumption regarding B may be largely avoided if C is assumed to be made up of two stars of equal luminosity and color. The components would still have to be of early spectral type in order to satisfy all criteria.

A very recent report of the Dominion Observatory states, with reference to Dr. Pearce's spectroscopic observations of Algol, that "during eclipse the spectrum of the class A companion has been repeatedly photographed." Since the eclipsing companion is probably an early G-type star, this "A-companion" must be a third body. Two companions to Algol have therefore been identified.

With the exception of the sun, probably no star has been so intensively studied by astronomers as the "demon" star, Algol. Since this star is so well known, no historical background is necessary. Its bibliography is so replete with references that only the more recent ones will be mentioned, as the opportunities arise.

OBSERVATIONAL PROCEDURE

All observations recorded in this paper were made with a photoelectric photometer containing a *Cs-O-Ag* photoelectric cell. Since this cell is sensitive over an extensive spectral region, one may compare Algol with another bright star in both the visual and infrared regions by merely changing the quality of the light admitted to its cathode. At the Sproul Observatory the starlight was broken up into spectra by means of fine-wire objective gratings. Since these were so constructed that even order spectra are missing, it is possible to observe the first-order infra red energy without interference from the second-order visual. At the Amherst College Observatory a replica grating, constructed by Professor R. W. Wood, having unusual efficiency in the first-order red, was used. This grating, mounted 351 mm in front of the focus of the 18-inch refractor, gives a dispersion only slightly less than that of the wire gratings used at Sproul. Its remarkable efficiency has more than made up for the loss of light experienced in changing from a 24-inch to an 18-inch telescope. In order to be sure that no second-order visual energy was confused with the first-order infrared, a Schott glass filter, OG5, was always used in addition to the replica grating for these observations. An especially constructed spectrometer, located in the focal plane of each telescope, enabled me to limit and, at the same time, to meas-

ure the wave length of the stellar energy striking the cell. This device also makes it possible to utilize the energy of both first-orders at the same time. In passing from measurements in the visual to measurements in the infrared, the focus was always changed in order to be sure that the energy falling on either side of the two slits of the spectrometer was sharply defined. A more detailed description of the arrangement and the method of calibration has already been published.[1]

TABLE 1

DESCRIPTION OF THE OBSERVATIONS

Observatory	Grating	Period	Slit Width	Eff. λ	Phase Observed
Sproul	Small (wire)	Nov., 1935—Nov. 27, 1936 (also Dec. 14, 1936)	2 mm (967 A)	5500 A 8660	Near primary minimum
	Large (wire)	Nov. 30, 1936—Mar. 22, 1937 (also Oct. 14, 1937)	1 mm (483.5 A)	5500 8660	Near primary minimum
	Large (wire)	Fall–winter, 1937–38	1 mm (483.5 A)	8660	All phases
Amherst College	R. W. Wood (replica)	Fall–winter, 1938–39	1 mm (500 A)	8660	All phases

The observations of Algol may be divided into two groups: comparisons with α Persei in two different wave-length bands; and spectrophotometric comparisons with β Tauri or α Persei in at least ten different spectral regions, made when Algol was near quarter-phase. We shall now discuss the first group.

Visual and infrared observations.—Details concerning this observational material are given in Table 1. The small wire grating mentioned in the second column of the table covered only 40 per cent of the 24-inch objective, while the large one covered 90 per cent. The unused portion of each grating was always shielded, in order to cut down background effects. The dispersion is that present at the visual focus, and has been determined with sufficient accuracy to predict

[1] *Ap. J.*, **84**, 372, 1936; **85**, 146, 1937.

the effective wave length at 8660 A, with a probable error of 20 A. In the case of the infrared observations, an error of 100 A would produce a magnitude error of $0^m.01$ in the comparisons with α Persei, an F5 star. Although Algol is classified as B8, its composite color temperature near 8000 A is more nearly A2 at maximum and Fo at primary minimum. The spectral regions admitted to the cell at any one time were so sharply defined that this change in color with phase could produce a change of effective wave length of no more than 10 A. In May, 1936, the photocell which had been in use for three years was damaged and was replaced by another similar one. No systematic differences were noted or expected from this fact. A similar advantage of the method was evident in moving from Sproul to Amherst.

Approximately 16 per cent of the energy incident on the wire gratings in each wave-length region actually reached the photocell. In the case of the smaller grating, each reading required about a minute near primary minimum, and the background current was about 25 per cent of the photocurrent. The time consumed in measuring these small photocurrents was so great that the comparison star was observed rather infrequently, compared with photoelectric observations of variable stars by other observers. Both the infrared and visual energy of Algol was compared with that of α Persei on nineteen different nights at Sproul. The comparison star was observed on an average of three times on each of these nights. The response from a standard lamp, measured at fifteen-minute intervals, served as an intermediate comparison star. The observations in the visual region undoubtedly suffered more in this procedure from short period irregularities in the atmosphere than those in the infrared region, where the extinction coefficient is about half as large.

All observations have been corrected for differential extinction. In general, an extinction coefficient of $0^m.25$ for the visual and $0^m.10$ for the infrared region, was used. On a few nights when Algol was observed at large hour angles or when repeated comparisons of the energy from α Persei and the standard lamp indicated that the extinction was unusual, the observed extinction coefficients were used. These averaged $0^m.22 \pm 0^m.04$ in the visual and $0^m.12 \pm 0^m.04$ in the in-

frared. At Sproul, Algol was never observed more than six, or at Amherst more than five, hours off the meridian.

Two readings in the visual, followed by two in the infrared, constituted one observation of the variable for each effective wave length for the early Sproul observations. A definite effort was made to keep the number of observations in the two spectral regions as nearly equal as possible. A few of the most recent Sproul observations near primary minimum were made in the following order: two visual, three infrared, and two visual. Since the comparison star was much brighter than Algol, more numerous readings were always secured whenever the telescope was pointed in its direction.

In the case of the observations between primary minima, when the light from Algol varies but slowly, only the infrared observations were continued, and a different procedure was used. At each observatory these observations were usually made in the following order: five on the standard lamp, five on Algol, five on the standard lamp, five on Algol, and five on the standard lamp. Such a series represents two observations. This sequence was alternated with eight or ten readings on α Persei, flanked by five readings on the standard lamp. The reason that the standard lamp has been observed so frequently throughout the course of these observations is because the Lindemann electrometer was used at such a high sensitivity that its response to the same photocurrent varies noticeably with the position of the telescope. All observations were, therefore, corrected for differential sensitivity of the photometer. It became increasingly evident, as the observations progressed, that a table could be constructed giving the relative electrometer response as a function of the hour angle for each star, which would be valid for any night. However, it seemed best to finish the observations by the method first used, despite its obvious inefficiency.

The general procedure in reducing the observations was as follows: They were first corrected for background effects. The difference in magnitude between each star and the standard lamp—this constitutes an observation—was then determined, and the extinction correction was applied. For the early Sproul observations near primary minimum the magnitude of the standard lamp was determined

from the mean of all the observations of α Persei after the latter had been corrected, of course, for background and extinction. For the remaining observations the mean of the two comparisons with α Persei flanking the Algol observations served to determine the magnitude of the standard lamp. Partly for this reason and partly because fewer readings are included in each observation, the magnitude differences observed prior to September, 1937, are given half the weight of the others in the discussion.

Infrared observations of Algol have been made on sixty-one different nights (thirty-nine at Sproul and twenty-two at Amherst). On nineteen nights at Sproul and four at Amherst, at least a portion of the principal eclipse was observed. The heliocentric Julian day, with the first three figures omitted (given in parentheses in Table 2), corresponds to the heliocentric phase directly below it. Zero heliocentric phase corresponds to heliocentric JD 2428113.5689 and suits all Sproul observations between November, 1935, and March, 1937, reasonably well. The mean period found by Hellerich,[2] 2.86731077 days, has been used. The observed difference in magnitude is in the sense: Algol *minus* α Persei. Since March, 1937, primary minima have been accurately observed on two nights—October 14, 1937, and December 1, 1938. These minima occurred at heliocentric JD 2428821.7917 and at JD 2429234.6859. While the latter of these seems to have occurred two minutes ahead of the minimum predicted from the previous data, the former is five minutes early. Although there is some doubt of the reality of this shift, the phases of all observations of October 14 have been corrected by the addition of 0.0012 to the computed phases for the discussion. The data given in Table 2 have not been so corrected. No corrections have been made for the light-time in the third-body orbit.

Spectrophotometric observations.—Algol was compared directly on four occasions and indirectly on three with β Tauri at Amherst. These comparisons were made in at least ten different wave-length regions, each 500 A in length and extending from 4250 A to 8790 A. They were made when the stars were at very nearly the same zenith distance, and they include four or more readings at each wave-length setting for each star. Differential extinction corrections were always

[2] *A.N.*, **209**, 231, 1919.

TABLE 2*

VISUAL AND INFRARED OBSERVATIONS

(Helioc. JD) Helioc. Phase	Δm 5500 A	Helioc. Phase	Δm 8660 A	(Helioc. JD) Helioc. Phase	Δm 5500 A	Helioc. Phase	Δm 8660 A
(8113.5078)[a]				(8173.5499)— *Cont.*			
Nov. .9787....	1m04	0.9794	1m50	.9432....	0m49	0.9397	0m99
6, .9884....	1.33	.9871	1.63	.9463....	0.48	.9407	0.99
1935 .0351....	0.81	.0346	1.34	.9526....	0.65	.9436	1.02
				.9567....	0.77	.9455	1.04
(8116.4952)[b]				.....	.....	.9520	1.16
.0206....	1.09	.0201	1.57	.....	.....	.9554	1.21
.0264....	0.93	.0260	1.47				
.0286....	0.92	.0291	1.44	(8182.4713)			
.0351....	0.79	.0354	1.39	.0303....	0.77	.0303	1.32
.0361....	0.81	.0434	1.25	.0320....	0.76	.0320	1.31
.0429....	0.67	.0458	1.23	.0397....	0.66	.0397	1.21
.0465....	0.63	.....	.....				
				(8193.5239)			
(8127.7013)[b]				.8850....	0.37	.9218	0.93
.9288....	0.36	.9274	0.98	.9226....	0.40	.9295	0.91
.9319....	0.45	.9307	0.98	.9287....	0.38	.9331	0.95
.9384....	0.44	.9350	1.02	.9301....	0.39	.9348	0.95
.9522....	0.59	.9391	1.02	.9323....	0.39	.9379	0.96
.....	.....	.9474	1.19	.9338....	0.42	.9418	1.05
.....	.....	.9536	1.16	.9360....	0.45	.9459	1.05
.....	.....	.9619	1.34	.9394....	0.48	.9469	1.05
				.9408....	0.48	.9508	1.10
(8136.4515)				.9430....	0.48	.....	.....
.9805....	1.06	.9807	1.59	.9452....	0.57	.....	.....
.9832....	1.15	.9825	1.63	.9483....	0.56	.....	.....
.9907....	1.31	.9900	1.75	.9505....	0.61	.....	.....
.9982....	1.45	.9965	1.84				
.0001....	1.45	.0009	1.85				
.0040....	1.42	.0023	1.87	(8196.6463)			
.0069....	1.35	.0050	1.84	.9740....	1.07	.9744	1.62
.0151....	1.18	.0074	1.80	.9783....	1.13	.9775	1.64
.0171....	1.12	.0166	1.63	.9800....	1.14	.9806	1.62
				.9875....	1.29	.9864	1.72
(8173.5499)[b]				.9885....	1.33	.9913	1.74
.9189....	0.36	.9106	0.93	.9936....	1.38	.9948	1.77
.9233....	0.43	.9179	0.93	.9955....	1.45	.9962	1.79
.9262....	0.38	.9235	0.97	.9969....	1.44	.9976	1.77
.9284....	0.35	.9257	0.92	.9981....	1.42	.9988	1.80
.9313....	0.37	.9291	0.89	.9993....	1.42	.0000	1.78
.9352....	0.37	.9308	0.91	.0007....	1.47	.0012	1.79
.9364....	0.37	.9320	0.90	.0019....	1.42	0.0036	1.69
.9386....	0.43	.9339	0.95	.0031....	1.39	.....	.....
.9415....	0.42	0.9375	0.95	.0043....	1.33	.....	.....

* The meaning of the symbols used in this table are:

[a] Observations interrupted by clouds.

[b] Observations stopped by clouds.

[c] Observations stopped by moonlight on grating.

[d] Hazy but uniform. Magnitudes interpolated with time.

[e] Observed extinction coefficients used.

[f] Uniformly hazy.

[g] Trouble checking standard lamp, owing to uncertainty in galvanometer.

TABLE 2—*Continued*

(Helioc. JD) Helioc. Phase	Δm 5500 A	Helioc. Phase	Δm 8660 A	(Helioc. JD) Helioc. Phase	Δm 5500 A	Helioc. Phase	Δm 8660 A
(8199.5222)				(8497.6603)—*Cont.*			
.9770	1^m11	0.9782	1^m57	.9766	1^m06	.....	1^m50
.9789	1.10	.9845	1.65	.9797	1.17	.....	1.52
.9837	1.29	.9879	1.61	.9845	1.27	.....	1.67
.9849	1.20	.9937	1.80	.9867	1.27	.....	1.73
.9871	1.25	.9956	1.75	.9906	1.34	.....	1.69
.9888	1.29	.9968	1.75				
.9932	1.37	.9980	1.75	(8500.5535)[gb]			
.9963	1.38	.9990	1.78	.9643	0.75	.....	1.34
.9973	1.40	.0002	1.77	.9682	0.75	.....	1.34
.9985	1.41	.0014	1.77	.9709	0.81	.....	1.39
.9997	1.41	.0027	1.77	.9765	0.99	.....	1.50
.0007	1.41	.0039	1.78	.9845	1.33	.....	1.77
.0019	1.41	.0051	1.78				
.0033	1.42	.0073	1.73	(8503.5602)[e]			
.0045	1.43	.0097	1.73	.0129	1.27	.....	1.60
.0057	1.43	.0155	1.63	.0158	1.21	.....	1.59
.0067	1.35	.....	.....	.0187	1.23	.....	1.64
.0079	1.42	.....	.....	.0223	1.06	.....	1.55
.0091	1.39	.....	.....	.0259	0.96	.....	1.47
.0144	1.30	.....	.....	.0290	0.84	.....	1.36
.0161	1.23	.....	.....	.0360	0.81	.....	1.38
				.0425	0.64	.....	1.21
(8612.5314)[ae]				.0459	0.68	.....	1.19
.0176	1.16	.0183	1.60	.0498	0.59	.....	1.14
.0188	1.12	.0190	1.61	.0556	0.49	.....	1.04
.0204	1.10	.0212	1.57	.0578	0.44	.....	0.98
.0234	1.01	.0231	1.56				
.0243	0.97	.0248	1.50	(8517.6682)[d]			
.0257	0.94	.0253	1.47	.9332	0.37	.....	0.95
.0279	0.91	.0280	1.41	.9388	0.57	.....	1.15
.0340	0.71	.0346	1.33	.9501	0.52	.....	1.16
.0358	0.69	.0360	1.28	.9552	0.57	.....	1.15
.0368	0.67	.0371	1.27	.9606	0.79	.....	1.36
.0385	0.63	.0378	1.26	.9686	0.94	.....	1.52
(8615.5037)[e]				(8529.5070)			
.0542	0.58	.0543	1.12	.0621	0.46	.....	0.98
.0555	0.49	.0550	1.08				
.0560	0.46	.0564	1.04	(8566.5472)[g]			
.0581	0.45	.0578	1.04	.9802	1.07	.....	1.55
.0584	0.45	.0588	1.03	.9826	1.08	.....	1.57
.0597	0.41	.0595	1.01	.9953	1.32	.....	1.78
.0638	0.36	.0640	0.97	.9980	1.45	.....	1.86
.0652	0.38	.0650	1.01	.0125	1.32	.....	1.73
.0666	0.38	.0672	0.99	.0200	1.22	.....	1.64
.0676	0.34	.0674	0.98				
.0696	0.30	0.0698	0.97	(8589.5416)			
				.9997	1.40	.....	1.83
(8497.6603)[b†]				.0036	1.37	.....	1.74
.9553	0.56	.....	1.02	.0058	1.37	.....	1.79
.9609	0.54	.....	1.08	.0123	1.34	.....	1.80
.9674	0.80	.....	1.28				

† The visual and infrared observations of the following nine nights were made in such a way that their mean phases are the same.

TABLE 2—*Continued*

(Helioc. JD) Helioc. Phase	Δm 5500 A	Helioc. Phase	Δm 8660 A
(8592.5104)			
.0351	$0^m.83$	.....	$1^m.36$
.0375	0.79	.....	1.29
.0397	0.77	.....	1.30
.0419	0.71	.....	1.25
.0479	0.57	.....	1.18
.0537	0.51	.....	1.09
.0593	0.45	.....	0.99
(8821.6590)			
Oct. .9527	0.638	.....	1.189
14, .9598	0.762	.....	1.290
1937 .9628	0.806	.....	1.357
.9659	0.886	.....	1.392
.9698	0.963	.....	1.440
.9731	1.001	.....	1.529
.9765	1.064	.....	1.564
.9795	1.108	.....	1.597
.9828	1.253	.....	1.662
.9996	1.430	.....	1.800
.0231	1.102	.....	1.592
.0270	0.998	.....	1.486
.0304	0.889	.....	1.390
.0341	0.809	.....	1.312
.0396	0.670	.....	1.238
.0435	0.602	.....	1.172

(Helioc. JD) Helioc. Phase	Δm 8660 A	Helioc. Phase	Δm 8660 A
(8795.8426)			
.9490	$1^m.14$	.....	.....
(8796.8536)			
.3016	0.912	.....	.....
(8807.7724)			
.1096	0.949	.....	.....
(8837.7682)			
.5709	0.900	0.5914	$0^m.878$
(8847.8250)			
.0783	0.919	.1052	.974
.0916	0.933	.....	.....
(8860.5157)			
.5043	1.078	.5491	.952
.5135	1.056	.5576	.929
.5215	1.014	.5641	.922
.5322	1.034	.5781	.881
.5395	0.945	.....	.....
(8871.6532)			
.3886	0.900	0.4082	0.930
.3970	0.906	.....	.....

(Helioc. JD) Helioc. Phase	Δm 8660 A	Helioc. Phase	Δm 8660 A
(8875.5519)			
.7483	$0^m.934$	0.7634	$0^m.910$
.7561	0.953	.....	.....
(8877.4844)			
.4223	0.853	.4827	1.008
.4328	0.896	.4921	1.002
.4420	0.947	.5066	0.972
.4490	0.927	.5156	0.982
.4583	0.955	.5263	0.981
.4723	0.995	.....	.....
(8879.5724)			
.1505	0.935	.1636	0.951
(8880.4805)[f]			
.4672	0.975	.5283	0.959
.4975	1.055	.5367	0.954
.5042	0.968	.5490	0.890
.5118	0.991	.5572	0.919
.5210	0.972	.....	.....
(8889.5346)[a]			
.6249	0.931	.....	.....
(8903.4714)			
.4855	0.957	.5075	1.013
.4930	0.980	.5147	1.032
.5002	1.026	.....	.....
(8904.4681)			
.8331	0.940	.8472	0.972
.8399	0.941	.....	.....
(8908.4884)			
.2352	0.962	.2539	0.937
.2456	0.917	.....	.....
(8917.5364)			
.3908	0.869	.4036	0.887
.3963	0.900	.4080	0.893
(8926.4787)			
.5095	1.017	.....	.....
(8934.5058)[f]			
.3090	0.851	.3211	0.900
.3155	0.881	.....	.....
(8946.5066)			
.4944	1.022	.5104	1.009
.5017	0.992	0.5181	0.991
(9189.6637)			
.2976	0.882	.....	.....

TABLE 2—*Continued*

(Helioc. JD) Helioc. Phase	Δm 8660 A	Helioc. Phase	Δm 8660 A	(Helioc. JD) Helioc. Phase	Δm 8660 A	Helioc. Phase	Δm 8660 A
(9193.5986)				(9248.4944)			
.6699	$0^m.963$	0.6960	$0^m.942$	.8153	$0^m.929$	0.8189	$0^m.940$
.6779	0.948	.7069	0.922				
.6876	0.934	.....	.....	(9249.4859)			
				.1611	0.908	.1642	.930
(9198.6052)[f]							
.4160	0.922	.4387	0.960	(9276.4613)[a]			
.4300	0.975	.....	.....	.5690	0.926	.6123	.894
				.5721	0.927	.6192	.864
(9202.5884)				.5782	0.916	.6308	.855
.8052	0.907	.8224	0.906	.5818	0.892	.6390	.879
.8151	0.949	.....	.....	.6009	0.901	.6426	.894
				.6026	0.889	.6499	.899
(9203.6330)				.6079	0.906	.....	.....
.1695	0.942	.1840	0.948				
.1768	0.917	.....	.....	(9278.6355)			
				.3273	0.853	.3464	.911
(9204.5795)				.3341	0.927	.3524	.913
.4996	0.989	.5246	1.026	.3372	0.912	.3553	.878
.5037	1.017	.5302	1.023	.3437	0.930	.....	.....
.5110	1.021	.5331	0.994				
.5142	1.022	.5730	0.937	(9279.5884)			
.5166	1.020	.5771	0.915	.6596	0.876	.6766	.859
				.6657	0.890	.6819	.881
(9223.5462)				.6684	0.895	.6867	.867
.1144	1.003	.1277	0.961	.6739	0.890	.....	.....
.1200	0.971	.1357	0.989				
.1236	0.920	.....	.....	(9284.5233)			
				.3807	0.862	.4159	.883
(9224.5179)[b]				.3880	0.871	.4195	.889
.4533	0.930	.4661	0.989	.3953	0.902	.4268	.888
.4562	0.913	.4740	1.005	.3989	0.903	.4309	.861
.4634	0.987	.4780	0.987	.4054	0.892	.4390	.898
				.4098	0.883	.....	.....
(9228.6073)[a]							
.8795	0.970	.9211	0.968	(9299.5345)[b]			
.8841	0.940	.9259	0.971	.6160	0.906	.....	.....
.8872	0.934	.9333	0.943				
				(9306.5279)[b]			
(9234.5327)				.0550	1.084	.0700	.955
.9460	1.053	.9609	1.251	.0584	1.070	.0731	.971
.9479	1.071	.9661	1.361	.0656	1.003	.....	.....
.9507	1.125	.9673	1.441				
.9520	1.162	.9712	1.449	(9308.4852)[e]			
.9532	1.161	.9732	1.483	.7377	0.921	.7619	.962
.9544	1.178	.9748	1.556	.7406	0.927	.7655	.891
.9585	1.221	.9980	1.807	.7493	0.936	.7772	.907
.9601	1.230	.0021	1.833	.7534	0.935	.....	.....
.0072	1.828	.0433	1.231				
.0387	1.305	.0445	1.180	(9311.5577)			
.0414	1.229	0.0464	1.159	.8092	0.914	.8354	.892
(9244.5200)[f]				(9318.5009)			
.4292	0.915	.....	.....	Feb. .2307	0.921	.2493	.914
				23, .2380	0.892	0.2541	0.900
				1939 .2409	0.938	.....	.....

applied. The indirect comparisons were made in connection with a general spectrophotoelectric intercomparison of about sixty bright stars, which I have been making during the last three years. The intermediate star for these observations was always α Persei. The mean of the three indirect comparisons is given in the tenth column of Table 3. The observations of December 13 are incomplete because of clouds. Weights are recorded after each magnitude difference, and

TABLE 3

MAGNITUDE DIFFERENCES (ALGOL$-\beta$ TAURI)

Effective λ (μ)	1938 Dec. 13	p	1938 Dec. 15	p	1938 Dec. 15	p	1939 Feb. 16	p	1938 Indirect	p	Weighted Mean
0.425	$+0^m528$	1	$+0^m553$	1.5	$+0^m513$	1.5	$+0^m552$	1.5	.....	...	$+0^m537$
.450	.498	1	.485	1.5	.464	1.5	.533	1.5	$+0^m52$	1	.499
.475	.504	1	.488	1.5	.462	1.5	.479	1.5	.....	...	.481
.500	.....	...	.498	1.0	.485	1.0	.479	1.5	.44	1	.476
.525	.....	...	.454	1.0	.459	1.0	.448	1.5	.....	...	.453
.550	.444	1	.427	1.5	.425	1.5	.412	1.5	.39	1.5	.418
.600	.407	1	.404	1.0	.392	1.0	.421	1.0	.42	1	.409
.650	.321	1	.379	1.0	.354	1.0	.337	1.0	.39	1	.356
.700	.368	1	.359	1.0	.290	1.0	.374	1.0	.31	1	.340
.749	.301	1	.347	1.0	.309	1.0	.253	1.0	.30	1	.302
.799	.305	1	.250	1.0	.350	1.0	.309	1.0	.30	1	.303
.849	.233	1	.328	1.5	.292	1.5	.312	1.0	.27	1	.291
0.879	+0.260	1	+0.250	1.0	+0.320	1.0	+0.262	1.0	+0.25	1	+0.268
Night correction	$+0^m014$	...	-0^m021	...	-0^m025	...	0^m000	...	$+0^m033$	...	.....
Phase of Algol	0.13	...	0.82	...	0.82	...	0.82	...	0.18	...	0.17

night corrections (the amount by which the differences of each night differ systematically from the mean) are included in the tabulated values and are given at the bottom of each column. The weighted mean difference in magnitude for each effective wave length is given in the last column of this table.

Three indirect comparisons have also been made when Algol was very near zero phase. These are not sufficiently accurate to justify publication at this time.

Several investigations of the scale of the photometer have been made in a manner already described.[1] There is every reason to believe that the observed response is linear with light intensity to better than 0^m02 per magnitude for the ranges involved in the observations given in this paper.

DISCUSSION

Visual and infrared observations of primary minimum.[3]—These observations were made in such a manner that the difference in the time of minimum light in the two wave-length regions could be accurately determined. The effective wave lengths were so widely separated that it seemed that this was a good opportunity to investigate the so-called "Nordmann-Tikhoff effect," or the alleged phenomenon whereby the time of minimum light is a function of the wave length.

Nordmann[4] discovered the effect from visual observations of Algol, using blue and red liquid filters. On the basis of his data he concludes that the red minimum (6800 A) precedes the blue (4500 A) by thirteen minutes. He estimates the accuracy of this interval as three minutes. When a plot of his data (published in steps and in sidereal time) is made, it appears that this discovery rests heavily on five visual estimates. It is evident, therefore, that he has been somewhat optimistic concerning the accuracy of these observations. Maggini,[5] Hnatek,[6] and Mustel[7] have all found that the minima observed in the red precede those observed in the blue, from observations of Algol. The most recent observer,[8] Skoberla, found the reverse to be true. Although he observed Algol visually on only two nights, it should be mentioned that he was the first of this group to apply corrections for differential extinction. This is particularly desirable in the case of Algol, since there are no close comparison stars of similar magnitude.

My own observations of primary minimum when both spectral regions were under observation (with the exception of October 14, 1937) were arranged according to phase, and normals were formed containing two successive observations. The observations of October 14 were given the phase correction mentioned in the previous section and are plotted together with these normals in Figure 1. The two curves drawn through the data are symmetrical with respect to a central line through zero phase.

[3] A more detailed description of this part of the discussion is published in the *Journal of the Franklin Institute*, **228**, 411, 1939.

[4] *B.A.*, **26**, 22, 1909.

[5] *B.A.*, **35**, 131, 1918.

[6] *A.N.*, **184**, 305, 1910.

[7] *A.J. Soviet Union*, **11**, 514, 1934.

[8] *Zs. f. Ap.*, **11**, 1, 1935.

The method of computing the times of primary minimum and its probable error for each of these wave-length regions was kindly suggested to me by Dr. Schilt and is as follows:

It was first assumed that the minimum of one curve is at phase P_0. Magnitude residuals, observed *minus* curve, were recorded and weighted according to the numerical slope of the curve. Let the sum

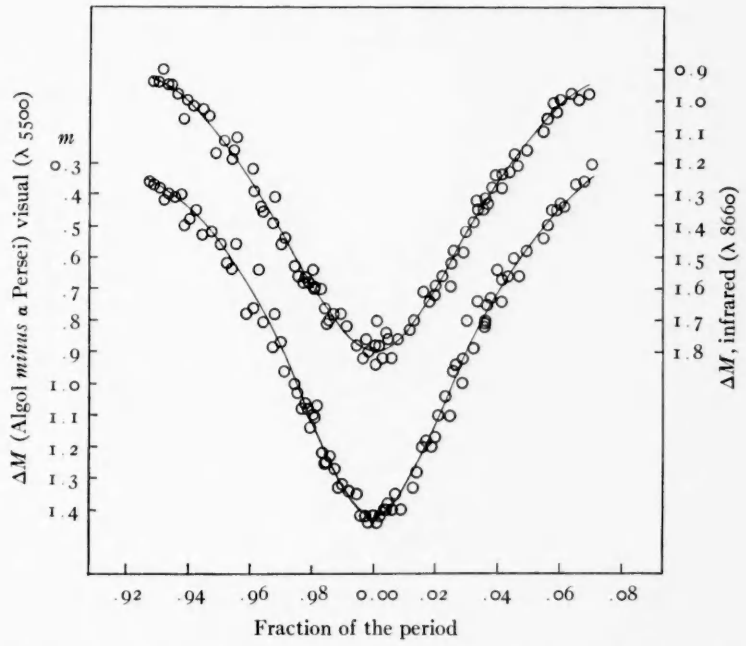

FIG. 1.—This graph includes observations obtained on those nights when both spectral regions were utilized. Consequently, only observations made at the Sproul Observatory are included. The infrared curve is above the visual curve.

of their squares (pvv) be denoted by S_2. A similar summation was then computed after the same curve had been shifted to $P_0 + 0.002$, and S_3 was found. The curve was next shifted to $P_0 - 0.002$, and S_1 was determined. If we assume that the sum of the squares of the residuals is a quadratic function of the phase, the true minimum is at

$$P_0 + 0.002 \frac{S_1 - S_3}{2(S_1 + S_3 - 2S_2)};$$

and if the mean error is the phase shift for which S is double its minimum value, then the mean error is given by

$$\pm 0.002 \sqrt{\frac{8S_2(S_1 + S_3 - 2S_2) - (S_1 - S_3)^2}{4(S_1 + S_3 - 2S_2)^2}}.$$

The phase of primary minimum and its mean error were computed in this manner for each curve. These computations showed that the infrared minimum preceded the visual by about twenty seconds. Since the computed times of minima depend somewhat on the shapes of the curves drawn through the data, the size and even the sign of this difference could be changed in this arbitrary manner.

The probable error of the determination of the time of minimum for each wave-length region is about six minutes, and therefore the probable difference in the times of minima is eight minutes. This latter figure should be the probable difference if the observations were made entirely independent of one another—for example, if the visual and infrared observations were made at different observatories. However, the manner in which these observations were made was such that the errors occurring in one wave-length band are not independent of those in the other. The error in the difference in the times of minimum is therefore less than eight minutes.

A good example of this reasoning is to be found in the observations of October 14, 1937. After 0.0012 has been added to all phases, the nine observations well distributed on the descending branch of each curve follow the mean curves very nicely, and the six observations after primary minimum cross the mean curves on the ascending branch. Since the infrared readings were sandwiched between the visual ones on this night, their phases are the same. Let us now read the phase of each mean curve on its descending branch corresponding to each of the six observed magnitude differences of the ascending branch. The mid-point between each phase on the descending branch so determined and the corresponding phase of the observation on the other branch is a determination of the phase of primary minimum and is given for each wave-length region in Table 4.

It is evident from these data that a systematic error has crept into the observations. Since it is evidently present in the observations in

both spectral regions, the systematic difference in the two phases of primary minimum is small—0.00025, or very nearly a minute. The probable error of this difference predicted from the errors at the bottom of the first two columns is 0.00044, as compared with the value 0.00018 derived from the observed differences in the third column. Although these data are not sufficiently numerous to place much reliance on the errors as given, nevertheless they do illustrate the advantage of making the observations practically at the same time when attacking this particular problem.

TABLE 4

PHASE OF PRIMARY MINIMUM

(Observations of October 14, 1937)

	5500 A	8660 A	Difference
	+0.0015	+0.0017	+0.0002
	+ .0011	+ .0006	− .0005
	+ .0003	− .0005	− .0008
	+ .0002	− .0008	− .0010
	− .0010	− .0007	+ .0003
	−0.0015	−0.0012	+0.0003
Mean...	+0.00010	−0.00015	−0.00025
P.E.....	±0.00032	±0.00030	±0.00018

I believe that my observations of Algol show that the visual (5500 A) and infrared (8660 A) times of minimum occur simultaneously, with an uncertainty of not more than three minutes.

Skoberla[8] has recently discussed data pertaining to the Nordmann-Tikhoff phenomenon. He has collected the results of studies of the times of minimum of thirty-five eclipsing stars in different wave-length regions. Subsequent papers by such experienced observers as Huffer,[9] Hellerich,[10] and Walter[11] relating to W UMa, RZ Cass, U Cep, and U Sag, as well as the data presented in this paper, all give strong indication that for these stars this effect, if it exists, is masked by the errors of observation. The results tabulated by Skoberla, with the possible exception of RZ Cass, indicate that the red minimum for each of the foregoing stars precedes the blue by

[9] *Ap. J.*, **79**, 370, 1934.

[10] *A.N.*, **256**, 405, 1935, and **261**, 120, 1937.

[11] *Zs. f. Ap.*, **16**, 167, 1938.

several times the errors of these more recent and more accurate observations.

The Nordmann-Tikhoff phenomenon, by its very nature, can never be proved not to exist. But it is interesting to note that, as observational accuracy increases, the effect seems to decrease in about the same proportion.

Since the actual times of minima are known with a probable error of six minutes in each spectral region, and since they seem to occur simultaneously, the combined data give us the time of primary minimum for the interval between November, 1935, and March, 1937, with a probable error of four minutes. It may be of interest to compare the results of these observations with the minimum of November, 1936, observed by Smart. The heliocentric Julian day he found for this minimum is 2428483.4560, from observations with a blue-sensitive photoelectric cell, while that predicted by my own observations is 0.0041 day, or six minutes earlier. These results seem to agree, within error of observation. This is particularly so since the correction for differences in the light-time of the long-period orbit have not been included in this comparison.

The results of observations of the times of primary minima given in this paper are not sufficiently numerous to contribute much to the problem relating to the change in the period of Algol. An interesting discussion of this puzzling problem has recently been made by Luyten.[12]

Infrared light-curve of Algol.—As has been previously mentioned, the infrared observations were continued after October, 1937, until the light-curve was completely covered. Also, at least a portion of the primary minimum was observed on four different nights in this spectral region at Amherst, in order to increase the weight of the infrared data and to check any possible changes in period since the Sproul observations. Neither these observations nor those made between minima show any definite systematic differences in magnitude from the Sproul observations.

The observations between minima were grouped according to phase, and eighteen normals were formed, having six observations each. These normals, together with those pertaining to observations

[12] *Zs. f. Ap.*, **15**, 97, 1938.

of secondary minimum, are shown in Figure 2. The latter contain five observations each. Conditional equations were formed giving the light-intensity between eclipse

$$l = a - b \cos\theta - c \cos^2\theta ,$$

where a is the brightness at $\theta = 90^\circ$, $2b$ is the difference in intensity between the side of the fainter star which is toward the brighter and the other side, $c = \frac{1}{2} z$ is the ellipticity constant that determines the equatorial eccentricity of the stars, and θ is the phase angle. No term has been included to allow for possible asymmetry due to orbital eccentricity. Several spectroscopic determinations indicate that the orbital eccentricity in the short-period orbit is very small. Since McLaughlin's[13] two determinations of ω separated by a year differ by 127°, it is probable that e is too small to be measured accurately. Furthermore, a careful discussion of the shape of the primary-minima-curves, for my own data as well as those of Stebbins[14] and Smart,[15] indicated that this portion of the light-curve is highly symmetrical.

The least-squares solution gave the following values for the light-intensity outside eclipse.

$$\begin{aligned} l = {} & 1.000 \;\; - 0.0344 \cos\theta - 0.0074 \cos^2\theta . \\ & \pm 0.0028 \pm 0.0029 \qquad \pm 0.0065 \end{aligned}$$

The difference in magnitude when $\theta = 90^\circ$ was $0^m.918$, and the probable error of a single normal is $0^m.008$. In the determination of the shape of primary minimum, normals were formed and rectified by means of the formula

$$l_r = \frac{l_0 + b(1 + \cos\theta) + c l_0 \cos^2\theta}{1 + b} .$$

The observations were arranged according to phase from primary minimum, without regard to whether or not they preceded or followed the minimum. The rectified normals resulting from this proc-

[13] *Bull. U. of Michigan Obs.*, **6**, 3, 1937.

[14] *Ap. J.*, **53**, 105, 1921. [15] *M.N.*, **97**, 396, 1937.

ess are given in Table 5. The first column gives the mean phase, and the second the mean observed difference in magnitude. The third column gives the argument $f = \sin^2\theta/(1 - z\cos^2\theta)$. The fourth column gives $1 - l_r$. The last column shows the number of observations included in each normal.

TABLE 5

NORMALS, PRIMARY MINIMUM

Phase	Δm	f	$1-l_r$	n
0.0698	$0^m.944$	0.1824	$-0^l.012$	5
.0661	0.968	.1647	+ .008	5
.0617	1.004	.1446	+ .038	5
.0576	1.034	.1269	+ .062	5
.0544	1.068	.1137	+ .089	5
.0502	1.132	.0974	+ .137	6
.0466	1.176	.0845	+ .169	5
.0450	1.162	.0788	+ .158	5
.0420	1.230	.0689	+ .205	5
.0396	1.254	.0615	+ .221	5
.0375	1.298	.0551	+ .249	5
.0346	1.346	.0470	+ .279	5
.0324	1.370	.0413	+ .292	5
.0290	1.452	.0331	+ .339	5
.0260	1.494	.0268	+ .362	5
.0237	1.562	.0224	+ .396	5
.0204	1.574	.0165	+ .403	5
.0179	1.624	.0128	+ .426	5
.0143	1.680	.0081	+ .451	5
.0091	1.744	.0034	+ .480	5
.0048	1.772	.0008	+ .491	5
.0026	1.806	.0002	+ .505	5
0.0009	1.800	0.0000	+0.502	6

I find by Russell's[16] method that these data are satisfied if k is 0.79 and a_0 is 0.683. Since the corrected depth of the primary minimum is only $0^m.76$ at 8660 A, it is difficult to determine k accurately from these observations. Although the theoretical curve corresponding to the foregoing values of k and a_0 represents the data in Table 5 with a probable error of $0^m.008$ for a single normal, a systematic error as large as this might change the computed value of k by as much as 20 per cent. I estimate the probable error of k to be 10 per cent.

Observations in the infrared, however, should be relatively free from limb darkening. According to Pannekoek,[17] "for B-type stars

[16] *Ap. J.*, **36**, 404, 1912. [17] *M.N.*, **95**, 733, 1935.

the limb darkening is small, for A-type stars it is very large in the blue, strongly decreasing in the longer wave lengths." The observations of the Smithsonian observers[18] have shown that darkening at the limb in the case of the sun is much less in the infrared than in the blue.

The discussion of the infrared light-curve is of particular interest when compared with the observations of others in the visual and photographic regions of the spectrum. In making a comparative discussion of this sort, it seems important to discuss the data of each observer by exactly the same method. Four other light-curves have, accordingly, been discussed in the manner already explained in connection with the infrared observations. Several points of interest concerning these light-curves are given in the following paragraphs.

1. *Stebbins' selenium photometer.*[19]—The observations of this series between minima and at secondary minimum are of particular interest. Stebbins found the difference in magnitude between Algol and α Persei to be $0^m.15$ at quarter-phase. Recent spectrophotometric comparisons of these two stars, which I have made, indicate that this value would obtain at about 5200 A. Consequently, if we assume that the relative brightness has remained unchanged during the last thirty years, this was the effective wave length of his series. Compared with the subsequent more accurate series made by Stebbins[14] ten years later, the early observations of primary minimum have very little weight. Consequently, these particular observations will not be used in the subsequent discussion. In accordance with the general policy of this discussion, a least-squares solution for the observations between minima, containing a term in $\cos^2 \theta$, was made in order to derive the ellipticity coefficient and its probable error.

2. *Stebbins' photoelectric photometer.*[14]—This photometer contained a *KH* photoelectric cell with an effective wave length near 4500 A. His reductions were made in practically the same way as the reductions of my own data; such differences as were found are very small and of negligible significance.

3. *Danjon's*[20] *cat's-eye photometer.*—Although Danjon claims a *precision* of about $0^m.01$ for these visual observations, a comparison

[18] *Handb. d. Ap.*, **3**, Part I, 149, 1930.

[19] *Ap. J.*, **32**, 185, 1910.

[20] *Ann. de l'obs. de Strassbourg*, fasc. 2, p. 1, 1933.

of his results with those of others gives the impression that their *accuracy* is not as high as is to be expected from such precision. He makes the interesting suggestion that the primary eclipse of Algol is annular and that the secondary is total. This solution is not compatible with the photometric results of others. I have used his data for the determination of the visual depths of the minima.

4. *Smart's*[15] *photoelectric photometer.*—Although Smart has not discussed his data, they are comparable with Stebbins' in both accuracy and spectral domain. Smart has grouped his observations into so-called "normals." Since some of these normals contain but one observation, I have derived new ones in an effort to equalize their weights. In view of the lack of any evidence to the contrary, the assumption is thus made that each observation has the same weight. Twenty-four normals were formed from his observations between minima, and also twenty-four during the principal minimum. It is interesting to note that Smart used δ Persei as the comparison star. Stebbins had found this star on several occasions to be "unmistakably faint to the extent of $0^m.04$ or $0^m.05$" about fifteen years previous to the time of Smart's observations. In view of the accuracy of both series of observations, it appears that this comparison star is at times variable, although its radial velocity is not known to vary.

In addition to these four series of observations, Maggini[21] has published a résumé of the results he has obtained from observations which he has made in two spectral regions (4080 A and 5800 A) by means of a photometer, using two photocells of different spectral response. Since he has not published the observational details, no comparable discussion of his data could be made. I look forward with interest to reading his complete paper, which he stated was in press at the time of the publication of the résumé.

Ellipticity and reflection.—The values I have found for the ellipticity and reflection coefficients, together with their probable errors for the five different spectral regions, are given in Table 6.

There is some evidence that the reflection coefficient b increases with the effective wave length. This conclusion is confirmed by the comparison of the results of accurate observations of similar stars

[21] *Soc. astron. Italiana* (3d ser.), p. 10, 1937.

made in the visual and photographic regions. These are given in Table 7.

The top value of *b* for each of the first four stars is that found from visual observations, mostly by Dugan. The value directly beneath

TABLE 6

Observer	Reflection		Ellipticity		Effective λ (A)
	b	P.E.	*c*	P.E.	
Stebbins	+0.0150	0.0010	+0.0132	0.0024	4500
Smart	.0149	.0012	.0027	.0023	4500
Stebbins	.0247	.0028	.0011	.0065	5200
Danjon	.0192	.0016	.0306	.0036	5500
Hall	+0.0344	0.0029	+0.0074	0.0065	8660

TABLE 7

Star	Reflection		Spectra	Observer and Reference
	b	P.E.		
RZ Cass	+0.0285	0.0038	A2 (G3)	Dugan, *Contr. Princeton Obs.*, No. 4, 1916
	.005	.0069		Hodgen, *Pub. Laws Obs.*, **34**
U Ceph	.0215	.0047	A0 G8	Dugan, *Contr. Princeton Obs.*, No. 5, 1920
	.020	.012		Baker, *Pub. Laws Obs.*, **30**, 1921
TV Cass	.037	.004	B9 (F5)	McDiarmid, *Contr. Princeton Obs.*, No. 7, 1924
	.016	.0037		Cummings, *Pub. Laws Obs.*, **27**, 1917
RS Vulp	.039	.....	B8 B9?	Dugan, *Contr. Princeton Obs.*, No. 6, 1924
	.033	.0047		Baker, *Pub. Laws Obs.*, **32**, 1921
U Sag	.0215	.0039	B9 G2	Walter, *Zs. f. Ap.*, **16**, 167, 1938
	+0.0130	0.0048		*Ibid.*

was found from photographic observations made at the Laws Observatory. In the case of the last star, the effective wave lengths given by Walter for the upper and lower values of *b* are at 6160 A and 4300 A, respectively. Krat's[22] spectrophotometric observations

[22] *Zs. f. Ap.*, **11**, 71, 1935.

of u Her also show that b increases with wave length. The only evidence which I have seen which tends to deny the tentative conclusion that b increases with effective wave length is that given by Maggini in his résumé. Since there is some doubt in this case as to which term was used in his derivation of the reflection coefficient, I prefer not to stress his results without first seeing his final paper.

Let $2b''$ be the additional energy radiated by the secondary component at full phase due to the presence of the primary, and $2b'$ be the corresponding radiation from the primary at full phase due to the secondary. The observed reflection from a hemisphere, $2b$, is then $2b' - 2b''$ and is expressed as the fraction of the total energy of the system when $\theta = 90°$. If the two stars were of equal size and surface brightness, $2b'$ would equal $2b''$, and no reflection would be observed. If a third body is present in the system, the observed reflection coefficient should be divided by $1 - L_C$, in order to reduce it to the unit involving only the eclipsing pair.

A crude explanation of the change of these coefficients with wave length may be illustrated by a comparison of the values of b found at 4500 A and 8660 A for Algol. Let us first assume that the energy reflected by the secondary has its color temperature. Stebbins has found from observations at 4500 A that the light from the fainter side of this body constitutes 0.045 that of the system, and that the reflection at full phase, $2b$, is 0.030 that of the system. The maximum reflected light is therefore two-thirds the light of the faint side of the secondary. If our assumption were correct, this result should be independent of the wave length used in the determination of the light-curve. At 8660 A the fainter side of the secondary contributes 0.193 of the light of the system, and the value of $2b$ would be $\frac{2}{3}$ (0.193), or 0.129. This is much larger than the observed value 0.069 ± 0.006.

If we now assume that the re-emitted energy has the same quality as that of the exciting star, and follow this same procedure, the value of $2b$ at 8660 A would be only 0.024. In each of these comparisons we have neglected the energy reflected from the primary and the corrections to be applied because of the influence of the third body.

If we assume that the B8 star has a color temperature of 15,000° and that of the fainter side of its eclipsing companion is 5600°, it can be shown by similar reasoning, using the data in Table 9 for the

ratio L_B/L_A, that the observed reflection coefficient at 8660 A would be predicted from that found at 4500 A if the energy striking the secondary is re-emitted at a black-body temperature of about 6500°.

In determining the ellipticity of the two principal components of Algol, I have followed the method developed by Walter and used in his discussion of U Sag.[11]

If a_i and b_j are the semimajor axes, the ellipticity of a star is defined as the square of its equatorial eccentricity, or

$$z_i = 1 - \frac{b_i^2}{a_i^2}.$$

Eddington[23] has shown that the observed ellipticity constant is partially masked by reflection and should be increased by 0.36 times the reflection constant. The corrected mean ellipticity for uniform disks is then

$$z_u = (2c + 0.72b) \operatorname{cosec}^2 i .$$

Walter has found that to a sufficient approximation

$$z_u = \frac{l_B z_B}{(1 - z_B)^{1/2}} + \frac{l_A z_A}{(1 - z_A)^{1/2}},$$

where l_B refers to the luminosity of the dark side of the secondary. Since the z's are independent of the wave length and the l's are not, by substituting the z_u's and l's found from observations at 4500 A and 8660 A, the two equations may be solved for the ellipticities of the individual stars. Stebbins' and Smart's values were used separately with my own, and the results are given in Table 8.

There is indication, therefore, that the more tenuous G star is more distorted than the B8 star. This result agrees in a qualitative way with that of Walter in his discussion of U Sag. He gives the density of the brighter and fainter components as 0.17 and 0.011, while the corresponding values given by McLaughlin[13] for Algol are 0.15 and 0.02. Walter finds the value 0.40 for z_B and zero for z_A, and he describes the shape of his red light-curve between minima as

[23] *M.N.*, **86**, 320, 1926.

the β Lyra type and that of the blue light-curve as the Algol type. No such obvious difference exists in the light-curves of Algol plotted in Figure 2. Further evidence that the secondary in Algol stars suf-

TABLE 8

ELLIPTICITY OF THE ECLIPSING COMPONENTS OF ALGOL

Observer	λ (A)	l_B	l_A	z_u	P.E.	z_B	z_A
Stebbins	4500	0.045	0.925	0.0380	0.0048	0.06	0.04
Smart	4500	.022	.948	.0165	.0046	0.16	0.01
Hall	8660	0.193	0.738	0.0404	0.0132	.....	.....
Mean	.....	.....	.....	.....	.....	0.11	0.025
b/a	.....	.....	.....	.....	.....	0.94	0.99

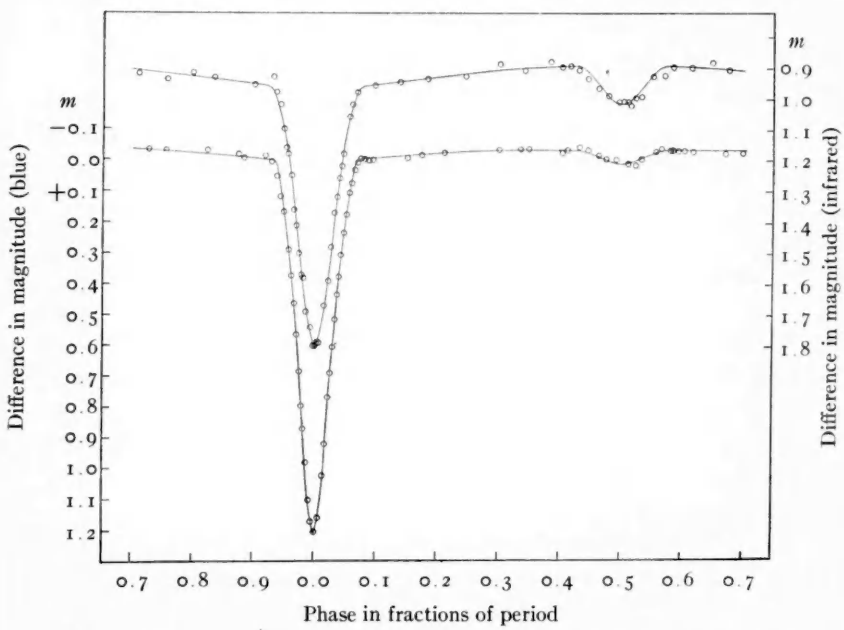

FIG. 2.—The lower curve is that found by Stebbins with his photoelectric photometer, in blue light (4500 A). The infrared (8660 A) light-curve shown directly above it includes both Sproul and Amherst observations. Four observations are included in each normal of the primary minimum for the infrared curve. The curves are theoretical curves derived from elements obtained from data they represent. Although the readings made for Algol by Stebbins in the blue are about 1½ times as numerous as those made in the infrared, the infrared data are distributed over nearly twice as many nights.

fers more tidal distortion than the primary is given in Kopal's[24] note on Krat's observations of u Her. Here again the value of L_A/L_B used in my discussion has not been corrected for the third body. If this body is similar to that suggested in the subsequent discussion, the results are similar to the foregoing in both cases.

Elements.—The elements were first derived on the assumption that the third body is completely dark. The results of these computations, which I have made, are given in Table 9 for Stebbins', Smart's, and my own data. In view of the difficulty of determining them in the case of Algol, the agreement of k and α_0 is reasonably good. It can be shown that the darkening at the limb would increase the value of k and decrease α_0. In other words, if darkening were introduced into Stebbins' solution, greater discordance would result between the violet and infrared values of k. In view of what is known about darkening at the limb as a function of the wave length, it does not seem reasonable to compare a darkened infrared solution with a uniform solution in the violet. The three solutions given in Table 9 are therefore uniform solutions.

Smart's depth of primary minimum is $0^m.031$ shallower than that found by Stebbins. It is difficult to attribute this to a possible difference in effective wave length, since his secondary minimum is $0^m.014$ shallower. As a result of this difference in the secondary minimum, there is considerable difference in the ratio of the surface brightnesses found from these two series of observations. Since Smart's secondary minimum is flatter than is to be expected from the shape of his primary minimum, and since his comparison star has been suspected of variability, I believe Stebbins' elements deserve greater confidence.

The data pertaining to the visual region, given in Table 9, were gleaned from various sources. The depth of the secondary minimum is the mean of that found from Stebbins' selenium observations and Danjon's visual observations. Danjon's rectified depth of primary minimum is $0^m.973$. I have found the difference in magnitude between Algol and α Persei, when the former is at quarter-phase, to be $0^m.325 \pm 0^m.006$ at 5500 A. When this value is compared with the

[24] *Zs. f. Ap.*, **16**, 304, 1938.

visual data of Table 2 pertaining to primary minimum and rectified by Stebbins' values of b and c (selenium photometer), the visual depth is $0^m.990$. The mean of these two determinations is given in

TABLE 9

ELEMENTS AND INFRARED LIGHT-CURVE

Observer		Stebbins	Smart	Hall	Misc.
Effective wave length	.....	4500 A	4500 A	8660 A	5500 A
Ratio of the radii	k	0.85	0.85	0.79	.....
Area of bright body obscured at minimum	a_0	0.700	0.673	0.683	.....
Light of bright body	L_A	0.925	0.948	0.738	.....
Light of faint body (bright side)	L_B	0.075	0.052	0.262	.....
Light of faint body (faint side)	L_B-2b	0.045	0.022	0.193	.....
Radius of bright body (orbit = 1)	r_2	0.207	0.206	0.204	.....
Radius of faint body (orbit = 1)	r_1	0.244	0.242	0.258	.....
Ratio of surface brightness (faint side L_B)	J_1/J_2	0.035	0.017	0.189	.....
Cosine of the inclination	$\cos i$	0.144	0.152	0.169	.....
Semiduration of eclipse	$d/2$	4^h49^m	4^h47^m	4^h55^m	.....
Range of primary minimum (rectified)	.....	$1^m.134$	$1^m.103$	$0^m.761$	$0^m.982$
Range of secondary minimum (rectified)	.....	$0^m.042$	$0^m.028$	$0^m.129$	$0^m.056$
Depth of primary minimum (rectified)	$1-\lambda_1$	0.648	0.638	0.504	0.595
Depth of secondary minimum (rectified)	$1-\lambda_2$	0.038	0.025	0.112	0.050

INFRARED LIGHT-CURVE

Phase	$(\beta-\alpha)$ Per	Phase	$(\beta-\alpha)$ Per
0.0000	$1^m.805$	0.3000	$0^m.906$
.0210	1.575	0.4017	0.894
.0319	1.386		
.0423	1.226	0.4281	0.892
.0534	1.084	.4467	.915
0.0719	0.958	.4578	.940
		.4681	.966
0.1000	0.953	.4790	.992
.2019	.930	0.5000	1.018
0.2500	0.918		

Table 9. Since the depth of the primary minimum is presumably more accurately determined than that of the secondary, the visual value of L_A was computed from the rectified loss of light at primary minimum, using Stebbins' value of a_0. The difference between L_A and unity is given for the luminosity of the bright side of the eclips-

ing companion. Stebbins' visual value for the reflection coefficient was used to find the luminosity of the dark side of this star.

The observed phases of secondary minimum have all been examined in order to see whether there was any definite photometric evidence of an eccentric orbit for the eclipsing pair. None was found. Although the chance of accurately determining the phase of secondary minimum is obviously greater in the longer wave lengths, I was prevented from doing this by unfavorable weather conditions.

The ratio of the surface brightness of Algol to that of its eclipsing companion in the three different spectral regions may be used to find the color temperature of the latter. We assume that the B8 star

TABLE 10

COLOR TEMPERATURE OF THE SECONDARY COMPONENT

Observer	Bright Side					Faint Side		
	Eff. λ	Obs.	5800° Comp.	5800° O−C	6000° O−C	Obs.	Comp.	5600° O−C
Stebbins	4500 A	0.059	0.056	+0.003	−0.001	0.049	0.060	−0.011
Misc. (vis.)	5500	.084	.095	− .011	− .018	.119	.109	+ .010
Hall	8660	0.222	0.222	0.000	0.000	0.262	0.262	0.000

has a color temperature of 15,000° and that both stars radiate as gray bodies. The ratio of the surface brightnesses when the brighter side of the secondary is used is merely the ratio of the rectified losses of light at the two minima, while that involving the fainter side of the companion for a given wave length is $J_1/J_2 = k^2(L_1 - 2b)/L_2$. Since we use $(J_1/J_2)_{\lambda i}/(J_1/J_2)_{\lambda j}$ in finding the color temperature, the k^2 cancels out. In the first case the computation is independent of the third body.

The observed ratio of the surface brightness of the bright side of the companion to that of the primary is given for different wave-length regions in the third column of Table 10. The computed value, assuming the companion has a color temperature of 5800°, is given in the following column. Agreement has been forced at 8660 A. For the sake of comparison, a similar computation is given for 6000°. If we assume that L_C is zero, we find the ratio of the surface brightness

of the fainter side of the companion to that of the primary shown in column 7. The color temperature of the secondary appears to be near 5600°. Maggini[21] finds a color index for the brighter and fainter side of this companion equivalent to an F6 and G5 star, respectively.

Spectrophotometric observations.—An attempt to detect the presence of the third body has been made by comparing the energy from Algol near quarter-phase with a normal B8 star. Since the color temperature and magnitude of the secondary component of Algol can be found to a first approximation from the light-curves in the different spectral regions, it should be possible to predict how the difference in magnitude between Algol and a B8 star of average color should change with wave length outside eclipse. Any deviations from these predicted differences may be attributed to additional light from the third or remaining bodies. When such deviations are found, it should be possible to correct the data from the light-curves and to repeat this process until all observed phenomena are satisfactorily explained.

We are assisted in this procedure by the fact that in regions of small or negligible obscuration the colors of B8 stars show very little dispersion. Since the eclipsing companion contributes relatively little light at the shorter wave lengths, we would naturally expect to find that the composite color of the system in this spectral region would be similar to that of a B8 star. The photoelectric observations at 4250 A and 4750 A given in Becker's[25] catalogue suggest that such is the case. These were made on two nights when Algol was at quarter-phase. On the other hand, colorimetric observations which I made at Yale[26] in 1932 at effective wave lengths 7000 A and 8200 A indicate a large positive color excess. In this spectral region the cooler secondary contributes a much larger percentage of the light of the system, and consequently the composite color at maximum is more nearly that of an A2 than a B8 star.

β Tauri was chosen, for the comparison star, since its color is typical of B8 stars over an extensive spectral region, its radial velocity is constant, and its position and magnitude are favorable. Perhaps the

[25] *Veröff. Sternwarte Berlin Babelsberg*, **10**, No. 3, 1933.

[26] *Ap. J.*, **79**, 145, 1934.

best reason for believing that β Tauri and the primary in Algol are similar in color is to be found in the spectroscopic determinations of their absolute magnitudes. Dr. Schlesinger's *General Catalogue of Stellar Parallaxes* gives the mean of four determinations of the spectroscopic parallax (made at the same observatories) of each of these stars as $0''.035$. This indicates that their absolute magnitudes differ by $0^m.5$ and that the two spectra, and hence their colors, are similar.

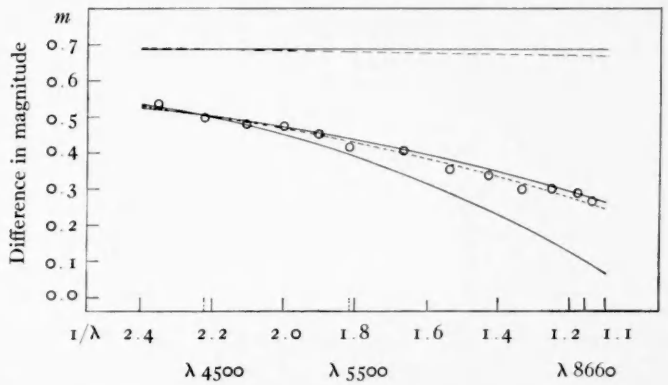

FIG. 3.—Spectrophotometric comparison with β Tauri. The heavy curve which passes just above the data represents the predicted departure from the horizontal line shown at the top of the figure, when C is assumed to be an A5 star of the proper bolometric magnitude. When this line is tilted by the amount indicated by the broken line, which implies that the primary in Algol is slightly redder than β Tauri, the predicted curve fits the data very well. The corresponding curves predicted when C is assumed to be completely dark are very similar to those just mentioned. The curve at the bottom of the figure would result if C were of the same magnitude and color as the eclipsing companion. It is therefore highly probable that the third body is not cooler than the eclipsing companion.

The mean observed difference in magnitude (Algol *minus* β Tauri) for thirteen different spectral regions, given in Table 3, is plotted against the reciprocal of the wave length, expressed in microns, in Figure 3. If the influence of the light from other bodies in the system is disregarded, one would expect these data to be satisfied by a straight line which differs but little from the horizontal. The mean phase of these observations is 0.17 of the period from primary minimum.

It has already been shown that, if the primary has a color temper-

ature of 15,000°, that of the dark side of the eclipsing companion is near 5600°. In order to predict the departure from a horizontal line caused by the presence of the eclipsing companion, we must find the ratio of L_B/L_A as a function of the wave length. In doing this, the values of L_B of Table 9 must first be corrected to phase 0.17 by the use of the reflection coefficients of Table 6. The resulting values of L_B/L_A are given in Table 11.

TABLE 11

RATIO OF LUMINOSITIES

Observer	Eff. λ	L_B/L_A (Obs.)	L_B/L_A (Comp.)	O−C
Stebbins	4500 A	0.057	0.069	−0.012
Vis. (misc.)	5500	.134	.124	+ .010
Hall	8660	.318	.304	+ .014
Hall	8660	0.286	0.304	−0.018

The first infrared value is that found entirely from the light-curve, while the second value is that found in the same manner as the visual luminosities, using Stebbins' value of a_0. The computed ratios were derived from Planck's law, using the foregoing temperatures and multiplying by a factor in order to represent the observed ratios. This same factor was then used to compute similar ratios for wave lengths not given in the table, and magnitude differences $m_A - (m_B + m_A)$ were formed. These represent the change in the magnitude of Algol caused by the addition of companion B. At 4500 A this amounts to $0^m.073$. A smooth curve drawn through the observations represented in Figure 3 passes through $0^m.506$ at this wave length. If the secondary were made completely dark, this magnitude difference would be increased to $0^m.579$. Since the primary and β Tauri have very similar spectra, we would expect this difference to hold approximately for other wave lengths as well. If we now subtract $m_A - (m_B + m_A)$ from $0^m.579$, we find a curve similar to the heavy one drawn through the normals shown in Figure 3. Had we assumed that the primary was slightly redder than β Tauri and that the difference in magnitude changed by $0^m.03$ in a linear fashion with $1/\lambda$ in the interval $1/\lambda = 2.22$ to 1.11, the broken curve would result.

It therefore seems evident that the spectrophotometric observations can be satisfactorily predicted from data derived from the light-curves if we assume that the third body is completely dark. This solution is not compatible with mass considerations.

Relative masses of the components of Algol.—If we let c_1 represent the mass function of the smaller, and c_2 that of the larger orbit, then

$$c_1 = \frac{(a_1 \sin i_1)^3}{P^2} = \frac{M_B^3 \sin^3 i_1}{(M_A + M_B)^2} = 0.026\,,$$

$$c_2 = \frac{(a_2 \sin i_2)^3}{P^2} = \frac{M_C^3 \sin^3 i_2}{(M_A + M_B + M_C)^2} = 0.058\,.$$

Assuming that $i_1 = i_2$, we have

$$\frac{M_C}{M_B} = \left(\frac{c_2}{c_1}\right)^{1/3}\left(1 + \frac{M_C}{M_A + M_B}\right)^{2/3}.$$

The value $(c_2/c_1)^{1/3}$, derived from McLaughlin's elements, is 1.31. Obviously, we must know the mass ratio of A to B before the last equation can be used to give us that of A to C.

A good approximation to the mass-luminosity law for the bright stars is given by

$$\frac{M_A}{M_B} = \left(\frac{L_A}{L_B}\right)^{2/5}.$$

The ratio of the luminosities, using the dark side of B, is 9.9 in the visual region. This ratio was found from the observations in a manner similar to that explained in the derivation of the computed ratios in Table 12. In this case the observed values of L_B were corrected by means of the reflection coefficients to phase 0.00 instead of 0.17, and the influence of a third body (to be discussed presently) has been taken into account.

The two components A and B are of different temperature; consequently, although the observed difference in visual magnitude is $2^m.5$, the bolometric difference is $1^m.8$. The computed mass ratio A/B is then 1.9, and A/C is only 1.1. In other words, the bolometric mag-

nitude of C is comparable with that of A; and if the inclination of C's orbit differs much from 90°, the mass-luminosity relationship implies that it should be even brighter than A. In view of both the spectroscopic and the photometric evidence, this seems highly improbable.

The parallax of Algol given in Dr. Schlesinger's *General Catalogue of Stellar Parallaxes* is $0''.031 \pm 0''.004$, suggesting an absolute magnitude of -0.4 for the primary. The spectroscopic value is practically the same. Although this evidence is by no means conclusive, yet we have no a priori reason to suspect that the B8 component has unusual luminosity or mass for its spectral type. Professor Russell suggests (by letter) that the eclipsing companion, which is well above the main sequence and is of low density, may be $1^m.5$ off the mass-luminosity curve. He draws an analogy between this star and the brighter component of ζ Herculis. The departure of the Go component of this star from the mass-luminosity curve is evidently well established. It has been discussed by Strömgren and by Chandrasekhar.[27] Van de Kamp[28] has very recently published a value for the mass of the bright Go component of 0.86 the sun's mass; but its absolute magnitude, determined from several series of trigonometric parallaxes, is 3.1, a value which seems to be well determined.

When we follow Professor Russell's suggestion and assume that B is $1^m.5$ too bright for its mass, we find that the mass ratio A/B is increased from 1.9 to 3.3 and that of A/C is increased from 1.1 to 2.0. The value 3.3 ($M_A = 1.60\odot$) agrees reasonably well with McLaughlin's[13] 1924 determination of 3.65 for this mass ratio from his study of the rotation effect. He states, however, that he believes his earlier value of 5.0, determined in 1923, merits greater confidence. A mass ratio of 4.5 would place A on the mass-luminosity curve if the trigonometric parallax is correct. When we adopt the ratio 3.3, the bolometric difference in magnitude ($C - A$) is $1^m.94$. Although this value is arbitrary, the discussion of the mass ratios still give strong indication that C is bolometrically brighter than the eclipsing companion, B.

[27] Chandrasekhar, *Introduction to the Study of Stellar Structure*, p. 279, Chicago: University of Chicago Press, 1939.

[28] *A.J.*, **47**, 168, 1938.

An upper limit to the visual luminosity of C is given at once from the photometric data. The sum of the visual depths of the two minima (corrected for reflection) represent about 0.62 the light of the system, and therefore C cannot possibly contribute more than 0.38 the visual light of the system. A more critical test is to be found in the spectroscopic observations. If C were half as bright as $A + B$ at primary minimum, its spectrum would be presumably more in evidence. McLaughlin found that his 1923 observations indicated that some of the lines of the primary near primary minimum are blended with those of the third body. He finds that his 1924 observations tend to contradict this hypothesis. It appears from the number and distribution of the observations shown in his diagrams that the 1923 observations support the hypothesis more strongly than the later ones refute it.

Consideration of the mass ratios and the spectroscopic data indicates that C *is bolometrically brighter than* B *but fainter photographically than* $\frac{1}{2}$(A + B) *at primary minimum.*

Miss Barney[29] has made a study of 250 spectrograms of Algol secured by Dr. Schlesinger and others at the Allegheny Observatory. She measured the radial velocities and recorded the phase distribution of numerous extra lines or lines of doubtful origin which had not been previously used by Dr. Schlesinger in the determination of the velocity-curve of the primary. She found that these lines were most numerous near primary and secondary minimum, and indicated radial velocities of the same sign as the primary but of smaller magnitude. Four of the extra lines are usually present in the B8 spectrum and one in A2; five are usually present in A5 and prominent in F5 stars. Miss Barney concluded that these lines belong to both the primary and the secondary and are visible when the light from the primary is reinforced by that of its eclipsing companion. She found that many of these extra lines were iron lines.

Since recent photometric data indicate that the eclipsing companion is an early G-type star, and since the ratio of the amplitudes of the velocity-curves of the short- and long-period orbits is 4.5, it is conceivable that the extra lines found by Miss Barney may belong in part to the third body.

[29] *A.J.*, **35**, 95, 1923.

If the discussion in the previous paragraphs is correct, C must be an early-type main-sequence star. It will presently be shown that such a possibility is not contradicted by the spectrophotometric observations. However, these observations would definitely rule out a star as cool as, or cooler than, the eclipsing companion having the required bolometric magnitude. This is illustrated by Figure 3.

Let us postulate an A5 star for C and assume that the bolometric difference in magnitude $(C - A)$ is that given above, or $1^m.94$. If the parallax is correct, C would then be a normal main-sequence star and would be about $0^m.9$ fainter than $A + B$ at primary minimum.

In the following computations, color temperatures of 15,000°, 10,000°, and 5600° for A, C, and B, respectively, are adopted. The bolometric difference in magnitude of 1.94 for $(C - A)$ and the temperatures of A and C enable us to compute the light-ratios L_C/L_A for different wave lengths. The ratio L_B/L_A must be determined from the light-curves. This was done in the following manner:

Let $L_A + L_B + L_C = 1$; and, since by our hypotheses, at 4500 A $L_C = 0.122L_A$, we have

$$1.122L_A + L_B = 1\,, \tag{1}$$

and in Russell's notation

$$a_0 L_A = 1 - \lambda_1\,, \tag{2}$$

$$k^2 a_0 L_B = 1 - \lambda_2\,. \tag{3}$$

After substituting Stebbins' data, we find from these:

$$a_0 = 0.727 + \frac{0.038}{k^2}\,.$$

The best values of k and a_0 can now be readily determined from the point of intersection of this curve and that found by setting $\chi(k, a_0, \frac{1}{4}) = 1.870$. This last value was determined from the shape of the primary minimum of the light-curve at 4500 A.

We find in this way that Stebbins' data give values of k and a_0 of 0.78 and 0.79, respectively, instead of 0.85 and 0.700 found for the two-body case. Cos i is 0.133 and r_1 and r_2 are 0.252 and 0.197, re-

spectively. The infrared data indicate that k is 0.69 and a_0 is 0.831. Since the primary minimum is much deeper in the blue than in the infrared, and since Stebbins' observations are more numerous than mine, I have adopted his values of k and a_0 and have computed L_A and L_B by means of equations (2) and (3), using the depths of minima for the visual and infrared regions shown in Table 9. L_C is then the difference between $L_A + L_B$ and unity. The three values of L_B were then corrected for reflection from phase 0.50 to 0.17, or to the mean phase of the spectrophotometric observations.

The ratios L_B/L_A and L_C/L_A found in this way are given in Table 12 for the three different effective wave lengths in the second and

TABLE 12

PREDICTION OF THE SPECTROPHOTOMETRIC OBS. $\theta = 0.17$

Wave length (A)	Obs. L_B/L_A	Comp. L_B/L_A	Obs. L_C/L_A	Comp. L_C/L_A	$\frac{L_A}{L_A+L_B+L_C}$	Comp. Δm
4000	.....	0.042	.....	0.110	0.868	0^m536
4500	0.071	.062	0.122	.122	.844	.506
5000	.....	.086	.....	.133	.820	.475
5500	.090	.112	.190	.144	.796	.442
6000	.....	.138	.....	.151	.776	.415
7000	.....	.192	.....	.166	.736	.357
8000	.....	.244	.....	.177	.704	.309
8660	0.287	.270	0.202	.182	.684	.278
9000	.....	0.290	.....	0.186	0.678	0.268

fourth columns. The computed ratios are those derived from blackbody considerations which seem to fit the values computed from the light-curves reasonably well. The ratios $L_A/(L_A + L_B + L_C)$ are derived from these computed ratios. The contribution of L_B and L_C to the magnitude of A was then found. When we force agreement by an additive constant at 4500 A, as in the two-body case, we find the predicted difference in magnitude between a star the color of A (in this case β Tauri) and the magnitude of the system as a function of the wave length. These differences are given in the final column of the table and are represented by the curve in Figure 3. The observed spectrophotometric data tend to fall slightly below this curve. If we assume, as before, that star A and β Tauri have slightly different colors and that their difference in magnitude changes with wave

length in the manner indicated by the broken line at the top of the figure, we find that the agreement between these independent data is very satisfactory.

In this discussion I have had to choose between slightly different methods of procedure in determining the luminosity of the eclipsing companion from the visual and the infrared data. However, such slight differences as would appear as the result of this arbitration are unimportant when compared with the uncertainty in the characteristics of the third body.

It is, of course, unfortunate that I have been forced to assume that B is not on the mass-luminosity curve; yet there is some outside justification for this procedure. It is otherwise difficult to predict a luminosity for C small enough to satisfy all other criteria. One could also avoid this difficulty to some extent by assuming that C consists of two stars of equal brightness. In this case the bolometric difference in magnitude $(C - A)$ would be 1^m66, and the photometric data would be satisfied, provided the third and fourth bodies are early-type stars. Results somewhat similar to those in Table 12 would still hold; in this case L_C would refer to the total light of the second system.

If the inclination of the long-period orbit differs greatly from 90°, the mass of C would be still larger and the difficulty in reconciling all data would be correspondingly increased. The value[13] of $a \sin i$ is 88,000,000 km; and, consequently, the light-time of the long-period orbit should be about five minutes. Smart has found, from his photometric observations near primary minimum, a change in period amounting to $2\frac{1}{2}$ times the expected value. Since these actually include this minimum on only four nights, his results are not convincing, despite the high accuracy of his observations. Dr. Schlesinger[30] has examined the rich photometric material accumulated during the second half of the nineteenth century and has found that this light-equation was actually present.

The determination of this orbital inclination, together with the value of the mass ratio $C/(A + B)$, will add greatly to our knowledge of Algol. It is gratifying to learn that astrometric plates are being

[30] *Science*, **41**, 115, 1915.

accumulated at the Sproul and Allegheny observatories for this purpose.

Since this paper was written, a report of the Dominion Astrophysical Observatory[31] has appeared in which it is stated, in reference to Dr. Pearce's spectroscopic observations of Algol, that "during eclipse the spectrum of the class A companion has been repeatedly photographed." My assumption that the third body is an A5 star rests mostly on considerations of mass, photometric data, and the Russell diagram. I have also been guided somewhat by the nature of the extra lines found by Miss Barney. Since the photometric data indicate that the eclipsing companion is an early G-type star, the A star observed by Pearce must be a third body. His statement strengthens the validity of my discussion and leads me to believe that the identity of two companions of Algol is now known to a first approximation. I look forward with much interest to reading the final discussion of his spectroscopic observations.

I wish to thank Dr. John A. Miller, former director of the Sproul Observatory, for the opportunity of using the 24-inch telescope to observe Algol. I am also grateful to Mr. R. W. Delaplaine, who voluntarily recorded observations and checked many of the reductions. Dr. John Merrill kindly sent me an advance copy of his extensive and very convenient table of χ functions; Professor Russell has given me valuable assistance in the discussion of the masses of the components; and Professor Dugan very kindly read and criticized the manuscript.

AMHERST COLLEGE OBSERVATORY
June 1939

[31] *M.N.*, **99**, 354, 1939.

THE MEAN ABSOLUTE MAGNITUDE OF CLASS-R STARS*

RALPH E. WILSON

ABSTRACT

Comparisons of the parallactic and peculiar motions derived from the proper motions of 28 and the radial velocities of 37 class-R stars indicate for the proper-motion stars a mean parallax, $\bar{\pi} = 0''.00180 \pm 18$. The mean absolute magnitude of these stars, uncorrected for dispersion, is $M_\pi = -0.22 \pm 0.22$. The mean absolute magnitude of the radial-velocity stars, as derived from the galactic-rotation factor, and also uncorrected for dispersion, is $M_r = -0.79 \pm 0.94$. If the distribution in $\log \pi$ is Gaussian, these results may be brought together with the dispersion $\sigma_{\log \pi} = \pm 0.222$. The concluded mean value for the stars of class R is $\bar{M} = -0.50 \pm 0.20$. There appears to be no evidence of a difference in $\bar{M}$ between the stars of subclasses Ro–R4 and R5–R9.

Owing to the rare occurrence and the apparent faintness of the stars of spectral class R, the accumulation of data concerning their motions has been very slow. Only one of these stars north of declination $-30°$ is brighter than magnitude 7.0, and that only at certain times (U Cygni, a variable with a large range, 6.1 to 11.8, period 453 days, classified as either R9 or Npe). The brightest typical R star is BD$-10°5057$, 7.0 mag., Ro. Sanford[1] has measured the radial velocities of all 22 stars brighter than 9.0 and of 20 fainter than that limit. He notes that 15 others are listed in the *Henry Draper Catalogue*, for six of which no magnitudes are given, while the mean visual magnitude of the remainder is 10.4. Since the early observations of stellar positions were, in general, confined to stars brighter than 9.0, one finds very few old data upon which to base determinations of proper motion. Hence, any knowledge of the mean absolute magnitude of these stars that may be acquired will necessarily be subject to considerable uncertainty.

The first attempt to estimate the mean distance of the R stars was made by Kapteyn and van Rhijn[2] in 1920. From the mean paral-

* *Contributions from the Mount Wilson Observatory, Carnegie Institution of Washington*, No. 618.

[1] *Mt. W. Contr.*, No. 525; *Ap. J.*, **82**, 357, 1935.

[2] *Groningen Pub.*, No. 30, 1920.

lactic motion of 16 stars of mean apparent magnitude 8.4 and an assumed group motion of 20.0 km/sec, they found $\bar{\pi} = -0''.0002 \pm 20$. From the concentration of the stars toward the galactic plane, however, they judged that the true parallax must be greater than the value they had found for the stars of class N. A year later Luplau-Janssen and Haarh,[3] using somewhat the same data, found $\bar{M} = 0.0$. In 1923 Wilson,[4] using 16 improved proper motions and Sanford's preliminary values of the group and peculiar motions ($V_0 = 21.0$ km/sec, $\theta = 26.0$ km/sec), found $\bar{M} = -1.2$. At about the same time Sanford made a preliminary estimate, $\bar{M} = -1.5$, which was published in Wilson's paper. Since then the subject has remained *in statu quo*, pending the accumulation of more data. Since it is unlikely that the material now available will be appreciably increased for some time, it seems worth while to attempt another estimate of the mean absolute magnitude.

DATA

Sanford's[1] radial velocities of 42 R stars were published in 1935, and none have been added since. They range from 0 to 383 km/sec; but 37 of them are less than 65 km/sec, with a small mean, +0.6, and an average of 26.2 km/sec. The five large velocities are all negative, between −128 and −383 km/sec; and two of the stars, BD+23°123 and BD+20°5071, are among the fastest-moving stars known. The proper motion of the former is outstanding, 0".145, while that of the latter is small, 0".011. In the solutions that follow, these five stars were omitted. All the others were used with equal weights.

Table 1 lists the proper motions of 28 stars which have been determined with probable errors not exceeding 0".015. These motions have been derived mainly by the writer; one is taken from the *Boss General Catalogue*, two from Kapteyn and van Rhijn,[2] and one from Luyten.[5] The total proper motions are, in general, small. In the solutions, BD + 23°123 was omitted and CD − 66°2978 was given

[3] *A.N.*, **214**, 388, 1921.

[4] *A.J.*, **35**, 129, 1923.

[5] *Harvard Circ.*, No. 293, p. 2, 1926.

TABLE 1

PROPER MOTIONS OF CLASS-R STARS

Star	α 1900	δ 1900	m_{vis}	Sp.	μ_α	μ_δ	μ	Auth.*
+53°66	0^h19^m2	+53° 44′	9.5	R5	−0″.013 ± 10	+0″.003 ± 10	0″.013	Ly
+23°123	0 48.9	+23 32	8.8	R5	+ .145 6	.000 6	.145	W
V Ari	2 9.6	+11 47	8.3–9.0	R8	+ .024 5	+ .024 5	.034	W
−10°513	2 30.2	− 9 53	8.3	R3	+ .001 8	− .001 7	.001	W
+57°702	3 3.7	+57 31	8.1	R5	+ .013 7	− .004 7	.014	W
UV Cam	3 57.2	+61 32	7.9– 8.3	R8	− .023 9	− .004 8	.023	W
S Cam	5 30.3	+68 45	7.8–11.4	R8e	− .011 12	− .057 13	.058	W
−69°642	6 39.6	−70 0	9.5	Ro	− .001 14	− .035 16	.035	K
−3°1685	6 56.1	− 3 7	7.5	R5	− .007 6	− .006 6	.009	W
RU Cam	7 10.9	+69 51	7.8–9.0	Roe	+ .018 6	+ .002 5	.018	W
+22°1680	7 20.2	+22 5	9.8	R5	+ .017 6	− .019 6	.025	W
+24°1686	7 25.8	+24 44	8.2	R8	+ .004 4	− .002 4	.004	W
W CMi	7 43.4	+ 5 40	9.8–10.3	R8	− .010 10	− .013 8	.016	W
−17°1442	8 15.2	−17 57	9.3	R5	− .031 14	− .001 12	.031	KW
−29°6735	8 42.4	−29 21	7.6	R8	− .023 9	− .010 8	.025	B
+34°1929	8 53.6	+34 9	9.2	Ro	− .001 9	− .019 10	.019	W
+50°1603	8 56.2	+50 29	9.5	R5	+ .004 6	− .005 7	.006	W
+14°2048	9 8.3	+14 37	8.9	R5	− .006 9	− .016 7	.017	W
−13°3407	11 30.7	−14 2	8.7	Ro	− .009 8	− .034 8	.035	W
+38°2389	12 54.7	+38 20	9.2–9.6	R6p	− .004 7	− .019 6	.019	W
−24°12084	15 21.9	−24 49	7.4	R3	.000 10	− .025 9	.025	W
−66°2978	16 25.8	−66 55	8.2	Ro	+ .003 9	− .071 10	.071	K
−15°4923	18 13.6	−15 39	9.0–9.8	R5	− .027 8	− .010 7	.029	W
−29°15574	18 52.4	−29 38	9.3	R1	− .012 13	− .010 11	.016	KW
−10°5057	19 17.6	−10 54	7.0	Ro	+ .006 4	+ .006 4	.008	W
U Cyg	20 16.5	+47 35	6.1–11.8	R9†	− .010 7	− .003 6	.010	W
+20°5071	21 59.7	+20 34	8.8	R3	+ .010 7	− .005 7	.011	W
+ 5°5223	23 44.0	+ 5 50	8.7	R3	+0.009 ± 6	−0.010 ± 60	.013	W

*Authorities: B, Boss; K, Kapteyn and van Rhijn; Ly, Luyten; W, Wilson.
† Also classified as Nep.

half-weight. Weights based upon the probable errors were assigned as follows:

P.E.	Weight	Stars
0″.001–0″.005	1.5	3
.006– .010	1.0	21
.011– .012	0.7	1
0.013–0.015	0.5	3

The visual magnitudes are mostly from the *Henry Draper Catalogue*.

GROUP MOTION AND GALACTIC ROTATION

An analysis of the radial velocities by means of the well-known relation[6]

$$V = K + X \cos b \cos l + Y \cos b \sin l + Z \sin b + du + ev$$

gives the results shown in Table 2. Although little precision is to be expected from such an analysis based upon only 37 stars, the right ascension and declination of the group motion derived from l_a and b_a,

TABLE 2

RESULTS FROM RADIAL VELOCITIES

K	$+2.9 \pm 5.8$ km/sec	l_a	40°.6
X	$-13.4 \quad 6.6$	b_a	$+17.1$
Y	$-11.5 \quad 8.1$	V_0	18.5 ± 7.8 km/sec
Z	$-5.4 \quad 8.7$	l_0	338°
u	$+10.2 \quad 7.1$	$\bar{r}A$	13.9 ± 6.9 km/sec
v	-9.5 ± 6.7	θ	25.2 ± 2.1 km/sec

namely, $A_0 = 282°$, $D_0 = +44°$, agree well with values derived from the motions of other late-type giant stars. Further, the group motion, V_0, and the longitude, l_0, of the galactic center agree much better with the conventional values of these co-ordinates than was to be expected.

The corrections to the Newcomb precessions plus a constant rotation, as determined by Wilson and Raymond,[7] were applied to the proper motions, which were then analyzed by means of the simple relations

$$\mu_\alpha = X \sin \alpha - Y \cos \alpha ,$$

$$\mu_\delta = X \cos \alpha \sin \delta + Y \sin \alpha \sin \delta - Z \cos \delta .$$

The results are given in Table 3. In view of the small number of stars involved, the agreement between the two determinations of the apex of the group motion is good. The use of the conventional values of the solar motion co-ordinates ($A_0 = 270°$, $D_0 = +30°$, $V_0 = 20.0$ km/sec) and of the longitude of the galactic center ($l_0 = 326°$) for

[6] For the significance of the symbols here used see R. E. Wilson, *Mt. W. Contr.*, No. 604; *Ap. J.*, **89**, 218, 1939.

[7] *A.J.*, **47**, 57, 1938.

the computation of mean parallaxes appears to be justified. With these co-ordinates one finds

$$K = +\ 1.0 \pm 3.2 \text{ km/sec},$$

$$\bar{r}A = \ 13.3 \pm 5.5 \text{ km/sec},$$

$$\theta = \ 23.2 \pm 2.2 \text{ km/sec}.$$

Values of the mean apparent magnitude, the mean observed and true total proper motion, and their components in the direction of,

TABLE 3

RESULTS FROM PROPER MOTIONS

$100X$	$+0''.23 \pm 0''.19$	A_0	285°
$100Y$	$-\ .85 \quad .23$	D_0	$+32°$
$100Z$	$+0.55 \pm 0.21$	$100q$	$1''.04 \pm 0''.21$

and at right angles to, the apex, as derived from both unreduced and reduced proper motions, are given in Table 4.

TABLE 4

MEAN PROPER MOTIONS

	μ Observed	μ Reduced
m_{vis}	8.50	8.50
$100\ \bar{\mu}_{obs}$	$1''.92 \pm 0''.19$	$1''.96 \pm 0''.19$
$100\ \tau_{av}$	1.24 ± 0.12	1.25 ± 0.12
$100\ \bar{\rho}$	0.83	0.83
$100\ \eta$	0.98	0.98
$100\ \bar{\mu}$	$1''.65 \pm 0''.16$	$1''.70 \pm 0''.17$
$100\ \tau_0$	$0.74 \quad .12$	$0.77 \quad .12$
$100q$	0.94 ± 0.17	0.86 ± 0.17

MEAN PARALLAX

Values of the mean parallax obtained by the relations

$$\pi_q = \frac{kq}{V_0}, \tag{1}$$

$$\pi_q = \frac{\sum(A\mu_\alpha + B\mu_\delta)}{\sum(A^2 + B^2)},^{8} \tag{2}$$

$$\pi_\tau = \frac{k\tau_0}{\theta}, \tag{3}$$

[8] G. Strömberg, *Mt. W. Contr.*, No. 558; *Ap. J.*, **84**, 555, 1936.

are given in Table 5. The relative weights of π_q and π_r, computed from the probable errors and by means of Russell's criterion,[9] are the

TABLE 5

MEAN PARALLAX

	μ Observed	μ Reduced	Relative Weight
(1)	$0''.00223 \pm 40$	$0''.00204 \pm 40$	1.0
(2)	.00216 40	.00218 40	1.0
(3)	.00152 24	.00158 24	2.8
$\bar{\pi}$	0.00180 ± 18	0.00180 ± 18	.....

same, namely, 1.0 and 2.8. The weighted mean values from the unreduced and the reduced proper motions are identical, namely,

$$\bar{\pi} = 0''.00180 \pm 18 .$$

MEAN ABSOLUTE MAGNITUDE

Values of the mean absolute magnitude may now be computed for the proper-motion stars from the mean parallax, and for the radial-velocity stars from the value of $\bar{r}A$, by means of the relations

$$M_\pi = \bar{m}_1 + 5 + 5 \log \bar{\pi} + 5C_1 - \frac{ac}{1000\,\bar{\pi}} ,$$

$$M_r = \bar{m}_2 + 5 - 5 \log \bar{r} - 5C_2 - \frac{a\bar{r}}{1000} ,$$

where

$$C_1 = \overline{\log \pi} - \log \bar{\pi} , \text{ and } C_2 = \overline{\log r} - \log \bar{r} ,$$

and a represents the absorption of visual light in magnitudes per kiloparsec. Since the R stars are well scattered over the sky, showing comparatively little concentration toward the galaxy, the effect of visual absorption cannot exceed a few hundredths of a magnitude and so may be neglected.

[9] *Mt. W. Contr.*, No. 215; *Ap. J.*, **54**, 142, 1921.

The data are

$$\bar{m}_1 = 8.50 \qquad \bar{\pi} = 0''.00180 \pm 18$$
$$\bar{m}_2 = 8.88 \qquad \bar{r}A = 13.3 \pm 5.5 \text{ km/sec}$$

Adopting for A the value 15.5 km/sec kpc,[10] one finds from $\bar{r}A$

$$\bar{r} = 0.86 \pm 0.35 \text{ kpc} .$$

With these values

$$M_\pi = \underset{\pm 0.22}{-0.22} + 5C_1 ,$$
$$M_r = \underset{\pm 0.94}{-0.79} - 5C_2 .$$

Since C_1 and C_2 are negative and in general nearly equal,[11] a fair approximation to the mean absolute magnitude is given by the assumption that $C_1 = C_2$, whence

$$\bar{M} = -0.50 \pm 0.20 .$$

To fulfil the condition, $M_\pi = M_r$, $C_1 = C_2 = -0.057$; and since $\log c = -(C_1 + C_2)$, $c = \bar{\pi} \cdot \bar{r} = 1.30$. If the distribution of $\log \pi$ is Gaussian, its dispersion is

$$\sigma_{\log \pi} = \pm 0.222 .$$

MEAN ABSOLUTE MAGNITUDES OF SUBGROUPS

The small amount of data available for the determination of $\bar{M}$ for all the stars makes impracticable attempts to estimate $\bar{M}$ for subdivisions according to characteristics such as type or variability, except possibly in one case, where a fairly equal division of the material may be made. The spectral types of 11 stars are classified as earlier than R5, while 16 of them are R5 or later. The data for these two groups were examined to see if there might be any evidence of a difference in $\bar{M}$. The results are shown in Table 6. As far as one may

[10] Plaskett and Pearce, *Pub. Dom. Ap. Obs.*, **5**, 167, 1933.

[11] R. E. Wilson, *Mt. W. Contr.*, No. 615; *Ap. J.*, **90**, 352, 1939.

judge from so few stars, there is no material change in $\bar{M}$ with type among the R stars.

TABLE 6

COMPUTATION OF $\bar{M}$ FOR EARLY AND LATE R TYPES

	R0–R4		R5–R8	
	μ Observed	μ Reduced	μ Observed	μ Reduced
m_{vis}	8.45	8.50	8.53	8.50
$100\,\bar{\mu}_{obs}$	1".92 ± 0".30	2".09 ± 0".32	1".92 ± 0".25	1".91 ± 0".24
$100\,\tau_{av}$	1.20 .19	1.18 .18	1.25 .16	1.31 .17
$100\,\bar{\mu}$	1.65 .25	1.85 .28	1.65 .21	1.64 .21
$100\,\tau_0$	0.69 .19	0.66 .18	0.78 .16	0.93 .17
$100q$	0.97 ± 0.31	0.92 ± 0.31	0.90 ± 0.28	0.82 ± 0.28
π_q (1)	0".0023	0".0022	0".0021	0".0019
π_q (2)	.0031	.0030	.0015	.0016
π_τ (3)	.0014	.0013	.0016	.0019
$\bar{\pi}$	0.0019	0.0018	0.0017	0.0018
M_π	−0.1	−0.2	−0.3	−0.2
$\bar{M}$	−0.4	−0.5	−0.6	−0.5

On the supposition that their individual absolute magnitudes are equal to the mean determined above, the parallaxes and the co-ordinates of space motion of the two high-velocity R stars are:

Star	π	A	D	V
BD+23°123	0".0014	127°	− 9°	529 km/sec
BD+20°5071	0.0014	147	−17	372

These stars, therefore, follow the asymmetric drift shown by the high-velocity stars in general.

CARNEGIE INSTITUTION OF WASHINGTON
MOUNT WILSON OBSERVATORY
August 1939

SPECTRA OF M SUPERGIANT STARS*

LYMAN SPITZER, JR.[1]

ABSTRACT

High-dispersion spectral plates of the late supergiant stars α Orionis and α Herculis have been reduced in the region λλ 4000–4300, and the line profiles measured for five multiplets of neutral iron and one of manganese. Approximate determinations of the energy distribution in the continuous background over this range and of the appropriate correction for finite resolving-power allow a reduction of the apparent relative intensities to true absolute intensities. A determination of the variation of a_λ, the atomic absorption coefficient, with increasing distance from the line center λ_0, shows that a_λ is given by the usual radiation-damping formula with a damping constant some five hundred times the classical value. For the greater widths shown by the *Na* lines, however, a_λ falls off much more rapidly than $(\lambda - \lambda_0)^{-2}$. These results are attributed to a turbulent distribution of velocities. Different properties of the atmosphere of α Orionis correspond to temperatures which range from 2100° for the excitation temperature, to 17,000° derived from the energy density of L_α radiation, and up to 200,000° for the value derived from the magnitude of the observed velocities. The evidence suggests that the atmospheres of these two stars are characterized by an almost complete lack of thermodynamic equilibrium.

Examination of these and other spectral plates of the stars α Orionis, α Scorpii, α Herculis, β Pegasi, β Andromedae, α Boötis, and α Tauri reveals asymmetries in the strong ultimate lines for the first three stars, the most extended of the seven. The general appearance is that of a wide line at the expected position, blended with a narrow, deep component a tenth of an angstrom or so to the violet. The asymmetry is attributed to a thin shell of outward-moving atoms; these absorb radiation from the violet side of the normal symmetrical lines which are formed by the underlying stationary reversing layer. The measurements indicate velocities for this shell ranging from 4 to 40 km/sec. An ionization cycle is suggested in which neutral atoms leave the surface, possibly accelerated by radiation pressure, and then become ionized and return to the star under the force of gravity. It is shown that such a cycle will operate only if the number of free electrons in the shell is less than $5 \cdot 10^6$ per cm^3 and if the intensity of the ionizing radiation is also restricted—for *Na* atoms this must be less than the equilibrium intensity at 3100°.

Previous spectrophotometric investigations of late supergiant stars have been largely confined to visual estimates.[2] The most important work of this type is probably that of Adams and Russell,[3] who used their calibration of the Rowland scale to determine stellar excitation temperatures. The great strength of the enhanced lines in

* *Contributions from the Mount Wilson Observatory, Carnegie Institution of Washington*, No. 619.

[1] This work was revised and prepared for publication while the author was holding a National Research Fellowship.

[2] F. E. Baxandall, *M.N.*, **86**, 524, 1926; F. E. Baxandall and F. J. M. Stratton, *Observatory*, **52**, 148, 1929; D. H. Menzel, *Harvard Circ.*, No. 258, 1924; L. H. Aller and L. G. Stoddard, *Ap. J.*, **87**, 53, 1938.

[3] *Mt. W. Contr.*, No. 359; *Ap. J.*, **68**, 9, 1928.

α Orionis and α Scorpii led them to suggest that these supergiants are surrounded by vastly distended envelopes, supported by radiation pressure. Research with calibrated plates has been carried through by Miss Payne;[4] more recently Wilson and Merrill[5] have found marked deviations from the square-root law for the *Ca* II infrared triplet in α Orionis and α Scorpii.

It is well known that both the radial velocities and the luminosities of the M supergiants fluctuate irregularly. Measurements at Mount Wilson also indicate[6] that lines of lower excitation potential are systematically displaced toward the violet relative to those of higher excitation potential, the effect amounting to as much as 5 km/sec for the strong ultimate lines. The double or asymmetrical nature of many of the strong ultimate lines has also been pointed out.[7]

The Mount Wilson high-dispersion plates make possible a quantitative examination of these spectra. In sections I–IV below, the observational data for the measured multiplet lines in α Orionis and α Herculis are given. Section I includes a description of the plates, the tracings, and the resolving-power corrections. Section II presents the observational data for the color gradient of the continuous background from λ 4000 to λ 4300. The measurements of line widths and intensities are given in section III; the analysis of these data in terms of width- and depth-curves for each multiplet is presented in section IV. The evidence for line asymmetries is discussed in section V. Section VI presents a theoretical discussion of the preceding sections, together with certain deductions as to the structure of these supergiant atmospheres.

I

Spectrograms covering the region λλ 3900–4600 were available for the giant stars α Orionis, α Scorpii, α Herculis, α Boötis, β Pegasi, β Andromedae, and α Tauri. For the first four stars additional plates extended the interval to λ 8000. These plates were all taken at the

[4] C. H. Payne and F. S. Hogg, *Harvard Circ.*, Nos. 300–307, 1927.

[5] *Mt. W. Contr.*, No. 575; *Ap. J.*, **86**, 162, 1937.

[6] C. E. St. John and W. S. Adams, *Mt. W. Contr.*, No. 279; *Ap. J.*, **60**, 43, 1924; R. A. Sanford and W. S. Adams, *Pub. A.S.P.*, **42**, 255, 1930; W. S. Adams and Miss E. MacCormack, *Mt. W. Contr.*, No. 505; *Ap. J.*, **81**, 119, 1935.

[7] Adams and Miss MacCormack, *loc. cit.*; W. S. Adams, *Pub. A.S.P.*, **49**, 156, 1937.

coudé focus of the 100-inch telescope, mostly with a 9-foot grating spectrograph. The dispersion amounts to some 3 A/mm in the second order (blue plates) and to 6 A/mm in the first order (red plates).

Selected tracings of the calibrated plates were reduced in the usual manner.[8] The continuous background does not exist in the usual sense (see tracings in Fig. 1); an effective background was determined from the points of highest intensity in each interval of 15–20 A. The moderately smooth curve thus found was taken as the continuous background in terms of which other intensities were measured.

To correct the observed central intensities for finite resolving-power it is customary to assume some standard shape both for the true line contours and for the instrumental profile. Since a dispersion-curve is the obvious form to assume for the instrumental profile, we shall also use it for the spectral lines, a procedure practically equivalent to assuming that the lines have exponential contours. For if x represents the wave-length distance $\lambda - \lambda_0$ from the line center λ_0 (x expressed, in general, in millimeters on the microphotometer tracing), then for $x < b$ the dispersion-curve $b^2/(b^2 + x^2)$ is virtually indistinguishable from the contour $\exp[-(x/b)^2]$. Values of $x > b$ correspond to the line wings, which in these late supergiant spectra are completely drowned out in a sea of blends.

With these assumptions the formula connecting s_0, the apparent relative intensity at λ_0, the line center, with r_0, the true central intensity, becomes very simple. The half-width of a dispersion-curve $y = (b^2 + x^2)^{-1}$ is defined as the distance across the profile when y has one-half its value for $x = 0$ and is thus equal to $2b$. Let the half-widths of the profiles assumed for the spectrograph, the true or actual line, and the apparent or observed line be $2b_0$, $2b_1$, and $2b_2$, respectively. Then from the integral equation relating observed to true intensity it follows directly that

$$r_0 = \frac{s_0 - \dfrac{b_0}{b_2}}{1 - \dfrac{b_0}{b_2}}, \tag{1}$$

$$b_1 = b_2 - b_0 . \tag{2}$$

[8] E. G. Williams, *Mt. W. Contr.*, Nos. 487, 541; *Ap. J.*, **79**, 280, 1934; **83**, 279, 1936.

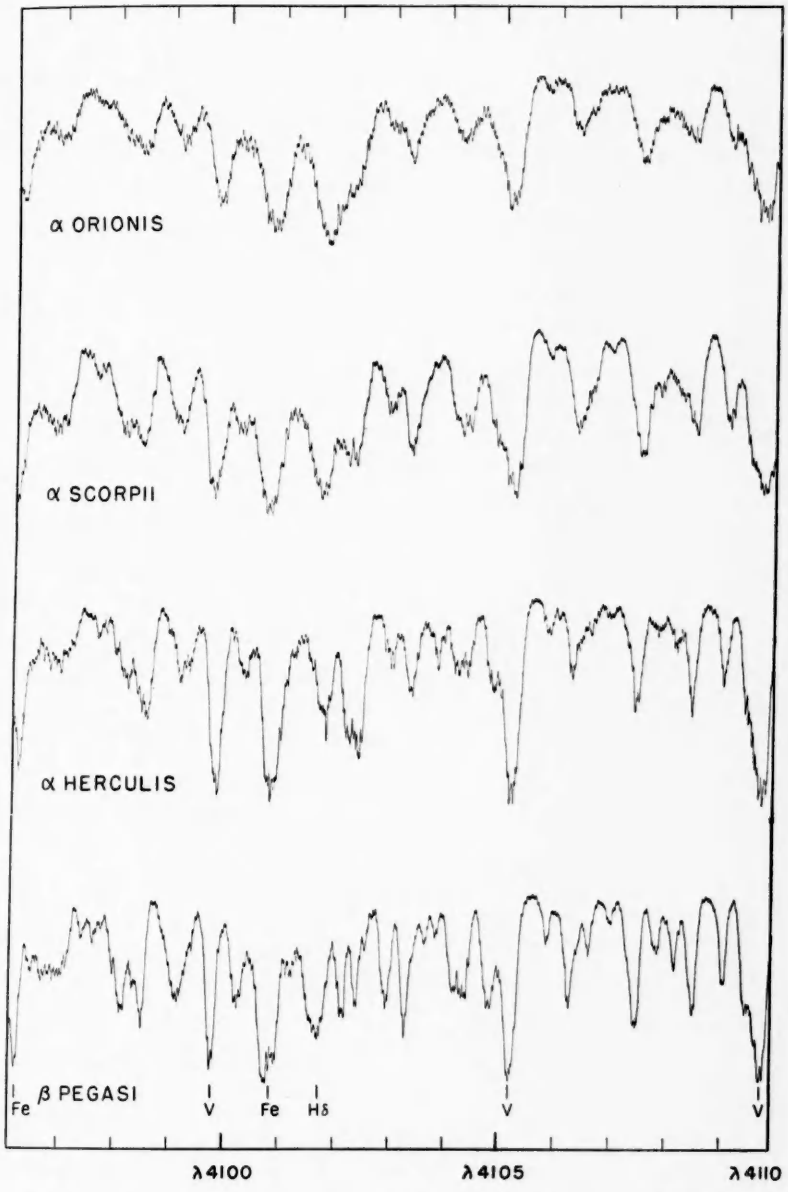

FIG. 1.—Microphotometer tracings on a uniform scale of four M supergiant stars

The most doubtful assumption made in deriving these formulae is that a uniform continuous background exists, or that the intensity outside the line is everywhere equal to the adopted intensity of the continuous background. The error so introduced may be found by calculating s_0 when the continuous background is uniformly reduced, the line core remaining unchanged. If we set $b_0/b_2 = 0.1$ and reduce the continuous background by half the depth of the line, then the correction $r_0 - s_0$ calculated from (1) will be 25 per cent too large in absolute value. This, for α Orionis at least, is an extreme case; and since $s_0 - r_0$ rarely exceeds 0.10 in this star, the error in r_0 produced by this cause will not be greater than 0.025 of the continuous background. For α Herculis, on the other hand, this error may be as great as 0.04.

The constant b_0 may be determined from lines of known r_0. First, there are 17 lines in the region $\lambda\lambda$ 4282–4298 whose central intensities have been given by C. W. Allen[9] and for which tracings were available from a Mount Wilson lunar plate. Second, there are the strong lines in the spectrum of α Boötis which have presumably very low central intensities. If $2b_2$, the apparent half-width, is determined for each line by methods to be discussed in section III, then we have the following values for $2b_0$:

1. From the solar lines, with Allen's values for r_0,

$$2b_0 = 0.086 \pm 0.017 \text{ A} ;$$

2. From the solar lines, with r_0 set equal to zero,

$$2b_0 = 0.115 \pm 0.025 \text{ A} ;$$

3. From 31 lines in the spectrum of α Boötis around λ 4400, with r_0 set equal to zero,

$$2b_0 = 0.090 \pm 0.017 \text{ A} ;$$

4. From the 13 of the foregoing lines that are stronger than 3 on the Rowland scale or that have excitation potentials of less than 0.4 e.v.,

$$2b_0 = 0.078 \pm 0.012 \text{ A} .$$

[9] *Mem. Commonwealth Solar Obs., Canberra*, 1, No. 5, Part II, p. 10, 1934.

The errors are average deviations (A.D.), which are used throughout. The second value is presumably of little significance and is given simply for comparison with the first, since Allen's values are thought[10] to be undercorrected.

It would be possible to determine $2b_0$ accurately from the apparent profiles of the Fraunhofer lines of known true profile; but since the "effective" b_0, chosen to make (1) correct, is likely to be different from the true b_0, it is scarcely worth while to carry out the extensive numerical integrations which this method would demand. It is not difficult to show, however, that the foregoing values are consistent with R. O. Redman's[11] data on the solar profile of λ 4227. A half-width between 0.09 and 0.10 A seems indicated by this method, provided that a 3 per cent correction for scattered light is made. No correction for scattered light is made in the rest of the work, however, since this would not affect the final interpretation of the results.

For the best value of $2b_0$ one may take 0.087 A. This is probably somewhat large. As will appear in section IV, however, it is less misleading to overcorrect than to undercorrect for finite resolving-power. In any case the scatter of b_0 from line to line with changes in individual profiles, adjacent lines, etc., will be at least as great as the statistical error in the assumed b_0. For extended wave-length regions, b_0 must be taken proportional to λ, but within the range λλ 4000–4345 it may legitimately be assumed constant.

II

From the standpoint of theory it is important to know the intensity of the continuous background, which may be denoted by $J_{c\lambda}$. For these late supergiants, $J_{c\lambda}$ has not the direct significance that it has for the earlier-type stars; the actual intensity averaged over a wave-length interval of several angstroms will rarely exceed half the so-called "continuous background" for α Orionis, the extreme case. Nevertheless, this average intensity does change with wave length, and $J_{c\lambda}$ is a useful function to characterize this change.

The determination of this function over extended wave-length regions presents many difficulties. For a range as short as 300 A, how-

[10] *Mt. W. Contr.*, No. 567; *Ap. J.*, **85**, 165, 1937.

[11] *M.N.*, **95**, 742, 1935.

ever, the problem is much simpler. The spectra of α Orionis and α Herculis were photographed on Eastman 40 and Cramer Hi-Speed plates, respectively, which in general vary in sensitivity by less than 15 per cent over the range λλ 4000–4345. The correction for atmospheric extinction is not large and may be approximately calculated from C. G. Abbot's[12] values for the mean coefficient of atmospheric absorption at Mount Wilson (1909–1910); the zenith distance of the star may be taken as equal to its value at mid-exposure. If the differential color sensitivity of the plates is neglected and Abbot's daytime values are taken for the atmospheric absorption, $J_{c\lambda}$ may then be determined directly from the reduced tracings.

In general this method would not be useful, since the errors involved are large. But here the change in $J_{c\lambda}$ is so unusually rapid that even this relatively crude method gives valuable results. To check the method one may determine $J_{c\lambda}$ for the sun from the lunar plates, which are also Eastman 40's and were taken with comparable exposure times. The result may then be compared with Abbot's[13] determination of $J_{c\lambda}$ for integrated solar radiation, since one may expect the albedo of the moon to change but little over the relevant range.

The resultant values of log $J_{c\lambda}$ (to the base 10) for the moon, α Orionis, and α Herculis are plotted in Figure 2. The distance between the values of $J_{c\lambda}$ for the lunar spectrum found by this method and the upper dashed line representing Abbot's values gives the logarithm of the correction for change in plate sensitivity with wave length, etc. The correction is clearly negligible. For α Orionis only the values of $J_{c\lambda}$ taken from the smoothed curve drawn on the tracings are shown. For α Herculis, however, the occasional high intensities which determine the continuous background are all represented by dots in Figure 2, giving some idea of the scatter involved. The absorption line λ 4227 is included for α Herculis since its wings are very broad, extending over several of the measured *Fe* multiplets. The higher intensities in the spectrum of α Herculis fall on the nearly flat section of the characteristic curve and are therefore poorly determined.

When this work had bee n completed, the data of Kienle, Strassl,

[12] *Ann. Astrophysical Obs. Smithsonian Inst.*, **3**, 198, 1913. [13] *Ibid.*, p. 197.

and Wempe[14] on the continuous energy distribution of various stars appeared in print. The results obtained for β Pegasi from each of

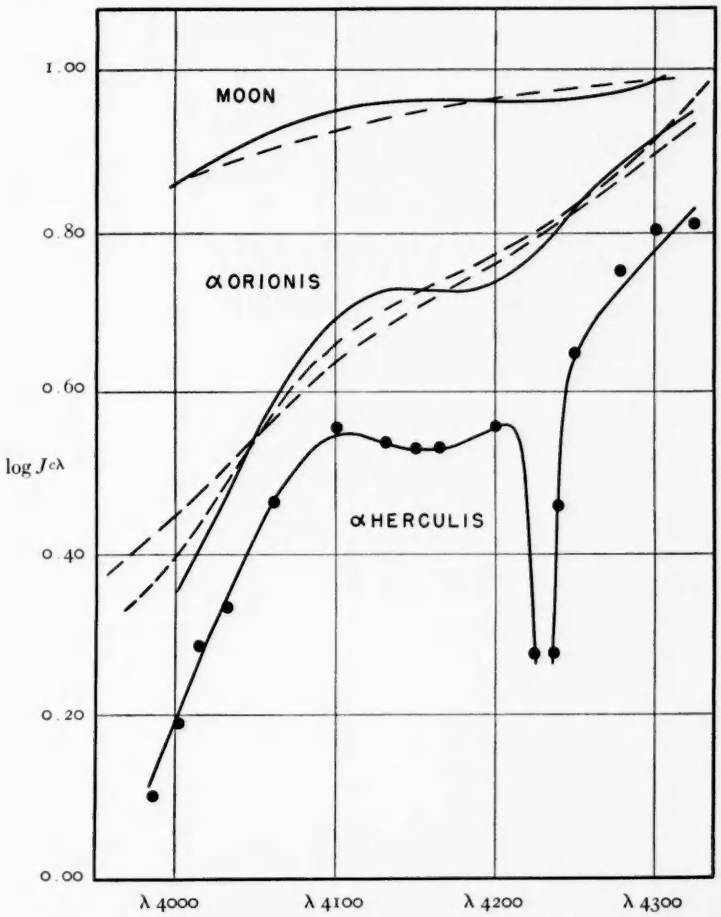

FIG. 2.—Full-line curves represent log $J_{c\lambda}$, the intensity of the continuous spectrum, for the moon, α Orionis, and α Herculis. Upper dashed curve, Abbot's determination of energy distribution of integrated sunlight; lower two curves, the data of Kienle, Strassl, and Wempe for β Pegasi, on the assumption that for Ao stars $J_{c\lambda}$ in this spectral region is constant.

their two spectrographs (S and T) are shown by the lower pair of dashed lines in Figure 2, where it has been assumed that $J_{c\lambda}$ is con-

[14] *Zs. f. Ap.*, **16**, 201, 1938.

stant for their standard of reference, the Ao stars. An assumed temperature of 14,000° for the reference stars would make little change in the appearance of the curves and would improve the agreement between the T-curve and that for α Orionis. Except for the depth of the depression at λ 4160, which may be a feature of only the most extended stars, there is remarkably good agreement between the values for α Orionis and those for β Pegasi. Since the spectral type and effective temperature of these two stars is the same, $J_{e\lambda}$ should be roughly the same for both. The values in Figure 2 may hence be used with confidence and are probably not in error by more than 25 per cent.

The investigations of H. Jensen,[15] on the other hand, are in serious disagreement with the foregoing results. For α Orionis he finds that the ratio of intensities relative to Polaris at λ 4300 and λ 4000 is 2.1 (from his Fig. 1), corresponding to a color temperature of some 2200° for this wave-length range, that for Polaris being taken as 7000°. The ratio found here, however, is 3.7, corresponding to a color temperature of 1500°. Jensen's results may possibly be explained by a change of the gradient of $J_{e\lambda}$ with time, since the factors determining the background intensity might well be expected to change with the pulsations of the star.

III

Quantitative measurements of the intensities of multiplet lines were restricted to α Orionis and α Herculis in the region $\lambda\lambda$ 4000–4345. Several strong, relatively unblended multiplets of neutral iron occur in this range, three of which have the further advantage that their relative $g \cdot f$ values have been accurately measured by R. B. and A. S. King.[16] Another *Fe* multiplet, with an excitation potential of 1 e.v., was also found to be relatively unblended and was included in the measurements. To examine lines from more highly excited states was also desirable. An *Fe* and a *Mn* multiplet, with excitation potentials of 2.5 and 2.0 e.v., respectively, were found to contain the most nearly unblended of such lines and were also included. For α Orionis the Balmer lines and one multiplet each of *Co*, *V*, and *Sc* II were added. Only one plate for each star was used for these measurements.

[15] *A.N.*, **248**, 217, 1933. [16] *Mt. W. Contr.*, No. 581; *Ap. J.*, **87**, 24, 1938.

It is evident from Figure 1 that the wings of all lines are so completely blended that individual equivalent widths, which depend largely on the extent of the line wings, cannot be determined here. It is therefore necessary to measure instead the actual line profiles or, more simply, the central intensities and the line widths for various intensities. The resolving-power of the spectrograph is fortunately great enough to make this procedure possible.

For each line a dispersion contour of the type discussed in section I was assumed so that the resolving-power correction could first be calculated. If we assume for s, the apparent intensity relative to the continuous background $J_{c\lambda}$,

$$s = 1 - \frac{1 - s_0}{1 + \left(\frac{x}{b_2}\right)^2}, \tag{3}$$

where s_0 is again the apparent central intensity, and x is the distance $\lambda - \lambda_0$ from the line center λ_0, then for an x such that

$$1 - s = L(1 - s_0), \tag{4}$$

we find

$$b_2 = \left(\frac{L}{1 - L}\right)^{1/2} x. \tag{5}$$

If the value of x corresponding to $L = 0.9$ be denoted by x', then $b_2 = 3x'$. The quantity $2x'$ may be measured in the unblended line core, since it is simply the total width of the line at an intensity one-tenth of the way from the lowest point in the line up to the continuous spectrum, an intensity which will be denoted by s'; by analogy with the half-width $2b_2$, we may thus refer to $2x'$ as the tenth-width. Since presence of blends makes it quite impossible to measure $2b_2$ directly for most lines, $2x'$ is a more convenient observational quantity.

Similarly, one may define a two-tenths width $2x''$ as the width of the line for $1 - s = 0.8(1 - s_0)$. The three-tenths width $2x'''$ corresponds to a value of s given by L equal to 0.7 in (4). The ratios x''/x' and x'''/x'' should equal 1.5 and $2(21)^{1/2}/7$, or 1.309, respectively, if the assumption of the contour (3) is justified.

The procedure for each line is first to determine s_0, the minimum

intensity of the line, directly from the reduced tracing, interpolating visually between the lines of constant intensity drawn on the tracings at intervals of 10 per cent or less. Then s', s'', and s''' are calculated from (4) with L equal to 0.9, 0.8, and 0.7, respectively. At each of these intensities the corresponding width of the line is measured, giving $2x'$, $2x''$, and $2x'''$. Finally, b_2 is set equal to $3x'$ and r_0 found from (1), with $2b_0$ taken equal to 0.087 A. Measurements of $2x'''$ were omitted for α Herculis.

These data for the two stars are given in Table 1. The first column lists the multiplets and their approximate average excitation potential, the second, the J-values for the lower and upper states, respectively, of each atomic transition, while the third column gives the wave length of the resultant line. For convenience the *Fe* multiplets are numbered in the order of increasing E.P.

The values of $g \cdot f$, the weighted oscillator strength of the line, in the fourth column, are taken largely from Miss Moore's *Multiplet Table*.[17] For the first, third, and fourth iron multiplets, however, the values are the Kings' quantitative measurements of laboratory absorption-line intensities derived from the linear portion of the curve of growth. For certain lines in these multiplets the intensities were too low to be measured accurately by this method. Visual estimates reduced to the same scale are given in parentheses for such lines. For three *Fe* lines no reliable intensity estimates were available, and the $g \cdot f$ values were accordingly found in a rough way from the Rowland intensities of the lines. Such values are followed by question marks. For the *Mn* multiplet, A. S. King's[18] arc intensity estimates are used except for λ 4041.4 and λ 4082.9, for which these values differ by more than one unit from the average of his arc, high-temperature furnace, and medium-temperature furnace intensities; for these two lines this average is taken instead.

In the remaining columns, containing the observed data, the upper figures for each line refer to α Orionis, the lower to α Herculis. The fifth column gives the apparent central intensity relative to $J_{c\lambda}$, the continuous background at that point, values for which may be found from Figure 2. The tenth-width $2x'$ in the sixth column is

[17] *A Multiplet Table of Astrophysical Interest*, Princeton, 1933.

[18] *Mt. W. Contr.*, No. 198; *Ap. J.*, **53**, 133, 1921.

TABLE 1

MULTIPLET LINES—WIDTHS AND CENTRAL INTENSITIES

Multiplet	$J-J$	λ	$g \cdot f$	s_0	$2x'$	x''/x'	x'''/x''	r_0
H	*Hδ*	4101.8	0.022	0.18	10.1	—	—	0.13
Balmer series	*Hγ*	4340.5	0.045	.12	12.2	1.26*	—	.077
E.P. = 10.2	*Hβ*	4861.3	0.119	.10?	11.3	1.47	1.22	.050?
	Hα	6562.8	0.641	.20	.....	.....	.....	.....
Fe 1	4–3	4134.3	(0.20)	.12	8.4	1.36	1.19*	.059
$a^5D - z^7P^o$				.15	6.8	1.12*	.....	.067
E.P. = 0	3–2	4149.8	0.15?	.17	6.2	1.61	—	.085
				.20	3.4	1.36	.....	.039
	2–2	4200.0	(0.20)	.18	6.1	1.34	1.27	.094
				.15	5.2	1.28	.....	.044
	3–3	4206.7	0.60	.13	7.1	1.38	1.29	.054
				.15	5.4	—	.....	.045
	4–4	4216.2	2.14	.10	7.0?	1.54*	1.12*	.019?
				.084	6.0	1.20*	.....	− .012
	1–2	4232.7	(0.20)	.14	7.1	1.39	1.37	.065
				.23	5.2	1.44	.....	.13
	2–3	4258.3	0.38	.11	7.9	1.47	1.20	.041
				.15	5.8	1.26	.....	.050
	3–4	4291.5	0.45	.075	10.2	1.45	1.18*	.020
				.047	6.6	1.38*	.....	− .042
Fe 2	3–2	4172.8	4	.25	6.4	1.52	—	.18
$a^5F - z^5D^o$				.16	3.9	1.38	.....	.017
E.P. = 1.0	2–1	4173.9	2	.24	7.2	1.48	—	.18
				.17	5.9	1.22	.....	.078
	4–3	4174.9	5	.26	6.4	1.38	—	.19
				.16	3.6	1.44	.....	.004
	1–1	4203.6	1	.33	4.9	1.47	—	.22
				.23	2.3	1.53	.....	− .027
	3–3	4237.1	0.5?	.29	4.4	1.34	—	.18
				.30	2.8	1.30	.....	.13
	1–2	4248.4	0.5?	.31	5.1	1.43	—	.22
				> .29	1.8*	—	.....	> .11
Fe 3	3–2	4005.3	1200	.23?	8.5?	1.47	—	.17?
$a^3F - y^3F^o$				.25	5.1	1.49*	.....	.16
E.P. = 1.5	4–4	4045.8	6000	.15	11.8	1.19	1.39	.11
				.13	9.8	1.39*	.....	.076
	3–3	4063.6	4300	.18	9.4	—	—	.13
				.14	7.2	1.79	.....	.062
	2–2	4071.8	3800	.18	8.6	1.24	1.36	.12
				.14	7.4	1.47	.....	.065
	2–3	4132.1	1100	.19	8.5	1.43	1.28	.13
				.18	7.4	1.25	.....	.11
	3–4	4143.9	1400	.19	11.0	1.27*	—	.15
				.15	5.7	1.43	.....	.050
Fe 4	4–3	4147.7	(350)	.23	5.6	1.41	1.25	.14
$a^3F - z^3G^o$				.20?	3.5?	1.44	.....	< .033
E.P. = 1.5	4–4	4202.0	890	.30	9.4	1.29	1.22	.26
				0.23	4.9	1.37	.....	0.12

TABLE 1—*Continued*

Multiplet	$J-J$	λ	$g \cdot f$	s_0	$2x'$	x''/x'	x'''/x''	r_0
	3–3	4250.8	880	0.13	8.8	1.52	—	0.069
				.16	5.1	1.38	.....	.049
	4–5	4271.8	2450	.10	10.0	1.52*	—	.046
				.10	8.3	1.38	.....	.037
	3–4	4307.9	3300	.28	—	—	—	.24
				.19	—	—	.....	.14
	2–3	4325.8	3800	.09	12.4	—	—	.047
				—	—	—	.....	—
Fe 5	3–2	4187.0	20	.31	6.9*	1.41	—	.25
$z^7D^o - e^7D$				.28	3.5	1.30*	.....	.14
E.P. = 2.5	4–3	4187.8	20	.38	6.7*	—	—	.35a
				.29	3.2	1.31*	.....	.14
	2–1	4191.4	15	.38	6.4*	—	—	.33a
				.25	4.1*	—	.....	.15
	5–4	4198.3	20	.36	8.4*	1.12?	—	.33
				.23	4.7*	—	.....	.13
	1–1	4210.3	15	.41	4.9	1.33	1.20	.33
				.34	3.1	1.54	.....	.18
	3–3	4222.2	12	.36	5.0*	—	—	.33a
				.52	3.1?	—	.....	.42
	1–2	4233.6	18	.27	4.0?	—	—	.21?a
				.39	4.9?	—	.....	.30
	4–4	4236.0	25	.28	7.1	1.52	1.24	.22
				.29	4.7	1.47	.....	.19
	2–3	4250.1	25	.23	6.0*	—	—	.20a
				.25	3.7	1.28*	.....	.10
	5–5	4260.5	35	.24	11.0	1.36	1.22	.20
				.19	4.7	1.38*	.....	.071
	3–4	4271.2	20	.19	7.4*	—	—	.19b
				.20	3.5	1.42*	.....	.048
Mn	$4\frac{1}{2}-3\frac{1}{2}$	4018.1	20	.37	5.2*	1.38	—	.30
$a^6D - z^6D^o$				.34	2.8*	1.1?	.....	.24
E.P. = 2.0	$3\frac{1}{2}-2\frac{1}{2}$	4035.7	15	.30	5.1*	1.50	—	.21
				.24	2.9*	1.45	.....	.13
	$4\frac{1}{2}-4\frac{1}{2}$	4041.4	38	.27	7.0	1.53	—	.20
				.24	3.6	1.46	.....	.097
	$2\frac{1}{2}-1\frac{1}{2}$	4048.8	15	.33	4.4	1.55	1.36	.23
				.24	3.6*	1.20	.....	.15
	$3\frac{1}{2}-3\frac{1}{2}$	4055.6	20	.34	4.4?	1.60	—	.24
				.24	2.7	1.45	.....	.034
	$1\frac{1}{2}-\frac{1}{2}$	4058.9	10	.38	4.4*	—	—	.33a
				.24	2.6*	1.25	.....	.18
	$\frac{1}{2}-\frac{1}{2}$	4070.3	5	.48	4.3*	1.32	—	.42
				.39	2.3	1.44	.....	.23
	$3\frac{1}{2}-4\frac{1}{2}$	4079.2	12	.30	—	—	—	.27a
	$\frac{1}{2}-1\frac{1}{2}$	4079.4	10	.26	—	—	.....	.18
	$1\frac{1}{2}-2\frac{1}{2}$	4082.9	14	.30	5.6	—	—	.26a
				.26	2.4	1.50	.....	.021
Sc II	4–3	4314.1	30	.20	9.2	1.31*	1.24*	.17a
$a^3F - z^3D^o$	3–2	4320.8	20	.22	6.4	1.72*	—	.15
E.P. = 0.6	2–1	4325.0	20	0.21	7.6	1.63*	—	0.17a

TABLE 1—*Continued*

Multiplet	$J-J$	λ	$g \cdot f$	s_0	$2x'$	x''/x'	x'''/x''	r_0
V	$1\frac{1}{2}-1\frac{1}{2}$	4330.0	30	0.28	7.3	1.34	—	0.22
$a^4F-z^4F^o$	$2\frac{1}{2}-2\frac{1}{2}$	4332.8	30	.28	5.6	1.48	1.34	.20
E.P.=0	$3\frac{1}{2}-3\frac{1}{2}$	4341.0	40	.18	7.6	1.74*	—	.18b
Co	$4\frac{1}{2}-4\frac{1}{2}$	4190.7	20	.26	6.2	1.35	1.18	.18
$a^4F-z^6F^o$	$3\frac{1}{2}-3\frac{1}{2}$	4252.3	12	0.29	5.8	1.50	—	0.21
E.P.=0								

defined above. The unit is 1 mm on the tracing, the equivalent of 0.051 A. Some of the values of $2x'$ for α Herculis were originally measured at excessive values of s, owing to a mistaken value of $J_{c\lambda}$. They have been corrected slightly on the basis of the dispersion-curve contours discussed below. The seventh and eighth columns give the ratios of x''/x' and, for α Orionis, of x'''/x''. Finally, in the last column, are the values of the true central intensity for each line, derived from formula (1). The quantity b_2 occurring in (1) is set equal to $3x'$ from (5). The third decimal place, given when r_0 is less than 0.10, is clearly of little significance and is inserted simply as a guard figure.

Several lines, particularly those of higher excitation potential, are blended on one side or another. If the blend does not extend to the core, the mid-point of the line is taken to be the frequency about which the core is symmetrical, and width measurements are made from this central wave length λ_0 to the unblended wing (and then, of course, doubled). The corresponding values of x''/x' and x'''/x'' are denoted with an asterisk.

If the value of $2x'$ is so marked, the line possesses no unblended core at all, and the appearance of the blend on the tracing is that of a single line. The true center of such lines was found with the aid of the lunar tracing, which was placed so that the cores of the unblended lines of the same multiplet coincided. To determine $2x'$, width measurements were then made from this line center to the nearest wing. Such results have some value only if it can be assumed that each wing is formed primarily by a single one of the two blended components. The resolving-power correction is found not from the $2x'$ so determined but rather from the directly measured width of the

blended combination of lines. This quantity was also measured for such cases but is not given in Table 1. The ratio x''/x' for such lines, however, if it is given at all, does refer to the directly measured widths of the apparent line, the presence of blends being disregarded.

For lines closely blended but still separate, a somewhat arbitrary resolving-power correction may be made. For closely blended lines of equal strength (*a*), one-half the usual correction (1) is used; for a weak line blended with a much deeper one (*b*), no correction is made. Values so found are denoted by an "a" or a "b" immediately following the intensities in the last column. Any data which are particularly doubtful for other reasons, such as irregularities of the plate or tracing, or unusually bad blends, are either omitted, and a dash inserted, or are followed by question marks.

The central intensities for the hydrogen lines may be compared with the values found by E. G. Williams,[19] namely, 0.14 and 0.22 for $H\gamma$ and $H\delta$, respectively, in the spectrum of α Orionis. The values of s_0 in Table 1 are 86 and 82 per cent, respectively, of Williams' values, which are apparently not corrected for the finite resolving power of his spectrograph. Since the value of $J_{c\lambda}$ used here is probably somewhat higher than that used by Williams, and the resolving power is greater as well, the agreement is satisfactory.

The values of x''/x' and x'''/x'' in Table 1 enable us to test the assumption that these profiles can be represented by dispersion-curves. An average of x'''/x'' was taken over all lines for which the data are available in α Orionis; x''/x', on the other hand, was averaged over only the first four *Fe* multiplets in both stars, since these include most of the unblended lines. We find the values:

$$\alpha \text{ Orionis: } \frac{x'''}{x''} = 1.256 \pm 0.061 \text{ (20 lines)},$$

$$\frac{x''}{x'} = 1.413 \pm 0.083 \text{ (23 lines)},$$

$$\alpha \text{ Herculis: } \frac{x''}{x'} = 1.377 \pm 0.094 \text{ (22 lines)},$$

where the errors are again average deviations.

[19] *Ann. Solar Physics Obs., Cambridge*, **2**, Part II, 25, 1932.

When these values are compared with 1.309 and 1.500, the theoretical values for dispersion contours, it becomes evident that the actual lines rise somewhat more steeply than the assumed profiles. This tends to offset any error of the resolving-power correction arising from the fact that the intensity on each side of the line is less than that of the assumed continuous background. It is of interest to note that within the errors of observation the observed lines may be represented quite accurately by parabolic contours. For a parabolic profile we should find $x'''/x'' = (3/2)^{1/2} = 1.225$, and $x''/x' = 2^{1/2} = 1.414$, values within 3 per cent of the observed average ratios.

To derive a line-profile formula which may be used to determine the true intensity at any point, a dispersion formula with a half-width $2b_1$ may again be assumed. One then finds by straightforward calculation that when r equals a value c, x_c is given by

$$\frac{x_c}{b_0} = \left(\frac{b_2}{b_0} - 1\right)\left(\frac{c - r_0}{1 - c}\right)^{1/2}. \tag{6}$$

An assumed parabolic contour gives substantially the same result when c is small, but in a more complicated form.

Before a program of quantitative measurements was undertaken, a series of visual estimates of line intensities had been made. Fifty-eight *Fe* lines distributed over the spectrum from λ 4143 to λ 6358, as well as 20 lines of other elements from λ 4206 to λ 4651, were found to be moderately free of blends. The central intensities of these lines were estimated in units of the continuous spectrum in ten visually equal steps, and the apparent widths were measured directly.

The tracings were originally expected to supplant entirely these rough measurements, but for weak lines the tracings are not of much use. Many weak lines of high excitation potential whose intensities and widths were visually determined with reasonable consistency appear as scarcely discernible depressions on the tracings. Intensity measurements are, of course, always possible in such cases, but any determination of widths from curves so poorly defined seems very difficult. For this reason the visual estimates provide information about weak lines which would otherwise not be so readily available. These data are shown graphically in Figure 5 and discussed in the next section.

IV

To interpret the data of the preceding section it is necessary to make some theoretical assumptions. As will be shown in section VI, the atmospheres of these supergiant stars are apparently characterized by an almost complete lack of thermodynamic equilibrium. Strictly speaking, we should develop at this point a theory of the formation of absorption lines applicable to such a non-equilibrium case. It is possible, however, to obtain most of the results of such an analysis from a single assumption that is both simple and theoretically reasonable.

Let J_λ be the intensity of radiation between λ and $\lambda + d\lambda$, and let a_λ be the average line-absorption coefficient per atom. We know in general that J_λ will be a function of λ and of a_λ and may also be a function of the upper and lower atomic states involved in the transition. The simplifying assumption which will be made here is that for lines in the same multiplet the difference in the properties of the various initial and final levels may be neglected, and that

$$J_\lambda = G_\lambda \cdot \chi(a_\lambda) , \tag{7}$$

where χ is some function of a_λ and G_λ is a slowly varying function of λ. Except for the fact that here a_λ replaces l_λ/k_λ, where k_λ is the continuous absorption coefficient, this is the result of the simplified Eddington-Milne theory of absorption lines, in which G_λ becomes simply $J_{c\lambda}$, or the intensity of the continuous background.

A theory of the absorption lines in the more general case has been developed by the author and will be presented elsewhere. The analysis indicates that (7) is an adequate approximation for the cores of strong lines and that G_λ is given by

$$G_\lambda = z_i B_\lambda(T_l) , \tag{8}$$

where $B_\lambda(T)$ is the Planck radiation function and z_i varies slightly with the lower level of the transition in question; T_l is a line temperature which characterizes primarily the quality, or color temperature, of the radiation responsible for ionization cycles.

Another assumption, however, is implied by the foregoing formu-

lation, namely, that the profile of the absorption coefficient a_λ is constant with depth, although the number of suitably excited atoms per cubic centimeter, and hence the mass absorption coefficient l_λ, may of course vary. Hence, if the variation of a_λ with wave length is produced by a velocity distribution of some sort, this distribution must be assumed constant with depth. Since the core of a strong line is formed in a relatively thin layer of the atmosphere, this is not a serious restriction. We may set

$$a_\lambda = a\Phi(x) , \tag{9}$$

where

$$a = \frac{\lambda_0^2}{c}\int a_\lambda d\lambda \sim g_i f \exp\left(\frac{-E_i}{kT_d}\right); \tag{10}$$

the integral is taken over the entire line; x measures $\lambda - \lambda_0$ in millimeters on the tracing, $g_i f$ is the weighted oscillator strength of the transition, E_i is the excitation energy of the lower level, and T_d is a distribution temperature characterizing the distribution of electrons among the different levels of a single term. One must assume, then, that the absorption-coefficient profile $\Phi(x)$ is not only the same function for all members of a multiplet but also does not vary with depth in the atmosphere.

It follows from (7) that, if for several multiplet lines a point on the contour of each is taken such that J_λ/G_λ is the same for all lines, then $\chi(a_\lambda)$ and a_λ must be constant for all such points and, from (9),

$$\Phi(x) \sim \frac{1}{a} , \tag{11}$$

where x for each line is the measured distance from the line center of the point so defined. Also, if we consider values of J_0 for each line, where λ_0 is the wave length of the line center, then we have

$$J_0 = G_\lambda \chi(a\Phi(0)) = G_\lambda \psi(a) , \tag{12}$$

which defines $\psi(a)$.

The purpose of the present section is to use (11) and (12) in a determination of the three functions G_λ, $\psi(a)$, and $\Phi(x)$. The second

and third of these will be called a "depth-curve" and a "width-curve," respectively. The practical determination of these curves is very much simplified by the fact that G_λ varies only slightly over the observed range; i.e., the absolute central intensities of the multiplet lines show little dependence on frequency, although the continuous spectrum increases by a factor of more than 3 over the same range. Thus J_0, or $r_0 \cdot J_{c\lambda}$, gives as good an approximation to $\psi(a)$ as the data will allow, while $J_0/\psi(a)$ then gives G_λ.

To the same approximation one may set G_λ constant in finding $\Phi(x)$, or rather in determining x for a known $\Phi \sim 1/a$. Let $2x_c$, the corrected width, be defined as the width of a line at an absolute intensity K, i.e., an intensity $K/J_{c\lambda}$ relative to the continuous background. Then x_c may be calculated from (6), setting $c = K/J_{c\lambda}$. The choice of K presents certain difficulties. It is desirable to choose this constant of proportionality so that the relative intensities at which x_c is calculated will at least be between s' and s''', i.e., the intensities at which the widths x' and x''' were measured. In this way no extrapolation is required to determine x_c from the measured x'. The values chosen (see Table 2) require little or no extrapolation for the weak lines, but for strong lines involve some extrapolation to widths greater than $2x'''$. This would seem a more accurate procedure than the alternative extension of the dispersion-curve profile to widths less than $2x'$. The unit for K in Table 2 is the value of $J_{c\lambda}$ at $\lambda = 4350$ A.

The results depend very much on the values of a. The data for $g \cdot f$ are taken from Table 1. The choice of T_d in (10) is somewhat arbitrary. In theory this temperature is determined by the gradient of $J_{c\lambda}$ in various regions of the spectrum and by the process of formation of the lower ultimate lines. The value 4900° was originally chosen as a mid-point of the range of probabilities; this value is used throughout. Fortunately, T_d does not affect the results appreciably, since the change of E_i in any multiplet is small.

The data do not permit an accurate determination of G_λ and $\Phi(x)$, although $\psi(a)$ can be obtained with relatively greater precision. It is therefore assumed that G_λ is linear in λ, with a slope m, and that $\log \Phi(x)$ is linear in $\log x$, with a slope $-n$. These slopes are determined from graphs of the two functions.

The depth-curve $\psi(\alpha)$ also makes possible a determination of $\Phi(o)$ for each multiplet—the value of $\Phi(x)$ at the line center. Equation (11) still holds when x equals zero, and thus $\Phi(o)$ is proportional to $1/\alpha$ for a line such that r_o, its relative central intensity, equals $K/J_{c\lambda}$. But this is just the value of α which we find from the depth-curve at the point where it intersects the horizontal line $J_o = K$. In practice it is convenient to calculate $\Phi_r(o)$, defined as $\Phi(o)/\Phi(x_1)$, where x_1 equals 5.9 mm, or 0.30 A. Thus, if the depth-curve is plotted logarithmically—$\psi(\alpha)$ against log α—log $\Phi_r(o)$ is the horizontal dis-

TABLE 2

COLLECTED MULTIPLET DATA

Multiplet	Number of Lines	$\Delta\lambda$	Δ log α	m	K	n	$\Phi_r(o)$	γ
Fe 1.....	8	157 A	1.22	−0.14	0.10*	2.4?	43	0.046 A
				—	.10	—	200	.021
Fe 2.....	6	76	1.11	− .17	.25	2.5	41	.047
				—	.20	1.8	115	.028
Fe 3, 4.....	12	320	1.23	− .141	.10	2.26	11	.095
				−0.131	.10	2.16	50	.043
Fe 5.....	11	84	0.52	—	.33	1.6	2.1	.29
				—	.20	1.4	8.1	.11
Mn.....	9	65	0.86	—	.20	1.5	4.7	.16
				—	0.20	2.1	36	0.051

* For each multiplet the upper data refer to α Orionis, the lower to α Herculis.

tance between the point on the depth-curve $\psi(\alpha) = K$ to the point log α = log α_1, where α_1 is determined from the width-curve for x_c equal to 5.9 mm.

As is shown below, the values of n obtained from the depth-curves average about 2. This is the value which would be obtained for a dispersion-curve $\Phi(x) \sim 1/(\gamma^2 + x^2)$. It is possible to calculate γ directly from $\Phi_r(o)$, and it is easily shown that γ in angstroms is given by

$$\gamma = 0.30(\Phi_r(o) - 1)^{-1.2}. \qquad (13)$$

To locate the point $\psi(\alpha) = K$ on the depth-curve and thus to determine $\Phi_r(o)$ and γ, it is necessary to extrapolate the depth-curves

to higher central intensities than are actually observed. To facilitate this extrapolation the depth-curves are plotted logarithmically.[20] In Figure 3 these curves are given for the *Fe* and *Mn* multiplets in α Orionis. In each curve J_0, or $r_0 \cdot J_{c\lambda}$, is plotted against log a, and a smoothed curve drawn to give $\psi(a)$. Since the third and fourth *Fe* multiplets have the same lower term, they are treated as one multiplet throughout. The curves for all the multiplets are assembled with the *Fe* 1 multiplet to form a consistent family, the curves of lower excitation potential lying lowest. The extrapolated curves are represented by dashed lines. The unit for J_0 is the value of $J_{c\lambda}$ at λ = 4350 A; for comparison with Figure 2, $J_{c\lambda}$ on this scale equals 0.55 when λ = 4200 A.

The lines designated by crosses in the *Fe* 3 and 4 multiplets are λ 4202.0 and λ 4307.9, respectively, with a common upper state. These have been observed as emission lines in long-period variables by A. D. Thackeray,[21] who attributed their anomalous intensities to the wave-length coincidence of λ 2795.00—an *Fe* line with the same upper state as the pair above—and the *Mg* II line λ 2795.52. The latter line is presumably excited by recombining hydrogen atoms.

The determination of m and n rests largely on the third and fourth *Fe* multiplets, whose lines cover the entire wave-length region examined and whose accurate $g \cdot f$ values vary by a factor of 17. In addition, the central intensities of these lines are higher and hence more accurate than those of the first *Fe* multiplet, which includes a comparable range of theoretical strengths. Figure 4 shows the values of G_λ plotted against λ and of log $\Phi(x)$ against log x_c for this pair of multiplets. The straight lines were determined by inspection for the case of α Herculis and by least-squares solutions for α Orionis.

The graphs for the other multiplets are not shown here, but the resulting values of m, n, $\Phi_r(0)$, and γ are listed in Table 2, together with the values found from Figure 4. For each multiplet the upper data refer, as before, to α Orionis; the lower, to α Herculis. The first four columns give the properties of the individual multiplets. The values of m in the fifth column give the increase of G_λ per hundred

[20] The depth-curves so plotted are analogous to Allen's[9, 10] *F*-curves, in which r_0 is graphed against log a.

[21] *Mt. W. Contr.*, No. 580; *Ap. J.*, **86**, 499, 1937.

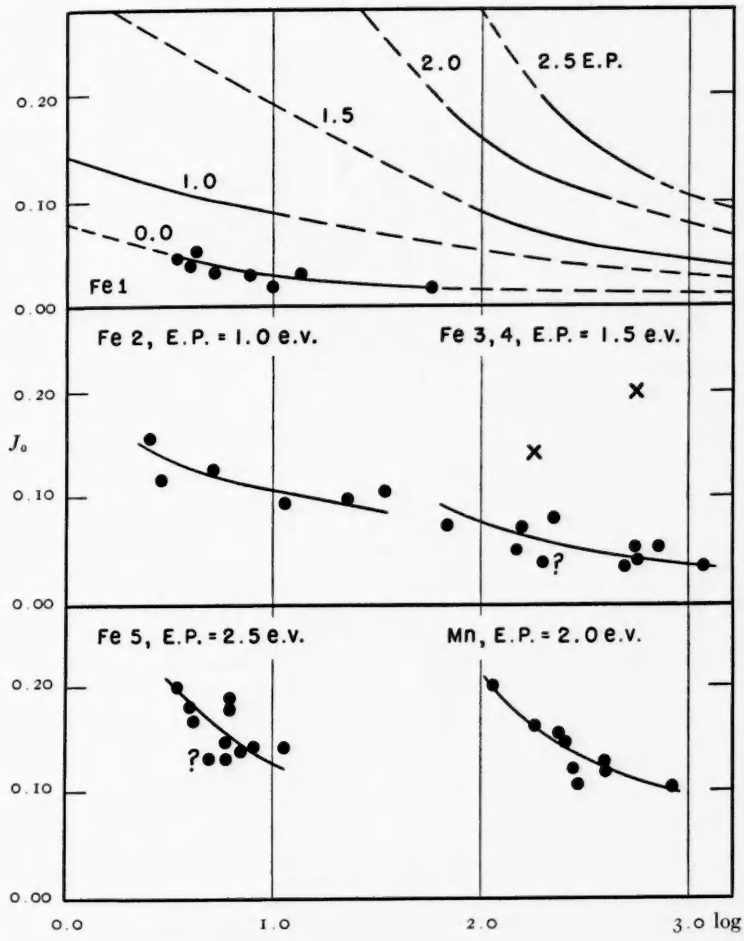

FIG. 3.—Central intensity J_0 of multiplet lines in α Orionis, corrected for resolving power and for dependence of continuous background on wave length, plotted against log α, the weighted oscillator strength; the zero point of the logarithmic scale is arbitrary for each multiplet. Unit for J_0 is the intensity of the continuous background at λ 4350. The smoothed curves are collected at the top, shifted horizontally by arbitrary amounts, and extrapolated (dashed lines) to form a consistent family of depth-curves, those of highest E.P. lying highest.

angstroms, which, since G_λ is nearly equal to 1, are also percentage increases in the same interval. The values of K are the intensities J_λ

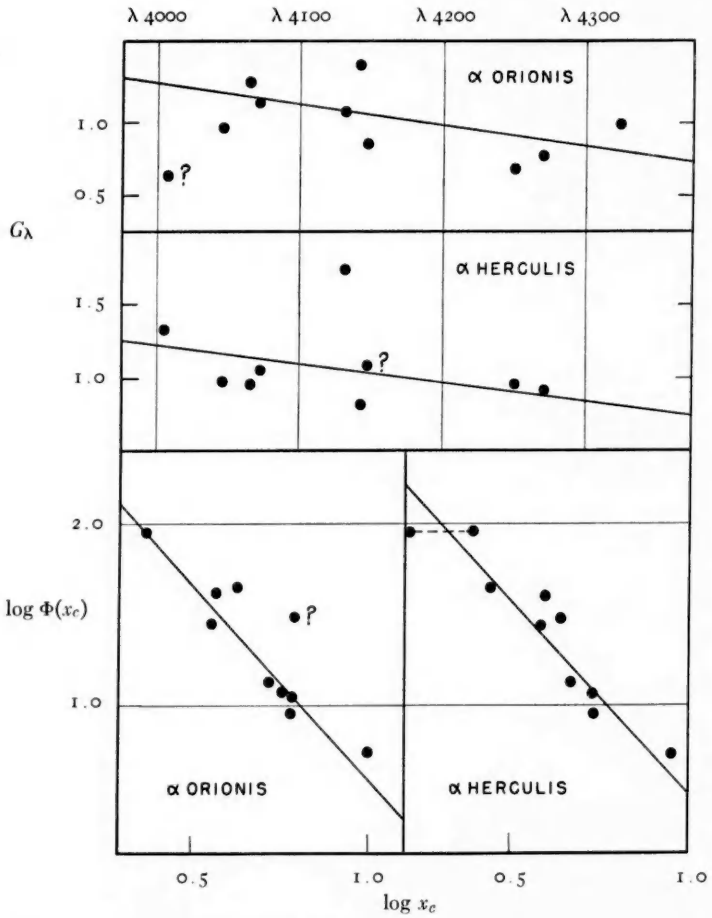

FIG. 4.—*Above*, the absolute central intensities G_λ of lines in multiplets *Fe* 3 and 4, corrected for resolving power and for differences in oscillator strength a. Ordinates, measured values of J_0 divided by the values of $\psi(a)$ found from the smoothed depth-curves shown in Figure 3. *Below*, the logarithm of the line-absorption coefficient plotted against the logarithm of the wave-length distance x_c from the line center. The two points connected by a dashed line represent the possible range of values for λ 4147.7.

for which the corrected widths x_c were calculated from (6). The slope n, found by graphing log $1/a$ against log x_c, follows. Values

with question marks in Table 1 were not used in the determination of m and n. In the last two columns are the values of $\Phi_r(0)$ and γ derived from the width-curves, the extrapolated depth-curves, and equation (13). These values are very dependent on the grouping of the different depth-curves at the top of Figure 3. For this reason the evident change of $\Phi_r(0)$ with excitation potential is not to be trusted. The scatter in γ is less, of course, and the order of magnitude seems clearly indicated.

Three conclusions may be drawn from Table 2. First, the values of m verify the statement that G_λ is sensibly independent of wave length. More accurately, while any variation of G_λ with the upper or lower state of a line is completely masked by the observational scatter, a slight general decrease with wave length, amounting to some 10 to 20 per cent per hundred angstroms, seems indicated. To put this result in a more familiar form, the relative central intensities of strong lines are inversely proportional to the intensity $J_{c\lambda}$ of the continuous background; these intensities therefore decrease by a factor of more than 3 in the observed range, provided we correct first for the differences in a, the weighted oscillator strength. The effect is similar to that observed by Thackeray[22] for the solar multiplet lines which are blended with H and K, and whose central intensities—relative to the continuous background outside of the calcium line, rather than to the intensity in the directly adjacent H or K wing—remain unaffected by the blending. The large scatter prevents a determination of m for the multiplets of higher excitation potential in α Orionis and for most of the α Herculis multiplets. Even these multiplets, however, are scarcely compatible with a value of m as high as 40 per cent, which would result from the case $G_\lambda = J_{c\lambda}$. As a probable value of m, we may take -0.14 ± 0.05, the average deviation being that from the least-squares solution for the *Fe* 3 and 4 multiplets in α Orionis.

The second result from Table 2 concerns the values of n. If the *Fe* 3 and 4 multiplet values are weighted four times as high as the others, the average values for n are 2.12 ± 0.30 for α Orionis and 1.92 ± 0.25 for α Herculis. The average deviations so obtained may be compared with the corresponding quantity ± 0.18 found from the

[22] *Mt. W. Contr.*, No. 555; *Ap. J.*, **84**, 433, 1936.

least-squares solution for the *Fe* 3 and 4 multiplets in α Orionis. These values justify the assumption of a dispersion-curve profile used in the calculation of γ and lead to the third conclusion—that the values of γ are about 0.1 A for α Orionis and 0.05 A for α Herculis. This is a quantitative statement of the observed fuzziness of all the α Orionis lines, previously noticed by Adams[7] and clearly evident from Figure 1. It is also clear from this same figure that the fuzziness is considerably less for α Herculis than for α Orionis. More quantitatively, if the value of γ for each multiplet in α Orionis is divided by the corresponding quantity for α Herculis and an average taken over all the multiplets, one finds that the value of γ in α Orionis is, on the average, 2.4 ± 0.4 times as great as that in α Herculis.

It is necessary to consider the possibility that systematic errors may affect all these results. The values of m, for instance, depend on $J_{c\lambda}$. Jensen's work gives a much lower gradient of $J_{c\lambda}$ with wave length than that found in section II. But a gradient less steep makes m more highly negative, which is unlikely on physical grounds, as will be shown in section VI. This is an additional reason to believe that the values of $J_{c\lambda}$ in Figure 2 are substantially correct.

A more serious possibility is that r_0 might be subject to some error which changed systematically with α. A choice of values of $2b_0$ such that the apparent intensities have been more overcorrected than undercorrected has the result that the intensities of weak, narrow lines are too low relative to those of strong broad lines. Hence the depth-curves are perhaps insufficiently steep, and $\Phi_r(0)$, too large. The average value of γ is accordingly a lower limit for this quantity.

Overcorrected central intensities lead also to a change in m, the apparent slope of G_λ. If 0.07 A is taken for $2b_0$, for instance, J_0 is increased 9 per cent for the *Fe* 3 and 4 lines at λ 4050 in α Orionis, and some 20 per cent for those at the λ 4300 end of the observed range. The slope m found with these new values is about -0.110. Since the change produced is less than the average deviation of m, it is evident that errors from this source have no very great effect.

Errors in s_0 changing systematically with wave length are of greater importance. If the apparent intensities at the violet end of the observed wave-length region are too low relative to those at the red end by some 4 per cent of the continuous background (a relative error of

some 50 per cent in s_0), then the true slope of m should be slightly greater than zero. Although further data are necessary to rule out this possibility entirely, the good agreement between the results for α Orionis and α Herculis makes such errors seem somewhat unlikely.

The most serious source of error in m is the combination of the *Fe* 3 and 4 multiplets to form a single multiplet. While it is a legitimate approximation to neglect differences in the properties of different levels in a given term, the neglect of corresponding differences between terms is more difficult to defend. A difference in the ionization probabilities of the *Fe* y^3F^0 and the z^3G^0 terms might seriously alter the value of m in the only case in which it is well determined. A separate determination of m for each of these multiplets in the two stars would yield values ranging up to 0.25 and would very much increase the average deviation. While the precise value of m would be completely unreliable in this case, the general conclusion would be unaffected, namely, that G_λ increases much more slowly with λ than does $J_{c\lambda}$ and is, in fact, roughly constant over the observed range.

The value of n is very much better determined than that of m. Various other methods for calculating n, such as measuring x_c directly or calculating x_c from (6), r_0 being assumed equal to zero, all lead to a result between 2 and 3. It is significant that for these other methods of reduction the scatter of points from the width-curves is in all cases much greater than that of Figure 4. If the *Fe* 3 and 4 multiplets are again treated separately, the average deviation is increased somewhat, but the value of n is not radically changed. Hence, for these two stars we may take n equal to 2.0 ± 0.3.

This value of n refers, however, to lines of moderate width. To find comparable data for very wide lines the profiles of the *Na* D lines were measured. Although these lines have asymmetrical cores, their profiles are quite normal when s is sufficiently large. These lines, furthermore, are strong, apparently unblended, and so close together that possible changes in the continuous background need not be considered. Their widths were accordingly measured for α Orionis, α Scorpii, and α Herculis at each of two apparent relative intensities, $s_1 = 0.45$ and $s_2 = 0.68$. The results in angstrom units are given in Table 3. These measurements may be compared with the values of the extrapolated half-widths $2b_2$ derived for the *H* lines; recalling

that $b_2 = 3x'$, we find from Table 1 that the half-widths of $H\beta$, $H\gamma$, and $H\delta$ in α Orionis are 1.73, 1.87, and 1.55 A, respectively.

The last column of Table 3 gives the values of n, equal to the logarithm of the theoretical-intensity ratio divided by the logarithm of the width ratio. This is the same quantity as occurs in Table 2 except that here the small resolving-power corrections to the measured widths are neglected. Except for the value 2.4 for α Herculis, the results for n here are much higher than any of those for the normal lines in Table 2. An examination of Table 5 in the following section

TABLE 3

WIDTHS IN ANGSTROMS OF D_2 AND D_1 OF SODIUM

STAR	D_2		D_1		D_2/D_1		n*	
	s_1	s_2	s_1	s_2	s_1	s_2	s_1	s_2
α Orionis	1.32	1.90	1.16	1.58	1.14	1.20	5.3	3.8
α Scorpii	1.63	2.28	1.48	2.05	1.10	1.11	7.3	6.7
α Herculis	0.64	1.15	0.48	0.92	1.33	1.25	2.4	3.1

* Defined by the equation $a_\lambda \sim (\lambda - \lambda_0)^{-n}$. Since the theoretical intensity of D_2 is twice that of D_1, n becomes $n = \log 2 / \log (D_2/D_1)$.

shows that both D_1 and D_2 in α Herculis are asymmetrical well above s_1; the value 2.4 is therefore not reliable. The average of the two values for α Orionis in Table 3 gives 4.6 ± 0.8, which may be taken as typical for the D lines.

The visual estimates alluded to in the preceding section show a remarkably consistent correlation of central intensity with excitation potential. Most of the estimated lines were classified in five groups according to width, lettered from A to E. Lines of neutral atoms occur in the first three in order of decreasing width, and those of ionized atoms in the last two in the same order. For each group a graph of visual central intensity r_v against excitation potential gave a determination of r_v for an excitation potential of 1 e.v., a quantity designated by $R_v(W)$, where W denotes the particular group. Let r_r, the related central intensity of a line in a group W, be defined as $r_v/R_v(W)$, the central intensity of the line divided by the central intensity of a line of the same width with an excitation potential of

1 e.v. The final r_r's were then plotted against excitation potential for all lines.

The results for the 70 lines in the five groups, except for one doubtful value which falls completely off the diagram, are shown in Figure 5. Five other doubtful values are indicated by question marks. All lines with an excitation potential greater than 2 e.v. are produced by *Fe* atoms. Of those below 2 e.v., the thirteen points marked with

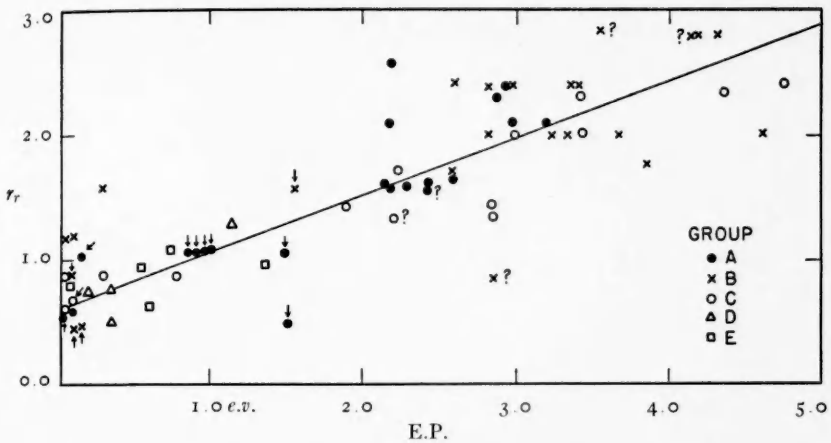

FIG. 5.—Ordinates of plotted points are visually estimated central intensities of absorption lines in the spectrum of α Orionis, divided by the corresponding intensity of a line of approximately equal width but of unit E.P. Neutral lines, groups A–C, arranged in order of decreasing width; enhanced lines, groups D and E, in the same order. Lines above 2 e.v. and those below marked with arrows arise from neutral *Fe*.

arrows represent *Fe* lines; these are in good agreement with the low excitation potential lines of other elements.

This change in r_r with excitation potential is similar to that found by Allen.[10] But here r_0 and s_0 change so much with excitation potential that the "mean depth of other lines of the same equivalent breadth and wave-length" which in Allen's paper replaces the $R_v(W)$ used here, becomes entirely dependent on the distribution of the excitation potentials of the lines chosen. In any case, the related central intensity r_r seems in α Orionis to be a more significant quantity than the relative depth d used by Allen. For with the latter quantity the uniform correlation with excitation potential for all lines is very much diminished. In other words, if r_0, the true central intensity for

each individual line, is plotted against the excitation potential of that line, a separate curve is obtained for each set of lines of the same width. If, as here, the curves are straight lines converging at $r_0 = 0$, E.P. = 0, then the reduction to r_r will bring the separate curves into coincidence. If, on the other hand, the convergence is at $r_0 = 1$, E.P. = 0, then Allen's d is more convenient. There are reasons to believe that the first method is likely to be the more useful one.

The results shown in Figure 5 are rather more qualitative than quantitative. Many sources of scatter are involved, as, for instance, the inverse variation of r_0 with $J_{c\lambda}$. It is possible to use the measured values of r_0 and $2x'$ for the multiplet lines in plotting curves similar to those of Figure 5. Even with these more accurate data, however, the scatter is not noticeably decreased, and, owing to the low range of excitation potential available, no strong trend is discernible in the plotted points. Thus the increase of r_r with excitation potential for lines of constant width shown by the visual estimates is at most an average effect. While the change is large—a factor of 5 or so for an increase of excitation potential from zero to 4.5 e.v.—the scatter is so great that the effect appears primarily when data are available for a considerable range of excitation potential.

The data of the last two sections may be summarized in the form of five experimental characteristics concerning the spectra of α Orionis and α Herculis, as follows:

1. The values of m, indicating roughly a slight decrease of the absolute central intensities of absorption lines with increasing wave length
2. The values of n, averaging 2 for most lines, and 4 or more for the *Na* D lines
3. The great widths of the observed lines and the high values for γ, twice as large in α Orionis as in α Herculis
4. The general increase of central intensity with excitation potential for lines of the same width
5. The great strength of the *H* lines, roughly the same as that of the *Na* D lines

V

A characteristic feature of these spectra is the asymmetrical nature of the profiles for the strong ultimate lines. These lines may be

divided into four general classes, depending on the change of J_λ as we pass from the violet core, the wave length of minimum intensity, to the red wing:

1. $dJ_\lambda/d\lambda$ becomes negative, and the line has a secondary minimum. This gives a true self-reversed line.

2. $dJ_\lambda/d\lambda$ becomes zero and then increases again, giving the line a sort of horizontal terrace on the red side.

3. $dJ_\lambda d\lambda$ is always greater than zero, but the line has a slight indentation in the red wing.

4. $dJ_\lambda/d\lambda$ has a single maximum on the long wave-length side.

These are roughly the classes which would describe a strong line blended with a progressively weaker one at a fixed distance to the red. Their meaning is best illustrated by the reproductions of microphotometer tracings in Figure 6.

The tracings were carefully examined for all evidences of asymmetry. The lunar spectrum was helpful in the elimination of blends. Suspected asymmetries were tested by tracing the spectral line on semitransparent paper, turning the paper over, and trying to fit the line to its mirror image.

Then for all asymmetrical lines the wave-length difference between the core and the line center was determined. The line center was taken to be the wave length about which the wings were symmetrical—in general this coincided very nearly with the position of the line in the solar spectrum relative to other neighboring lines. The core is the wave length at which the intensity is a minimum. In general the shift of the core relative to the line center was toward the violet, and thus v_1, the shift of the core in velocity units, was relatively negative. For each line, in general, an intensity could be found above which the line was symmetrical; the width of the profile at this point was also measured, divided by 2, and reduced to velocity units. The result is denoted by v_2. This quantity is, of course, more sensitive to the presence of blends than is v_1.

A list of the observed asymmetrical lines, together with their classes, and both v_1 and v_2, expressed in kilometers per second, is given in Table 4. The first three columns give the element producing the line, the wave length of the line, and the theoretical values of

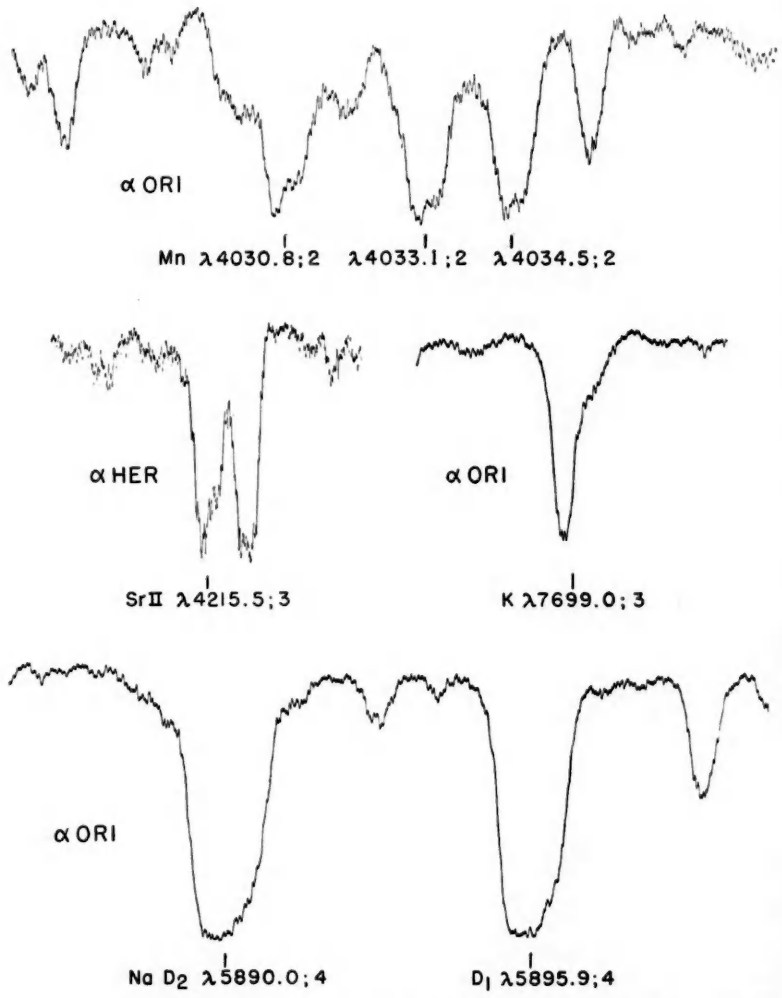

FIG. 6.—Profiles of the *Mn* triplet, the *Na* doublet, and lines of *Sr* II and *K*. Vertical dashes bisect the wings of each line. The indicated solar wave length is followed in each case by the class of asymmetry shown by the line.

TABLE 4

ABSORPTION LINE SHIFTS

Element	λ	g·f	Plate	Class	$v_1 \pm$ A.D.	No. of Tracings	$v_2 \pm$ A.D.	No. of Tracings
Al	3944.0	1	O 9	—	6.5	.....	28?	.....
	3961.5	2	O 9	—	7.6	.....	25?	.....
Mn	4030.8 γ	4	O 2	—	9.1	.....	.....	.....
	4033.1 β	3	O 2	3	6.1	.....	.....	.....
	4034.5 α	2	O 2	4	4.8	.....	.....	.....
	γ	.....	O 7	1, 2	12.8 ±1.1	3	20 ±2	4
	β	.....	O 7	1, 2	11.8 ±0.3	3	20 ±3	4
	α	.....	O 7	1, 2	7.1 ±1.1	4	16 ±1	4
	γ	.....	O 9	2	11.7 ±0.7	2	20 ±1	4
	β	.....	O 9	1, 2	9.6 ±0.8	2	17 ±0.6	4
	α	.....	O 9	1, 2	7.5	.....	15 ±1	4
	γ	.....	S 4	4?	9.0 ±0.6	2	25?	.....
	β	.....	S 4	1?	9.4 ±0.7	2	22 ±3	2
	α	.....	S 4	1, 4	4.4 ±0.2	2	24? ±3	2
	γ	.....	H 3	1	6.2? ±1.2	2	20	.....
	β	.....	H 3	1, 3	9.2 ±2.3	3	17.5	.....
	α	.....	H 3	1, 4	3.9 ±2.0	3	15	.....
Cr	4254.3 γ	9	O 3	—	13.2	.....	.....	.....
	4274.8 β	7	O 3	—	11.4	.....	.....	.....
	4289.7 α	5	O 3	—	—	.....	.....	.....
	γ	.....	O 6	3	11.0	.....	39	.....
	β	.....	O 6	3	13.8	.....	28	.....
	α	.....	O 6	3?	11.0	.....	21	.....
	γ	.....	O 9	1	10.8 ±0.4	2	22 ±2	2
	β	.....	O 9	2	11.3 ±0.2	2	24 ±2	2
	α	.....	O 9	2	9.7 ±0.1	2	—	.....
	γ	.....	S 4	4	4.7	.....	16	.....
	β	.....	S 4	4	3.6	.....	18	.....
	α	.....	S 4	—	—	.....	13	.....
	γ	.....	H 3	4?	6.8	.....	19	.....
	β	.....	H 3	2	9.9	.....	18	.....
	α	.....	H 3	2	8.5 ±0.7	2	15	.....
Ca	4226.7	.....	O 9	2, 3	9.8 ±0.7	2	21?	.....
Mg	4571.1	.....	O 9	4	3.3?	.....	12	.....
		.....	S 3	4	4.4	.....	17	.....
Fe	4375.9	.....	O 6	4	4.2	.....	—	.....
		.....	O 9	4	5.5	.....	11	.....
		.....	S 3	—	—	.....	9	.....
		.....	H 3	4	—	.....	13	.....
	5110.4	.....	O 11	4	4.5	.....	13	.....
		.....	S 2	4	3.4	.....	13	.....
		.....	H 1	.....	0.0?	.....	.....	.....

TABLE 4—*Continued*

Element	λ	$g \cdot f$	Plate	Class	$v_1 \pm$ A.D.	No. of Tracings	$v_2 \pm$ A.D.	No. of Tracings
Sr II	4077.7 β	2	O 2	3	12.9	.....	>42	.....
	β	.....	O 7	3	7.6	.....	28	.....
	β	.....	O 9	3	8.3	.....	>34	.....
	4215.5 α	1	O 9	—	3.2?	.....	—	.....
	β	.....	S 4	.....	0.0	.....	0.0	.....
	β	.....	H 3	1?	7.4?	.....	—	.....
	α	.....	H 3	3	6.5	.....	14	.....
Ba II	4554.0 β	2	O 3	3	6.9	.....	>34	.....
	β	.....	O 6	3	8.1	.....	>25	.....
	β	.....	O 9	3	11.1	.....	>29	.....
	4934.1 α	1	O 9	3	4.4	.....	14	.....
	β	.....	S 3	4	1.3?	.....	10	.....
	β	.....	H 3	4	3.0	.....	15	.....
H	4101.8 δ	0.022	O 9	4	1.7? ±1.7	2	—	.....
	4340.5 γ	0.045	O 9	4	1.4? ±1.4	2	—	.....
	4861.3 β	0.119	O 9	4	6.9	.....	33	.....
	6562.8 α	0.641	O 11	4	10.6	.....	>42	.....
	α	.....	O 10	4	8.4	.....	>49	.....
	α	.....	O 1, 4, 5	.....	0.0	.....	0.0	.....
	δ	.....	S 4	4	2.3	.....	—	.....
	α	.....	S 1	4	9.3	.....	47	
	α	.....	S 2	4	8.7	.....	48	.....
	δ	.....	H 3	.....	0.0?	.....	.....	.....
	γ	.....	H 3	.....	0.0?	.....	.....	.....
	α	.....	H 2	—	> 6.5	.....	—	.....
Na	5890.0 D_2	2	O 1	4	6.0	.....	24	.....
	5895.9 D_1	1	O 1	4	3.9	.....	19	.....
	D_2	.....	O 4	4	3.6?	.....	22	.....
	D_1	.....	O 4	4	2.7?	.....	21	.....
	D_2	.....	O 5	.....	0.0	.....	0.0	.....
	D_1	.....	O 5	—	6.9?	.....	32?	.....
	D_2	.....	O 11	4	9.4	.....	32	.....
	D_1	.....	O 11	4	8.3	.....	30	.....
	D_2	.....	S 1	4	7.6 ±0.3	2	37	.....
	D_1	.....	S 1	4	8.3 ±0.2	2	39	.....
	D_2	.....	H 2	4	10.9	.....	22	.....
	D_1	.....	H 2	4	7.3	.....	22	.....
K	7699.0	.....	O 8	3	8.7	.....	23	.....

$g \cdot f$,[23] the weighted oscillator strength of the line, respectively. For convenience all multiplet lines are denoted by Greek letters in the order of increasing frequency, as in the Balmer series, and the wave length and strength of the line are printed only once. The fourth column indicates the star and plate from which the tracing was made; the letters "O," "S," and "H" refer to α Orionis, α Scorpii, and α Herculis, respectively; the plates for each star are numbered chronologically, the earliest having the lowest numbers. The class of the line, as defined above, appears in the fifth column. When the classification of a line differed for different tracings, both classes are listed. The values of v_1 in the sixth column are in some cases followed by the average deviations and in the seventh column by the number of tracings measured. In such cases all the tracings were, of course, made from the same plate. The last two columns relate similarly to v_2. The absolute values of v_1 and v_2 are given; actually the shifts are all negative according to the usual convention. In several cases overexposed plates, bad blends, or, as in the case of λ 4227, the width of the line made some of the data uncertain; such data are either omitted, a dash being inserted instead, or, if given, are followed by question marks. Lower limits for v_2 are given for those cases in which the asymmetry extended as far up as the line remained unblended.

Asymmetries were also noted in these three stars for several lines of *Fe*, *Cr*, *Ti*, and *Sc* II. These were either weak ultimate lines or strong lines of excitation potential less than 1 e.v. They were all entered as class 4, but the values of v_1 were small, mostly 2 and 3 km/sec, with only one as much as 4.1. Also, these shifts were apparently not self-consistent—the cores of two lines showed shifts toward the red. Since asymmetry in line profiles is very dependent on plate grain and other errors, these small shifts were regarded as unreliable and were omitted from the table.

The spectra of α Boötis, β Pegasi, β Andromedae, and α Tauri were similarly examined; no clear asymmetry could be found except perhaps in the *Mn* triplet, where the effect is so doubtful that it may well be attributable to plate grain.

Except for the Balmer lines, Table 4 is simply a list of all the ulti-

[23] H. N. Russell, *Mt. W. Contr.*, No. 537; *Ap. J.*, **83**, 129, 1936; D. H. Menzel and C. L. Pekeris, *M.N.*, **96**, 77, 1935.

mate lines identified in the sun with Rowland intensity 5 or greater, omitting only the *Ca* II doublet, which was too far in the ultraviolet for accurate measurements. Values for the *Al* lines in α Orionis are uncertain for the same reason. Within the table the velocity shifts from a single plate increase roughly with the strength of the line. Except for the *Cr* line λ 4254.3, this relationship is followed within experimental error for all multiplets.

A comparison of the D lines on different plates indicates that these asymmetries actually vary from time to time for the same star; the differences seem larger than can be explained away by various photographic effects. There is, however, a distinct lack of correlation in α Orionis, the only case where sufficient data are available, between the asymmetries and the radial velocity of the star as averaged over all lines. Plates O 4 and O 5, with different radial velocities of 15 and 22 km/sec, respectively, both show no asymmetry for *Hα* and relatively little for the D lines. While this is by no means conclusive proof, it suggests that the asymmetries have perhaps no direct connection with the rate of expansion or contraction of the general atmosphere.

Several tracings showing these asymmetrical lines were reduced to intensity units. The profiles of these lines do not resemble the dispersion-curves assumed for the normal multiplet lines of the preceding sections, and thus a simplified resolving-power correction is no longer possible. Most of these lines are so wide, however, that the difference between apparent and true intensities will not be very large—less than 4 or 5 per cent of the continuous background.

The uncorrected intensities have, therefore, considerable significance. For each line three such intensities were measured: s_c, the intensity of the core, or the minimum apparent intensity; s_o, the central intensity, defining λ_o as before—the wave length about which the upper part of the line is symmetrical; and s_a, the intensity above which the line is symmetrical—half the width of the line at s_a gives v_2. These three intensities are collected in Table 5 for all the lines measured. Two tracings were measured for each line for which an average deviation is listed, except for the *Mn* lines, for which the mean of four tracings was taken. Lines which are asymmetrical as far out as they are comparatively unblended yield only a lower limit

TABLE 5

INTENSITIES OF ASYMMETRICAL LINES

Element	λ	Plate	$s_c \pm$ A.D.	$s_o \pm$ A.D.	$s_a \pm$ A.D.
Mn	4030.8	O 7	0.16 ±0.04	0.23 ±0.02	0.26 ±0.02
		O 9	.11 ±0.02	.20 ±0.02	.24 ±0.01
		H 3	.20	.22	.25
	4033.1	O 7	.13 ±0.04	.21 ±0.02	.24 ±0.02
		O 9	.08 ±0.02	.16 ±0.02	.18 ±0.01
		H 3	.12	.18	.23
	4034.5	O 7	.15 ±0.04	.18 ±0.05	.23 ±0.03
		O 9	.11 ±0.02	.15 ±0.01	.17 ±0.01
		H 3	.12	.12	.21
Cr	4254.3	O 9	.07 ±0.01	.12 ±0.01	.16 ±0.01
		H 3	.11	.12?	.16
	4274.8	O 9	.04 ±0.01	.10 ±0.02	.17 ±0.01
		H 3	.09?	.10	.12
	4289.7	O 9	.05 ±0.00	.11 ±0.01	> .17? ±0.03
		H 3	.03	.05	.08
Sr II	4077.7	O 9	.06 ±0.01	.10 ±0.01	> .30
		H 3	.12	.13	.16?
	4215.5	O 9	.10	—	—
		H 3	.11	.17	.21
Ba II	4554.0	O 9	.12?	.15	> .40
	4934.1	O 9	.18	.20	.30
H	4861.3	O 9	.10	.10	.39
	6562.8	O 9	.20	.22	> .70
		S 2	.17	.17?	> .70
		S 1	.18	.19	> .80
Mg	4571.1	O 9	.18	.18	.23
Na	5890.0	O 11	< .15	.15?	.42
		S 1	< .10	.10?	.36
		H 2	0?	.25	.55
	5895.9	O 11	< .15	.15?	.45?
		S 1	< .10	.10?	.46
		H 2	0?	.25	.65
K	7699.0	O 8	0.22	0.41	0.72

for s_a. As usual, question marks denote doubtful values; dashes indicate that measurements could not be made because of obvious blends or peculiarities of the tracing.

From Table 5 it is evident that the strongest members of the *Mn* and *Cr* multiplets tend to give higher intensities than those of the other theoretically weaker lines. This tendency is much stronger than the average deviations would indicate. If Δs_0 designates the value of s_0 for the strongest line in a multiplet *minus* the same quantity for the next strongest, the average values of Δs_0 for the *Mn* triplet on plates O 7 and O 9 are 0.023 ± 0.008 and 0.048 ± 0.008, respectively; for the *Cr* triplet $\Delta s_0 = 0.025 \pm 0.015$. The corresponding Δs_a for the *Mn* triplet averages 0.02 ± 0.02 for the four tracings of plate O 7, and 0.06 ± 0.02 for the two of plate O 9. For the *Mn* lines on O 9 these differences are considerably greater than can be accounted for by any resolving-power corrections, particularly since λ 4030.8 and λ 4033.1, as shown in Figure 6, have nearly the same width.

From the data of the present section it is possible to give five observational characteristics in addition to the five already set forth at the end of the preceding section:

6. The occurrence of strong asymmetries in the spectra of α Orionis, α Scorpii, and α Herculis, but not in the other four stars observed
7. The general nature of the observed profiles
8. The rough correlation of the velocity shifts v_1 and v_2 with relative line strengths in multiplets
9. The zero excitation potential of nearly all asymmetrical lines
10. The variation of these asymmetries with time

VI

The observational data of the last two sections allow a consistent theoretical interpretation. Results based on a single plate are, of course, untrustworthy from a quantitative standpoint, but the agreement between the data for the different stars and the general consistency of the final results increases considerably the reliability of this investigation.

To take up separately each of the ten observational characteristics outlined above, we have first the slight change observed in G_λ. From this it follows that the corrected central intensities must be real and cannot be attributed to uncorrected resolving-power, rotation, expansion, or large-scale turbulence. Any of these effects would fill up the line center to an extent proportional to $J_{c\lambda}$, the intensity in the continuous background. Even small-scale turbulence (motion of a gas in masses of small optical thickness) would, in the absence of other effects, produce broadened lines with central intensities proportional to $J_{c\lambda}$.

Since these central intensities are real, they convey definite information about the emission of radiation from the atoms forming the line. From (8) it follows that the color temperature of this emitted radiation is simply T_l, provided we neglect the change in z_i, which in the present case is less than the observational scatter involved. The value of $-m$, and hence the relative decrease of G_λ per hundred angstroms, was found in section IV to be 0.14 ± 0.05, if the combination of the *Fe* 3 and 4 multiplets is justified, and otherwise about zero, with a maximum error of not more than 0.25. If follows from the usual formula for the Planck radiation function that the maximum theoretical value for $-m$ is 0.12, its value for T_l infinite. If the true error is taken to be twice the average deviation above, $m = -0.04$, and $T_l = 10{,}000°$. When $m = 0$, $T_l = 7000°$; but if m is as high as 0.25, T_l will be as low as 2300°. We may tentatively set T_l at about 8000°, with the realization that this value is most uncertain. The evidence definitely points to the conclusion, however, that T_l in α Orionis is probably higher than the effective temperature of 3400° for this star.

The value $n = 2$ found from the *Fe* multiplets strongly indicates that the absorption-coefficient profile $\Phi(x)$ is given simply by the ordinary radiation-damping formula, and that the observed multiplets fall on the familiar square-root section of the curve of growth. The values of γ in Table 2, however, make this hypothesis untenable. The radiative value of γ is $\Gamma = 3f\omega/4\pi$, where ω is the classical damping constant and f is the oscillator strength of the downward transition, which we may set equal to $1/3$. In wave-length units, $\Gamma = 5.91 \times 10^{-5}$ A, independent of frequency. This is less than one

five-hundredth of the values of γ in Table 2. Since there is apparently no form of pressure broadening which would not be effective in other less rarefied atmospheres as well, the suggestion that n arises from resonance scattering or from any form of pressure broadening must be ruled out.

The only alternative explanation for the observed line broadening lies apparently in the Doppler shift; the low central intensities, moreover, rule out large-scale in favor of small-scale turbulence. While it is a priori improbable that the distribution of atomic velocities in a given direction should mimic a dispersion-curve, the general lack of thermodynamic equilibrium in these supergiant atmospheres makes such a distribution less surprising. It should perhaps be noted that the velocity distribution denoted by small-scale turbulence has probably little connection with the terrestrial concept of turbulent motion.

This hypothesis of turbulence is strongly supported by the behavior of the *Na* D lines. Here the values of n in Table 3 range from 3 to 6 and must almost certainly be attributed to turbulence; one may expect, moreover, that a velocity-distribution function, whatever its behavior at moderate velocities, would begin to fall off exponentially for sufficiently great velocities.

On the basis of this assumption the values of γ correspond to velocities of about 8 km/sec for α Orionis and half this for α Herculis. A large proportion of *Fe* atoms, however, will have velocities ranging up to 18 km/sec, and the root-mean-square velocity will be of the order of magnitude of about 10 km/sec. The usual formula $\overline{v^2} = 3kT/m$ indicates that such a velocity for an atom of atomic weight 56 corresponds to a temperature of about 200,000°. It is not, of course, intimated that this temperature has any significance other than to indicate the magnitude of the observed velocities.

Individual depth-curves give no very particular information about the process of line formation. We have seen in section IV, however, that the visual estimates clearly show an increase in the central intensities with increasing excitation potential, even for constant line width. There are several possible explanations for this increase. An increase of ionizing radiation with depth would explain the effect,

since the lines of higher excitation potential are formed deeper in the atmosphere; a systematic change of the various transition and ionization probabilities from the upper state with increasing energy of the upper state would also provide an adequate explanation. No quantitative treatment of this and other similar effects is apparently possible, but the observed change of r_r with excitation potential is a wholly reasonable one.

The strength of the hydrogen lines fits consistently into the nonthermodynamic model presented here. *Hα*, for instance, has a half-width of nearly 2 A in α Orionis and is one of the strongest lines in the entire spectrum. Apparently the only consistent explanation for this fact is that the energy density of L_α radiation is very high, corresponding to a temperature of about 17,000°, if we assume ten times as much hydrogen, by mass, as neutral sodium. For on these assumptions the number of hydrogen atoms in the second quantum state equals the number of neutral sodium atoms; since the oscillator strengths are comparable, this leads to the roughly equal strengths of the *H* and *Na* D lines noted in point 5 at the end of section IV.

The enormous strength of the enhanced lines noted by Adams and Russell[3] also fits into the same general picture of a complete departure from equilibrium conditions. In comparison with their results on stellar excitation temperatures it is possible to derive here a corresponding value of the excitation temperature from the multiplets of known $g \cdot f$ values. The theoretical strength of a line is proportional to $g \cdot f \exp(-E_i/kT_x)$. The assumption that lines of equal strength, but arising from different terms, have the same width x_c, regardless of other differences in the process of line formation, gives at once a determination of T_x. This assumption is almost certainly not valid but provides a legitimate first approximation. The vertical distance between the $\Phi(x)$ curves for the *Fe* 1 and the *Fe* 3 and 4 multiplets, the only ones of accurately known $g \cdot f$ values, gives $\Delta E_i \theta_x$ directly, where θ_x is $5040/T_x$ and ΔE_i is the difference of excitation potential for the two lower states concerned. In this way we find that T_x equals 2100°. This is in satisfactory agreement with the revised value of 2200° obtained from the Adams and Russell results, if we take the solar excitation temperature to be 4150°, the value found by

Menzel, Baker, and Goldberg[24] from the *Fe* I multiplets, instead of the 5300° used by Adams and Russell.

This excitation temperature T_x has a different significance from T_d and T_l discussed above. While T_d gives the distribution of electrons among the various levels of a spectroscopic term, T_x gives their distribution among wholly different terms. The line temperature T_l, on the other hand, characterizes the energy distribution of the ionizing radiation. One may expect these three temperatures to differ widely in an atmosphere which is not in thermodynamic equilibrium.

The various temperatures derived for the atmosphere of α Orionis are given in Table 6. The enormous discordance between these values, together with the general non-Maxwellian nature of the velocity distribution, indicates the extent of the deviations from thermodynamic equilibrium which are apparently present in these late-type supergiant atmospheres.

We next consider the asymmetrical line profiles discussed in section V. These may be explained by a simple kinematical model. One may suppose that the star has the usual photosphere and a stationary reversing layer in which normal, symmetrical lines are formed. Above this may be assumed a thin shell of outward-moving atoms; by the usual Doppler effect these atoms will absorb the radiation emitted by the reversing layer only in frequencies which are considerably greater than the central frequency of the line emitted by stationary atoms. Such an expanding shell is also indicated by the measures of Adams and MacCormack[6] and others on the systematic displacement to the violet shown by the lines of low excitation potential.

It is clear that such a model explains most of the observed features of the asymmetrical lines. By a suitable distribution of velocities among the atoms in the shell it is possible to produce any of the observed profiles of the strong ultimate lines. The situation is perhaps more complicated than would first appear. A moving atom will not only absorb radiation to the violet of the line center but will also scatter such radiation back to the reversing layer. To an observer in the reversing layer the atoms in the shell are moving away; hence the returning radiation will be shifted as far to the red of the line center as it was originally to the violet. In this way any radiation absorbed

[24] *Ap. J.*, **87**, 81, 1938.

by the moving atoms from the violet wing of the line and returned to the reversing layer reappears immediately in the red wing. This may possibly explain the relatively higher central intensities of the theoretically strongest members of the *Mn* and *Cr* multiplets, a fact noted in section V.

The correlation between v_1, v_2, and the line strength $g \cdot f$ is readily explicable. One need only assume that the number of atoms in the

TABLE 6

TEMPERATURES OF α ORIONIS

Temperature	Method of Determination
$T_x = 2100°$	Excitation temperature: found from widths of strong iron lines of different excitation potential and known oscillator strengths
$T_e = 3400°$	Effective temperature: determined by the total flux per unit area and found from measurements of angular diameter and apparent bolometric magnitude
$T_l = 8000°?$	Line temperature: given by equating $B_\lambda(T_l)$ to G_λ, the energy density in the centers of the strong iron lines, corrected for differences in oscillator strength
$T_H = 17{,}000°$	Hydrogen temperature: determined from the energy density in L_α necessary to give the observed strength of the Balmer series, on the assumption that the mass abundance of hydrogen is ten times that of neutral sodium
$T_v = 200{,}000°$	Velocity temperature: derived by substituting the magnitude of the observed turbulent velocities into the formula $\overline{v^2} = 3kT/m$

line of sight with a given velocity v decreases as v increases. For very strong lines the few atoms with very large velocities will be readily noticeable, while for weak lines a very large number of atoms will be required to produce an observable effect. Thus, any asymmetry will extend farthest to the violet for the strongest lines.

As regards point 9, it is reasonable to expect that only ultimate lines should show asymmetries. The radiation incident on the asymmetry-producing shell will show roughly the same spectrum as that

observed; i.e., all the normal lines will be fully formed. Since it is line radiation that maintains atoms in excited states, and since, furthermore, the line shifts are less than the line widths, these excited states will be largely depopulated for all the atoms in the shell, and such atoms will therefore produce asymmetries only in the ultimate lines.

These arguments are not inconsistent with the asymmetries observed for the Balmer lines. The mass absorption coefficient for L_α is so high that this Lyman line will form at higher levels than other ultimate lines and will keep its full intensity high in the reversing layer and conceivably well into the shell.

Very few atoms are required to produce the observed asymmetries. If N_a equals the number of outward-moving atoms in the line of sight and t_λ is the optical depth of the shell in the wave length λ, then we find, with the aid of the usual quantum-mechanical expression for the atomic absorption coefficient a_λ,

$$N_a \int a_\lambda d\lambda = \int t_\lambda d\lambda \,, \tag{14}$$

$$N_a = \frac{m_e c^2}{\pi e^2 f \lambda^2} \int t_\lambda d\lambda = 7.4 \cdot 10^{11} \frac{E_v^2}{f} \int t_\lambda d\lambda^\circ \,, \tag{15}$$

where $d\lambda^\circ$ is the wave-length interval in angstrom units, E_v is the energy in electron volts of a quantum of radiation in the center of the line, and the integrals extend over the line. For the observed lines of Figure 6 the integral of $t_\lambda d\lambda^\circ$ necessary to produce the asymmetries is scarcely greater than 5. For E_v and f equal to 3 and to 0.5, respectively, N_a will therefore not exceed 6.7×10^{13} atoms/cm^2.

We see that this model explains the observations satisfactorily. It is possible to go farther and deduce other properties of the assumed shell of outward-moving atoms. In the first place this shell must cover most of the observed stellar surface, since otherwise it would be difficult to explain the large observed difference in intensity between the red and the violet wings of asymmetrical lines. This difference is particularly striking in the case of the K line, λ 7699 (see Fig. 6).

Secondly, since the line cores are always shifted to the violet, one

may conclude that the atoms in the shell return to the star as unobservable ions. It is most unlikely that many atoms could leave the star entirely. Radiation pressure is apparently the only agency that could remove many atoms to infinity, but most atoms will become highly ionized before they have gone very far, and their lines will then be so far in the ultraviolet that radiation pressure will be negligible. If the electron density were appreciable, the ions would recombine before they had fallen back into the star. In such a case, however, the number of atoms in the line of sight would be much greater either than the observed line profiles would indicate or than the available radiation pressure would support. Hence the atoms must return to the star as ions.

The proposed model therefore consists of a sort of ionization cycle, the neutral atoms rising, the ionized ones returning.[25] Such a process is possible only if neither the ionizations nor the recombinations take place too rapidly. These restrictions provide upper limits on both the density of atoms in the shell and the amount of ionizing radiation incident on the shell.

Let us assume that the outgoing atoms are ionized when they have a velocity V and that they then decelerate under gravity and return to the star in a time which will be at least $2V/g$, where g is the acceleration of gravity. The condition that most of the ions do not recombine with electrons until they have returned to the reversing layer gives the restriction that $P_r 2V/g < 1$, where P_r is the probability of recombination per ion per unit time. If we replace the ionizing transitions by a single line of wave length λ_i corresponding to an ionization potential E_{vi} e.v., then we may calculate P_r from the Saha ionization equation, the probability of ionization, and the principle of detailed balancing in thermodynamic equilibrium. In this way we find, letting f equal the upward oscillator strength of the ionizing transition, and equating the internal partition functions of the neutral and ionized atom,

$$P_r = \frac{3f\omega_{el}}{2}\left(\frac{h^2}{2\pi m_e k T_V}\right)^{3/2} n_e = 2.5 \cdot 10^{-14} n_e f \theta_V^{3/2} E_{vi}^2 , \qquad (16)$$

[25] This applies to lines absorbed by neutral atoms. In the case of the *Ba* II and *Sr* II lines the asymmetries are presumably produced by a shell of outward-moving singly ionized atoms, the doubly ionized ones falling back to the surface.

where ω_{cl} is the classical damping constant, T_V is the temperature characterizing the relative motion[26] of ions and electrons, θ_V is defined as $5040/T_V$, and n_e is the number of free electrons per cubic centimeter. If we assume that n_e is roughly constant along the path of the moving atoms, the restriction on $P_{r2}V/g$ yields

$$Vn_e < 2.0 \cdot 10^{13} \frac{g}{f\theta_V^{3/2}E_{vi}^2} . \tag{17}$$

For the three supergiant stars observed, g is approximately 10 cm/sec^2; if we set $E_{vi} = 6$, $f = 0.1$, and $\theta_V = 1.6$ (corresponding to $T_V = 3100°$), (17) gives $Vn_e < 2.8 \times 10^{13}$/cm^2 sec. Since actually $P_{r2}V/g$ must be considerably less than unity if no asymmetries to the red are to be observed, we may take 10^{13} as an upper limit for Vn_e. If V is equal to 20 km/sec, this gives $n_e < 5 \cdot 10^6$; if hydrogen atoms are predominant, this corresponds to densities of 10^{-17} gm/cm^3.

To derive an upper limit for the energy density of ionizing radiation, we consider a simplified case in which atoms stream from the reversing layer at some constant velocity V and become ionized with a probability P_i per unit time. If $n_a(h)$ represents the number of neutral atoms of a particular element per cubic centimeter as a function of the height h above the reversing layer, and N_a, as in (14), equals the total number of outward-moving neutral atoms per square centimeter, then

$$N_a = \int_0^\infty n_a(h)dh = n_a(0) \int_0^\infty e^{-P_i t(h)} dh , \tag{18}$$

and, since we assume that $V(h)$ is constant,

$$t(h) = \frac{h}{V} ; \qquad N_a = \frac{Vn_a(0)}{P_i} . \tag{19}$$

It is known that for an upward transition of oscillator strength f and energy E_{vi} e.v. the transition probability is given by

$$P_i = 3\omega_{cl} f \, 10^{-E_{vi}\theta} , \tag{20}$$

[26] V is not to be confused with the initial velocity of the outgoing stream of atoms; the latter is much greater than the relative velocity of ions and electrons in the same stream.

provided that $E_{vi}\theta > 1$; θ, or $5040/T$, characterizes the energy density of the radiation producing the transition. We again replace all ionizing transitions by a single transition; substituting (20) into (19) and solving for θ, which in this case corresponds to an ultraviolet temperature T_{uv} and will be denoted by θ_{uv}, we have

$$\theta_{uv} = \frac{1}{E_{vi}} \left\{ 7.64 + \log \frac{N_a}{V n_a(0)} + \log f + 2 \log E_{vi} \right\}. \qquad (21)$$

Assuming $f = 0.1$, $N_a = 2 \times 10^{13}$, and taking for $V n_a(0)$ the value 10^{13} derived above for $V n_e$, we find that for $E_{vi} = 5.1$ and 13.1 e.v., respectively, $\theta_{uv} = 1.6$ and 0.70. The temperatures corresponding to the ionization of Na and H are accordingly 3100° and 7200°, respectively. Since $V n_a(0)$ can be very much less than 10^{13}, these are clearly upper limits for T_{uv}.

The fact that these ultraviolet temperatures vary so with the ionization potential E_{vi} need not be particularly surprising in view of the general lack of equilibrium. Also, it is not unreasonable to expect that the intensity of ultraviolet radiation should be very much less in the extreme outermost layers of a supergiant atmosphere than in the reversing layer and the photosphere.

These upper limits on $V n_e$ and T_{uv} are rough approximations and depend on several simplifying assumptions. If, however, the tentative model of a fountain atmosphere—the neutral atoms rising, the ionized ones decelerating and falling—is essentially a correct explanation of the line asymmetries, then these limits should be roughly correct.

The dynamical explanation for the existence of such an atmosphere is a rather more difficult problem. Such an explanation is presumably connected with the fact that the line asymmetries are observed in only the most extensive of the stars observed, and that these stars are the ones which show large turbulent velocities. There are two obvious possibilities. First, the very presence of high velocities in the reversing layer might explain the existence of a shell of outward-moving atoms, since the atoms with the largest outward velocity would naturally rise highest in the atmosphere. Second, the surface gravity of these stars is so low that radiation pressure is rela-

tively very great. The ratio of radiation pressure to gravity for an atom of α Orionis exposed to the full continuous background varies from 360 for an atom of neutral manganese to 18,000 for a neutral potassium atom. It seems likely, therefore, that radiation pressure will certainly play a part in any complete theory of the structure of supergiant atmospheres.

In any case, it is not difficult to see why asymmetrical lines should be observed in only a few exceptional stars. The disappearance of turbulence, the increase of surface gravity, an increase in the free electron density in the shell, an increase in the intensity of ionizing radiation in the shell—any of these changes might render impossible an ionization cycle of the type discussed here and might thus eliminate the effects discussed in section V. In view of the general variability of late-type supergiant stars, both in magnitude and in radial velocity, any variation of these asymmetries with time need also occasion no surprise.

It is a pleasure to close with an expression of sincere appreciation for the assistance received in the course of this research. The author is very much indebted to Dr. Adams and the staff of the Mount Wilson Observatory, both for the generous offer of such valuable observational material and for the helpful advice and co-operation which were constantly available. Particular thanks are due to Professor Russell for many helpful discussions on numerous problems; Professor Stewart and Dr. Wildt have also contributed several valuable suggestions.

Carnegie Institution of Washington
Mount Wilson Observatory,

Princeton University Observatory
July 1939

ON THE STABILITY OF SPHERES OF SIMPLE MECHANICAL FLUID HELD TOGETHER BY NEWTONIAN GRAVITATION

RICHARD C. TOLMAN

ABSTRACT

A sphere of simple mechanical fluid held together by Newtonian forces of gravitation will be in stable equilibrium if its total potential energy is a minimum. Using the principles of the calculus of variations, it is shown that any equilibrium distribution of fluid would, in general, automatically satisfy all tests for a minimum except that of Jacobi as to the location of conjugate points. The circumstances which lead to failure of the Jacobi test and the consequences which arise from such failure are discussed and illustrated.

1. *Introduction.*—In the case of spheres of fluid held together by gravitational attraction, the condition for hydrostatic equilibrium consists in an increase of pressure with depth, as we proceed inward from the surface of the sphere, at just the rate necessary to support the gravitational forces acting on the fluid. Using Newtonian gravitational theory, this condition for hydrostatic equilibrium is expressed by the equation

$$\frac{dp}{dr} = -G\frac{m\rho}{r^2}, \tag{1.1}$$

where p and ρ are the pressure and density of the fluid at any distance of interest r from the center of the sphere, m is the mass of fluid inside this radius, and G is the constant of gravitation. Although a distribution of fluid which satisfies the condition given by equation (1.1) is necessarily in a condition of mechanical equilibrium, further investigation is necessary to determine whether the equilibrium would be mechanically stable against displacements of the distribution. This circumstance was specially emphasized by Landau,[1] who gave a simple argument showing in the special case of Emden's so-called "polytropic spheres," composed of fluid obeying an "equation of state" of the form $p = \kappa\rho^{\gamma}$, that an equilibrium distribution of fluid satisfying equation (1.1) would be unstable when the constant γ is less than $4/3$. It is the purpose of the present article to in-

[1] *Phys. Zs. der Sowjetunion*, 1, 285, 1932.

vestigate the fundamental nature of the conditions which determine stability of equilibrium in spheres of fluid held together by Newtonian forces of gravitation, and to determine in the case of instability the type of displacement which would be sufficient to make the sphere depart from its equilibrium configuration.

In Part I of this article we shall proceed, as far as possible, with a general analysis of the stability of fluid spheres, making the assumption that the fluid is of a simple mechanical nature such that its pressure p is a definite function of its density ρ, but without introducing any special assumption as to the particular form of the "equation of state" connecting those two variables. We shall base the analysis on the principle that the total potential energy of the fluid—mechanical plus gravitational—must be a minimum toward small variations in the distribution of the fluid if the sphere is to be in *stable equilibrium*. This application of a well-known general principle of mechanics finds its immediate justification in the present example in the consideration that the existence of any diminution in potential energy, accompanying a small displacement in the distribution of fluid in the sphere, would provide the necessary kinetic energy to increase the extent of displacement.

To carry through the analysis, we shall first need an expression for the total potential energy of the sphere. This we shall be able to obtain in the form of an integral over the contents of the sphere, depending on one independent variable, the distance from the center of the sphere r over which the integration is taken, and on one dependent variable together with its first derivative, the mass m of fluid out to any particular value of r. The integral thus has the form commonly treated in the calculus of variations, and we can apply to it the known tests for a minimum, when the distribution of fluid is subjected to small variations.[2]

We shall first consider the tests for a minimum which would apply when variations in the distribution of fluid are contemplated which do not alter the total radius of the sphere r_b, locating the boundary of the fluid. We shall then find that the integral which expresses the potential energy would automatically satisfy (*a*) the Euler test for

[2] See, e.g., Bolza, *Lectures on the Calculus of Variations*, reprint of edition of 1904, New York, 1931, and *Vorlesungen über Variationsrechnung*, Leipzig, 1909; Bliss, *Calculus of Variations*, Chicago, 1925; and Forsythe, *Calculus of Variations*, Cambridge, 1927.

an extremum toward small variations, this being equivalent to the condition (1.1) for hydrostatic equilibrium; (*b*) the Legendre test, necessary for the extremum to be a minimum toward weak variations; and (*c*) the Weierstrass test, necessary for a minimum toward strong variations. Hence, in accordance with the calculus of variations—neglecting the special case of a pair of conjugate points located exactly at the limits of integration—the potential energy would or would not be a minimum toward small variations which do not alter the total radius, depending (*d*) on the satisfaction or failure of the Jacobi test, which requires that the range of integration should include no pair of conjugate points.

We shall next consider, in the case of spheres of finite size, the additional tests which would apply when alterations in the total radius of the sphere are contemplated. For this purpose we shall examine the change in the integral of potential energy when we change to neighboring distributions of the fluid which leave the Euler test satisfied but change the radius r_b of the boundary. We shall then find (*e*) that the integral would, in any case, automatically satisfy the so-called "transversality condition" that the value of its first derivative with respect to the radius r should be zero at $r = r_b$ and could also be expected, at least in general, to satisfy the further condition that its value would actually increase when a small finite change is made in the radius r_b of the boundary. We shall therefore conclude, also when changes in the radius of the boundary are permitted, that the Jacobi test—at least in typical cases—would still remain as a necessary and sufficient condition for minimum potential energy.

Having thus found that the equilibrium would be stable or unstable according as the Jacobi test is or is not satisfied, we shall then conclude Part I by setting up, in the general form appropriate for the present problems, the Jacobi differential equation whose solutions determine the location of conjugate points, and by making some qualitative remarks as to the kind of circumstances which might be expected to lead to failure of the Jacobi test and as to the kind of instability which would then arise.

In Part II we shall undertake the treatment of spheres of fluid obeying the Emden "equation of state," $p = \kappa\rho^{\gamma}$, since it is only by considering some specific equation of state that actual applications of the Jacobi test can be made. After presenting the so-called "Emden

differential equation" which determines the equilibrium distribution of such a fluid, we shall proceed to obtain expressions for the potential energy of such a fluid, both for the special case of equilibrium and for the more general case of any spherically symmetrical distribution. We shall first use the equilibrium expression to show, in any case when $\gamma < 4/3$, that the potential energy for an equilibrium distribution of the kind of fluid under discussion would actually be greater than the potential energy if the fluid were dispersed to infinity. We shall then use the general expression for potential energy to give a somewhat more detailed exposition of Landau's original argument showing, when $\gamma < 4/3$, that a particular kind of variation in the distribution of fluid can be found toward which the potential energy would exhibit at equilibrium the properties of a maximum rather than a minimum, thus demonstrating the necessary existence of instability in such cases.

Finally, we shall consider the relation of the Jacobi test, as a general condition for stability in fluid spheres, to Landau's finding that spheres of fluid obeying the "equation of state" $p = \kappa\rho^{\gamma}$ would, in any case, be unstable when $\gamma < 4/3$. For this purpose we shall substitute the consequences of the Emden "equation of state" into our previously obtained form of the Jacobi differential equation whose solutions determine the location of conjugate points. The equation thus obtained is a difficult one to handle, but it will prove possible to obtain explicit analytic solutions for the cases $\gamma = \infty$, $\gamma = 2$, $\gamma = 4/3$, $\gamma = 6/5$, and for a class of singular distributions of fluid which exist with $\gamma < 4/3$. In pleasing agreement with expectation we shall find that there is no point conjugate to the center lying within the boundary of the sphere for the cases where $\gamma > 4/3$, that a point conjugate to the center appears just at the boundary of the sphere when we reach the critical case $\gamma = 4/3$, and that there is at least one point conjugate to the center within the boundary for the cases where $\gamma < 4/3$.

We shall then conclude with some remarks as to the possibility of extending the considerations of the present article to more complicated cases.

PART I. GENERAL TREATMENT

2. *The condition of mechanical equilibrium.*—Since fluids cannot withstand transverse stress, the state of equilibrium for a gravitating

mass of fluid will be characterized by spherical symmetry. The condition for mechanical equilibrium, at any distance r from the center, can then be obtained by equating the difference in total pressure, acting on the two surfaces of a spherical shell of the fluid of thickness dr, to the gravitational force acting on that shell. The result thus obtained has already been given by the so-called "equation of hydrostatic equilibrium" (1.1). For our further purposes it will be convenient to assume units of mass, which make the gravitational constant G equal to unity, and to re-write this equation in the form

$$\frac{1}{\rho}\frac{dp}{dr}+\frac{m}{r^2}=0\,, \tag{2.1}$$

where ρ and p are the density and pressure of the fluid at the radius r of interest, and m is the mass of fluid *inside* that radius. In what follows we shall be concerned with distributions of fluid which satisfy the foregoing necessary and sufficient condition for mechanical equilibrium (2.1) and, in investigating the stability of the equilibrium, shall evidently only have to consider the effect of displacements in the distribution which preserve spherical symmetry.

Although equation (2.1) applies to the hydrostatic equilibrium of fluids in general, our present treatment will deal only with *simple mechanical fluids*, where the pressure can be regarded as a definite function of the density, in accordance with some "*equation of state*" of the general form

$$p=p(\rho)\,, \tag{2.2}$$

where, however, we shall in any case assume that we shall have $p\geqq 0$, $\rho\geqq 0$, and $dp/d\rho\geqq 0$, in accordance with the physical character of our spheres of fluids and with a necessary character of the dependence of pressure on density if we are to have any possibility at all for stability.

In carrying out the treatment it will be useful to note that we can express the *density of the fluid*, at any point in the distribution, in terms of the increase in mass with radius, by the equation

$$\rho=\frac{1}{4\pi r^2}\frac{dm}{dr}=\frac{m'}{4\pi r^2}\,, \tag{2.3}$$

where we use an accent to denote differentiation with respect to r.

3. *The potential energy expressed as an integral over the sphere.*—In the case of a sphere of simple mechanical fluid it is convenient to choose the zero of potential energy as corresponding to a condition of such complete dispersion that the pressure and gravitational forces acting on the fluid can be taken as having gone to zero, and then to treat the potential energy as the sum of the amounts of work which would have to be done against the mechanical forces of pressure and against the gravitational forces of attraction to transfer the fluid to the condition which it has in the sphere. It will be noted that the mechanical part of the potential energy will then be positive and the gravitational part negative.

To calculate the *mechanical part* of the potential energy, it is convenient to begin by considering the mechanical potential energy u per unit mass of the fluid at any density ρ of interest. For this we can write

$$u = -\int_{\rho_0}^{\rho} p d\left(\frac{1}{\rho}\right) = \int_{\rho_0}^{\rho} \frac{p}{\rho^2}\, d\rho\,, \tag{3.1}$$

where we integrate the work done in compressing unit mass of the fluid from the density ρ_0, which it has when the pressure p is zero, to the density of interest ρ. In accordance with the assumed dependence of pressure on density (2.2), it will be noted that u can be regarded as a function of ρ, with the derivative

$$\frac{du}{d\rho} = \frac{p}{\rho^2}\,. \tag{3.2}$$

And in accordance with the dependence of density in the sphere on radius and rate of change of mass therewith as given by (2.3), it will be noted that u can also be regarded within the sphere as a function of r and m' with a partial derivative with respect to the latter quantity satisfying

$$\frac{\partial u}{\partial m'} = \frac{du}{d\rho}\frac{\partial \rho}{\partial m'} = \frac{p}{4\pi r^2 \rho^2}\,. \tag{3.3}$$

In terms of the mechanical potential energy u per unit mass, we can now write, as the desired expression for the total mechanical potential energy,

$$U_{\text{mech}} = 4\pi \int_0^{r_b} u\rho r^2 dr = \int_0^{r_b} u m' dr\,, \tag{3.4}$$

where we integrate over the whole sphere from the center $r = 0$ to the boundary $r = r_b$. As a result of the discussion given above to the quantity u, it will be noted that the integrand in (3.4) can be regarded as a function of r and m'.

To calculate the *gravitational part* of the potential energy, it is convenient to consider the work against gravitational forces which would be needed to remove the material in the sphere, layer by layer, to infinity. In this way we readily obtain the desired expression

$$U_{\text{grav}} = -4\pi \int_0^{r_b} \frac{m}{r} \rho r^2 dr = -\int_0^{r_b} \frac{mm'}{r}\, dr\,, \tag{3.5}$$

where we again integrate over the whole sphere from $r = 0$ to $r = r_b$. The integrand is this time a function of r, m, and m'.

Adding (3.4) and (3.5), we now have the desired expression for the *total potential energy*,

$$U = \int_0^{r_b} \left(um' - \frac{mm'}{r} \right) dr\,. \tag{3.6}$$

This gives the integral which must be a minimum toward small variations in the distribution of fluid if the equilibrium is to be stable. The integrand in the expression which is to be a minimum,

$$f = um' - \frac{mm'}{r}\,, \tag{3.7}$$

is seen to be a function of the independent variable r and of the dependent variable m and its derivative m'. With respect to these latter quantities, it has the first and second partial derivatives

$$f_m = \frac{\partial f}{\partial m} = -\frac{m'}{r}\,, \tag{3.8}$$

$$f_{m'} = \frac{\partial f}{\partial m'} = m' \frac{\partial u}{\partial m'} + u - \frac{m}{r} = \frac{p}{\rho} + u - \frac{m}{r}\,, \tag{3.9}$$

$$f_{mm} = \frac{\partial^2 f}{\partial m^2} = 0\,, \tag{3.10}$$

$$f_{mm'} = \frac{\partial^2 f}{\partial m \partial m'} = -\frac{1}{r}\,, \tag{3.11}$$

$$f_{m'm'} = \frac{\partial^2 f}{\partial m'^2} = \frac{\partial}{\partial m'} \left(m' \frac{\partial u}{\partial m'} + u \right) = \frac{1}{4\pi r^2 \rho} \frac{dp}{d\rho}\,, \tag{3.12}$$

where use has been made of (2.3) and (3.3) in obtaining alternative forms of expression. We are now ready to apply the known tests for a minimum furnished by the principles of the calculus of variations, beginning with a discussion of the conditions for a minimum when the radius r_b of the boundary is not subject to variation, and postponing until section 7 a discussion of the additional conditions which must be satisfied when variations in r_b are also permitted.

4. *The Euler test.*—The first test to be considered is the well-known one of Euler, which in the present example requires the validity of the equation[3]

$$\frac{d}{dr}\frac{\partial f}{\partial m'} - \frac{\partial f}{\partial m} = 0 . \tag{4.1}$$

We readily find that this equation is valid, however, since it proves to be equivalent to the condition for hydrostatic equilibrium.

To show this we have merely to substitute (3.8) and (3.9) into the left-hand side of (4.1) and to make use of (3.2) to cancel two of the terms which appear. We thus obtain

$$\left.\begin{aligned} \frac{d}{dr}\frac{\partial f}{\partial m'} - \frac{\partial f}{\partial m} &= \frac{d}{dr}\left(\frac{p}{\rho} + u - \frac{m}{r}\right) + \frac{m'}{r} \\ &= \frac{1}{\rho}\frac{dp}{dr} - \frac{p}{\rho^2}\frac{d\rho}{dr} + \frac{du}{d\rho}\frac{d\rho}{dr} + \frac{m}{r^2} - \frac{m'}{r} + \frac{m'}{r} \\ &= \frac{1}{\rho}\frac{dp}{dr} + \frac{m}{r^2} = 0 . \end{aligned}\right\} \tag{4.2}$$

This is seen to be our previous equation for hydrostatic equilibrium (2.1), which holds in any case of equilibrium, whether stable or unstable.

The satisfaction of the Euler test is a necessary requirement in order that the potential energy, as given by (3.6), should be an extremum toward small variations in the distribution of mass m, which vanish at the limits of any range of integration that we desire to test.

5. *The Legendre test.*—The second test to be considered is that of Legendre, which is necessary if the integral is to be, in particular, a

[3] See, e.g., Bliss, *op. cit.*, p. 130.

minimum toward weak variations. In the present example it requires the validity of the expression[4]

$$f_{m'm'}(r, m, m') \geqq 0 , \tag{5.1}$$

where we consider values of this second derivative, at any point in the distribution, as a function of the values of r, m, and of the slope m' at that point. We readily find that this expression is valid, however, since by substituting (3.12) it is seen to have the form

$$\frac{1}{4\pi r^2 \rho} \frac{dp}{d\rho} \geqq 0 , \tag{5.2}$$

where ρ is the density and $dp/d\rho$ is the rate of change of pressure with density, at any point r in the fluid. Since pressure increases with density for all actual one-phase fluids of interest, the test is satisfied in the stronger of the two forms, with the sign of inequality holding throughout.

The fact that this further test is satisfied with the sign of inequality shows that the potential energy will at least behave as a minimum toward variations in the distribution of mass m, which involve changes that are sufficiently small in m' as well as in m, and which do not extend over a range in r large enough to include conjugate points.

6. *The Weierstrass test.*—The third test to be considered is that of Weierstrass, which is necessary if the integral is to be a minimum toward strong, as well as toward weak, variations. In the present example it requires the validity of the expression[5]

$$f_{m'm'}[r, m, m' + \theta(M' - m')] \geqq 0 , \tag{6.1}$$

where we now consider values of this second derivative, at any point in the distribution, as a function of the actual values of r and m at that point and of an altered slope, which differs from that of the actual distribution m' by the arbitrary amount $[\theta(M' - m')]$, where M' is any physically realizable value of the increase in mass with radius and θ lies between zero and one. We readily see that this expression

[4] See, e.g., *ibid.*, p. 131.

[5] See, e.g., *ibid.*, p. 139.

is valid, however, since by substituting (3.12) it again reduces to the same form as (5.2)

$$\frac{1}{4\pi r^2 \rho} \frac{dp}{d\rho} \geqq 0 , \tag{6.2}$$

where ρ and $dp/d\rho$ are now the density and rate of change of pressure with density that correspond to the altered slope $m' + \theta(M' - m')$. Since ρ and $dp/d\rho$, however, would be positive for any physically possible rate of increase of mass with radius, we may conclude in the present case that the test is satisfied in the stronger of the two forms, with the sign of inequality holding throughout. It is of interest to note that the previous Legendre test may be regarded as the limiting case of the present Weierstrass test when θ goes to zero.

The fact that this further test is thus satisfied now shows that the potential energy will behave as a minimum toward any kind of small variations in the distribution of mass m which do not extend over a range in r large enough to include conjugate points. Hence—neglecting the special case of a pair of conjugate points located exactly at the limits of integration—the Jacobi test, which requires that no pair of conjugate points shall fall within the range of integration, provides, in accordance with the principles of the calculus of variation, the only further condition that must be satisfied actually to insure a minimum value of the potential energy toward variations in the distribution of the fluid that do not change the total radius of the sphere. The method of applying the Jacobi test will be discussed later, in section 8.

7. *The mobile-boundary tests.*—Up to this point we have considered the conditions for minimum potential energy when variations are made in the distribution of fluid which do not alter the total radius of the sphere. To include the possibility of alterations in the radius r_b in our considerations, let us now examine the potential energy,

$$U = \int_{r=0}^{r=r_b} f(r, m, m')dr , \tag{7.1}$$

as a function of the limit of integration r_b, when we consider neighboring distributions of fluid, subject to the condition that the various

distributions shall in each case satisfy the Euler test for an extremum, and subject to the further condition that the connection between mass and radius at the boundary must necessarily satisfy the equation

$$\tilde{m} = \text{constant}, \tag{7.2}$$

since we have a definite amount of fluid available.

Differentiating (7.1) with respect to r_b, we then obtain, for the first derivative of U with respect to r_b, an expression of the known form[6]

$$\frac{dU}{dr_b} = f(r, m, m') + (\tilde{m}' - m')f_{m'}, \tag{7.3}$$

where the values of the two terms are to be taken at the boundary $r = r_b$, the first term arising directly from the differentiation of the upper limit of the integral, and the second term arising from the differentiation behind the integral sign, taking r_b as a parameter which determines the form of $f(r, m, m')$, and making use of the circumstance that the form of f is, by hypothesis, such as to satisfy the condition for an extremum given by the Euler equation (4.1). Noting from equation (7.2) that the curve determining the possible boundary values of m and r is a straight line for which the value of the derivative $\tilde{m}'$ is identically equal to zero, and substituting from (3.7) and (3.9), we can now reduce (7.3) to the form

$$\frac{dU}{dr_b} = um' - \frac{mm'}{r} - m'\left(m'\frac{\partial u}{\partial m'} + u - \frac{m}{r}\right) = -m'^2\frac{\partial u}{\partial m'}. \tag{7.4}$$

Making use of (2.3) and (3.3), and remembering that we are to take the value of the right-hand side at the boundary of the distribution, we can then finally re-express this result in the physically more significant form

$$\frac{dU}{dr_b} = -4\pi r_b^2 p_b, \tag{7.5}$$

where r_b and p_b are the values of the radius and pressure at the boundary of the distribution.

[6] See, e.g., Bolza, *Lectures*, p. 106, eq. 32.

In the first place, this expression immediately shows that the first derivative of the potential energy with respect to the boundary radius will have the value zero, in the case of any finite isolated sphere of fluid in a condition of equilibirum which we wish to test for stability, since the pressure p_b at the boundary will then be zero, owing to the circumstance that there will be no fluid beyond the boundary to exert pressure thereon. The so-called "transversality condition" for a minimum, that the first derivative of the integral with respect to a mobile limit should be equal to zero, is thus immediately satisfied.

In the second place, the foregoing expression also shows that we can usually expect the potential energy actually to increase when we change to a neighboring distribution of different boundary radius, which still satisfies the Euler test for an extremum, since, on physical grounds, we can then usually expect an increase in boundary pressure when we make a small finite decrease in boundary radius; and this, in accordance with (7.5), will lead to an increase in potential energy. For example, in the case of the Emden spheres of fluid, obeying an equation of state of the form $p = \kappa\rho^\gamma$, which will be treated in Part II of this article, it can readily be shown that the pressure at the boundary would, in general, have to be increased above zero if we should change to a neighboring Emden solution with the same mass of fluid in a smaller radius, this result occurring not only in the cases $\infty > \gamma > 4/3$, which lead to stable equilibrium, but also in the cases $4/3 > \gamma > 6/5$, which lead to unstable equilibrium, the only exception—with the boundary pressure remaining equal to zero—occurring in the special case $\gamma = 4/3$, which leads to neutral equilibrium. Hence, we shall take as the "typical cases" that concern us those in which the potential energy would be increased by the above-described kind of change from the original boundary radius.

In accordance with the foregoing, we now have the following situation when the original integral of potential energy does satisfy the Jacobi test as to conjugate points. The potential energy of the original equilibrium distribution of fluid will then be less than that of any varied distribution of fluid with the same boundary radius r_b, since the Euler, Legendre, and Weierstrass tests for a minimum are automatically satisfied. The potential energy of the original distribution,

as we have just seen above, will also in general be less than that for a varied distribution which still satisfies the Euler test for an extremum but has a slightly altered boundary radius. The potential energy for this extremal distribution with altered boundary radius will, however, also in general be less than that for any varied distribution with the new boundary radius, since we note that the Legendre and Weierstrass tests will automatically continue to be satisfied, and since by continuity considerations we may prove that the Jacobi test will also continue to be satisfied, owing to the small variation from a distribution which by hypothesis does not entail conjugate points within the range of integration. Hence, we are now led to the desired conclusion that the Jacobi test—neglecting the special case of a pair of conjugate points located just at the limits of integration—will remain, in typical cases, as the necessary and sufficient condition for minimum potential energy, also even when changes in the boundary radius are permitted.

8. *The Jacobi test.*—Having thus found that we can expect the equilibrium in general to be stable or unstable according as the Jacobi test is or is not satisfied, we must now inquire into the location of conjugate points, since the test requires that no pair of such points should be included within the range of integration—except possibly at the limits of integration—if the potential energy is to be a minimum. In the present example the location of conjugate points would depend on the behavior of a quantity $z(r)$, which is defined by the differential equation[7]

$$\frac{d}{dr}\left(f_{m'm'}\frac{dz}{dr}\right)+\frac{df_{mm'}}{dr}z-f_{mm}z=0\,. \tag{8.1}$$

Solving this equation, with boundary conditions so chosen as to make $z = 0$ at any initial point of interest r_1 but not identically equal to zero as we proceed therefrom, the nearest point in either direction conjugate to r_1 would then be, by definition, the first point r_2 in that direction where z again becomes equal to zero. It is to be remarked in this connection, as a consequence of the linear, homogeneous, second-order character of (8.1) and of the separation theorem which ap-

[7] See, e.g., Forsythe, *op. cit.*, §§ 18 ff.

plies to the roots of such equations, that the location of such a conjugate point r_2 would be independent of the particular value assigned to the initial slope at r_1, and that no other pair of points conjugate to each other could lie within such a range r_1 to r_2.

Substituting for f_{mm}, $f_{mm'}$, and $f_{m'm'}$ the values given by (3.10–11–12), the Jacobi equation (8.1) can be re-written in the present case in the form

$$\frac{d}{dr}\left(\frac{1}{4\pi r^2 \rho}\frac{dp}{d\rho}\frac{dz}{dr}\right) + \frac{z}{r^2} = 0 . \tag{8.2}$$

Actual solutions of this equation can, of course, be obtained only when we have some specific dependence of ρ on r and p on ρ. It hence becomes necessary to make a separate application of the Jacobi test to each particular equilibrium distribution of fluid which we wish to study. In Part II we shall make such separate applications of the Jacobi test to different distributions of fluid obeying "equations of state" of the Emden form.

Before proceeding to these specific applications, however, it is of interest to point out that we can already obtain a qualitative idea of the kind of circumstances which may be expected to lead to instability. In accordance with the form of the differential equation (8.2) for the quantity z, the zeros of which determine the location of conjugate points, it will be seen that the frequency of oscillation of z will depend qualitatively on the ratio

$$\frac{\frac{1}{r^2}}{\frac{1}{4\pi r^2 \rho}\frac{dp}{d\rho}} = \frac{4\pi\rho}{\frac{dp}{d\rho}} \tag{8.3}$$

and will tend to be large for large values of ρ and small values of $dp/d\rho$. Furthermore, in agreement with the evident expression for central pressure

$$p_c = -\int_0^{r_b} \frac{dp}{d\rho}\frac{d\rho}{dr}\,dr , \tag{8.4}$$

we see that the distance from the center to the boundary of the distribution will tend to be large for large values of p_c and small values of $dp/d\rho$. Hence, in a rough way we can already say that high central density, high central pressure, and high compressibility will be the

factors which tend to make a point conjugate to the center appear before reaching the boundary, and thus to lead to instability.

It is also of interest to emphasize, as a consequence of the character of the Jacobi test, that a failure of the test in the present application, with a point conjugate to the center lying inside the boundary of the fluid, definitely implies that the potential energy of the fluid at equilibrium is neither a true minimum nor a true maximum. Under such circumstances we may then expect to find some kinds of displacement toward which the potential energy at equilibrium would exhibit the properties of a minimum, and others (see later remarks in connection with [10.13]) toward which the potential energy would actually exhibit the properties of a maximum.

In connection with failure of the Jacobi test, however, it is to be emphasized that we must regard the kinds of displacements toward which the potential energy fails to continue to exhibit the properties of a minimum as forming only a limited class. Displacements which lead to such failure have to extend over the whole range between conjugate points and must be of an appropriate character over that range.[8] A simple example is provided by the case of geodesics on the surface of a sphere. In this case conjugate points are antipodal to each other, and a geodesic—i.e., the arc of a great circle—which passes more than halfway around the sphere fails to exhibit the properties of minimum length only toward displacements which are appropriately chosen over the whole range between antipodal points. Hence, returning to the situations of present interest, it may be said in a somewhat rough way, in the case of failure of the Jacobi test, that the chance for a fluctuation in fluid distribution leading to decreased potential energy would increase as the conjugate points come nearer together. Thus we may regard the proximity of conjugate points as a rough measure of degree of instability.

PART II. APPLICATIONS TO POLYTROPIC SPHERES

9. *Emden's equations.*—In accordance with the terminology of Emden,[9] equilibrium distributions of fluid may be called polytropic when the fluid satisfies an "equation of state" of the form

$$p = \kappa\rho^{\gamma} = \kappa\rho^{1+1/n}, \tag{9.1}$$

[8] See, e.g., Bolza, *Vorlesungen*, § 14.

[9] *Gaskugeln*, Leipzig, 1907.

with

$$n = \frac{1}{\gamma - 1}, \tag{9.2}$$

where p and ρ are the pressure and density of the fluid and κ and γ, or κ and n, are parameters that depend on the properties of the fluid, n being called the "index of the polytrope."

Substituting (9.1) into (2.1), the condition for hydrostatic equilibrium in such a distribution can be written in the form

$$\kappa\gamma\rho^{\gamma-2}\frac{d\rho}{dr} + \frac{m}{r^2} = 0\,; \tag{9.3}$$

or, differentiating with respect to r, noting (2.3), this can also be written in the more convenient form

$$\frac{d}{dr}\left(r^2\rho^{\gamma-2}\frac{d\rho}{dr}\right) + \frac{4\pi\rho r^2}{\kappa\gamma} = 0\,. \tag{9.4}$$

Analytic solutions of this equation will be found in Emden's treatise for the cases $\gamma = \infty$, 2, and $6/5$, when ρ is taken as finite and $d\rho/dr$ as zero at the center, and for all cases $\gamma < 4/3$, when ρ is taken as infinite at the center. Numerical quadratures will be found for other cases.

10. *The potential energy of a polytropic sphere.*—Useful expressions for the potential energy of a spherical distribution of fluid, obeying the Emden "equation of state," can be readily obtained both for the general case in which the distribution is not necessarily in equilibrium and for the special case of equilibrium.

For the *mechanical* potential energy per unit mass of the fluid at density ρ, we can evidently write, in accordance with (3.1) and (9.1),

$$u = \int_{\rho_0}^{\rho}\frac{p}{\rho^2}\,d\rho = \int_{\rho_0}^{\rho}\kappa\rho^{\gamma-2}d\rho = \frac{\kappa}{\gamma - 1}\,(\rho^{\gamma-1} - \rho_0^{\gamma-1})\,. \tag{10.1}$$

Furthermore, since we shall continue to choose the zero of potential energy as corresponding to such complete dispersion that the pressure and gravitational forces acting on the fluid have gone to zero, and since in accordance with (9.1) the density ρ_0 will be zero when

the pressure p is zero, this expression reduces, with $\gamma > 1$, to the simple form[10]

$$u = \frac{\kappa}{\gamma - 1} \rho^{\gamma - 1} . \tag{10.2}$$

For the physically less interesting case $\gamma < 1$, equation (10.1) would give $u = +\infty$ for any finite value of ρ, which makes further computations for that case unnecessary. Substituting (10.2) into (3.4), we then obtain

$$U_{\text{mech}} = \frac{4\pi}{\gamma - 1} \int_{r=0}^{r=r_b} \rho^{\gamma} r^2 dr \tag{10.3}$$

as the desired expression for the total mechanical potential energy when $\gamma > 1$. With $\gamma < 1$ the value of U_{mech} would be positive infinite.

For the *gravitational* potential energy we can write, in accordance with (3.5), the *general* expression

$$U_{\text{grav}} = -4\pi \int_0^{r_b} \frac{m}{r} \rho r^2 dr , \tag{10.4}$$

where m is the mass of fluid inside the radius r. Substituting for m from (9.3), we can also write for the more special case of an *equilibrium* distribution of fluid, obeying the Emden "equation of state,"

$$\left.\begin{aligned} U_{\text{grav}} &= 4\pi \int_0^{r_b} \kappa\gamma \rho^{\gamma - 1} \frac{d\rho}{dr} r^3 dr \\ &= 4\pi\kappa\rho^{\gamma} r^3 \Big|_{r=0}^{r=r_b} - 12\pi\kappa \int_0^{r_b} \rho^{\gamma} r^2 dr \\ &= -12\pi\kappa \int_0^{r_b} \rho^{\gamma} r^2 dr , \end{aligned}\right\} \tag{10.5}$$

where the integrated term in the second form of writing drops out, since $r = 0$ at one limit and $\rho^{\gamma} = 0$ at the other.

[10] It is of interest to note that the variable u, introduced in the present treatment to denote the potential energy per unit mass of the fluid, turns out to be proportional to the variable u, introduced in Emden's treatment from a different point of view.

Adding (10.3) first to (10.4) and then to (10.5), we now obtain

$$U = \frac{4\pi}{\gamma - 1} \int_0^{r_b} \rho^\gamma r^2 dr - 4\pi \int_0^{r_b} \frac{m}{r} \rho r^2 dr \,, \tag{10.6}$$

as the desired *general* expression for the total potential energy of a spherical distribution of fluid obeying the Emden "equation of state," and obtain

$$\left.\begin{aligned} U &= \frac{4\pi\kappa}{\gamma - 1} \int_0^{r_b} \rho^\gamma r^2 dr - 12\pi\kappa \int_0^{r_b} \rho^\gamma r^2 dr \\ &= \frac{4\pi\kappa(4 - 3\gamma)}{\gamma - 1} \int_0^{r_b} \rho^\gamma r^2 dr \end{aligned}\right\} \tag{10.7}$$

as the desired *special* expression when the distribution satisfies the conditions for equilibrium.

The special equilibrium expression for potential energy (10.7) shows that the potential energy of an equilibrium distribution of fluid obeying the Emden equation of state would be a finite positive quantity with $4/3 > \gamma > 1$, and the remarks made in connection with (10.3) show that the potential energy would be an infinite positive quantity with $\gamma < 1$. Thus, in any case with $\gamma < 4/3$, we see that the potential energy of the equilibrium distribution,whether stable or not toward small displacement, would actually be greater than if the fluid were dispersed to infinity.

The general expression for potential energy (10.6) can be used to show, in agreement with the original argument of Landau, that a type of displacement can be found when γ lies in the range $4/3 > \gamma > 1$, toward which the potential energy of the distribution would actually behave as having a maximum, rather than a minimum, value at equilibrium. For this purpose let us consider a "uniform" expansion (or contraction) of the sphere such that the radius r out to any specific particle in the fluid is increased in the ratio θ from its equilibrium value r_e. After such an expansion we can then write

$$r = \theta r_e \qquad \rho(r) = \theta^{-3}\rho_e(r_e) \,, \qquad m(r) = m_e(r_e) \tag{10.8}$$

for the new values of the quantities listed. Substituting in the general expression for potential energy (10.6), this gives us an expression of the form

$$U = \alpha\theta^{3-3\gamma} - \beta\theta^{-1} \tag{10.9}$$

for the potential energy of the expanded distribution, where α and $-\beta$ are the mechanical and gravitational parts of the potential energy at equilibrium. And making use of the ratio between those quantities, given by the expression for potential energy at equilibrium (10.7), this can be re-written in the form

$$U = \alpha[\theta^{3-3\gamma} - 3(\gamma - 1)\theta^{-1}], \tag{10.10}$$

with the derivatives

$$\frac{dU}{d\theta} = \alpha[-3(\gamma - 1)\theta^{2-3\gamma} + 3(\gamma - 1)\theta^{-2}] \tag{10.11}$$

and

$$\frac{d^2U}{d\theta^2} = 3\alpha(\gamma - 1)[(3\gamma - 2)\theta^{1-3\gamma} - 2\theta^{-3}]. \tag{10.12}$$

Substituting the value $\theta = 1$, which applies at equilibrium, we then finally obtain the desired expressions,

$$\frac{dU}{d\theta} = 0 \quad \text{and} \quad \frac{d^2U}{d\theta^2} = 3\alpha(\gamma - 1)(3\gamma - 4), \tag{10.13}$$

for the derivatives of U with respect to θ at the point of equilibrium. These then show that we have, indeed, found a type of displacement toward which the potential energy would exhibit at equilibrium a maximum, rather than a minimum, value when we proceed from values of $\gamma > 4/3$ to values lying in the range $4/3 > \gamma > 1$.

11. *Application of Jacobi test to polytropic spheres.*—It will now be of interest to apply the Jacobi test for a minimum of potential energy to different classes of polytropic sphere, since we have seen in Part I that this is the fundamental test which distinguishes between the stability and instability of equilibrium distributions of fluid, and since we can hope to gain a better understanding of the nature of

unstable distributions by examining the manner in which the Jacobi test then fails. The starting-point for the investigation is provided by the Emden "equation of state" (9.1), which describes the fluid to be considered,

$$p = \kappa \rho^{\gamma} ; \tag{11.1}$$

by the Emden differential equation (9.4), which describes the equilibrium distribution of fluid,

$$\frac{d}{dr}\left(r^2 \rho^{\gamma-2} \frac{d\rho}{dr}\right) + \frac{4\pi \rho r^2}{\kappa \gamma} = 0 ; \tag{11.2}$$

and by the Jacobi equation (8.2), the zeros of which determine the location of conjugate points, and which by the substitution of (11.1) can be written for our present purposes in the form

$$\frac{d}{dr}\left(\frac{\rho^{\gamma-2}}{r^2} \frac{dz}{dr}\right) + \frac{4\pi z}{\kappa \gamma r^2} = 0 . \tag{11.3}$$

We may now consider those cases in which it is possible to give a simple analytic treatment which will let us compare the distance from the center to the boundary of the sphere, as determined by (11.2), with the distance from the center to the first point conjugate thereto, as determined by (11.3).

Case $\gamma = \infty$, n = 0 (*incompressible fluid; stable*):

With

$$\gamma = \infty , \tag{11.4}$$

Emden's equation (11.2) has the known physically interesting solution

$$\rho = \text{constant} , \tag{11.5}$$

corresponding to a sphere of incompressible fluid with a radius determined by the total amount of fluid available. Substituting (11.4) and (11.5), the Jacobi equation (11.3) and its general solution can then be written in the forms

$$\frac{d}{dr}\left(\frac{1}{r^2} \frac{dz}{dr}\right) = 0 , \qquad z = C_1 + C_2 r^3 , \tag{11.6}$$

where C_1 and C_2 are arbitrary constants. Choosing C_1 equal to zero, so as to make $z = 0$ at the center, we see that z will never return to the value zero. Hence, in the present case there is no point conjugate to the center, and the distribution is in *stable* equilibrium.

Case $\gamma = 2$, n = 1 (*typical stable distribution*):

With

$$\gamma = 2 , \tag{11.7}$$

Emden's equation (11.2) has the known physically interesting solution

$$\rho = \text{constant} \frac{\sin \sqrt{\frac{2\pi}{\kappa}} r}{r} , \tag{11.8}$$

corresponding to a sphere of compressible fluid with a boundary at

$$r_b = \pi \sqrt{\frac{\kappa}{2\pi}} . \tag{11.9}$$

Substituting (11.7), the Jacobi equation assumes the form

$$\frac{d}{dr}\left(\frac{1}{r^2}\frac{dz}{dr}\right) + \frac{2\pi}{\kappa}\frac{z}{r^2} = 0 , \tag{11.10}$$

which has the general solution

$$z = C_1(\sin ar - ar \cos ar) + C_2(\cos ar + ar \sin ar) , \tag{11.11}$$

with

$$a = \sqrt{\frac{2\pi}{\kappa}}$$

and with C_1 and C_2 as arbitrary constants. Choosing C_2 equal to zero, so as to make $z = 0$ at the center, we see in the present case that z will return to that value when

$$\tan ar = ar , \qquad r = 4.4934 \sqrt{\frac{\kappa}{2\pi}} . \tag{11.12}$$

Since this value of r falls outside the boundary of the fluid as given by (11.9), we have a typical case of a sphere of compressible fluid in *stable* equilibrium.

Case $\gamma = 4/3$, n = 3 (*critical case; neutral equilibrium*):

With

$$\gamma = \tfrac{4}{3}\,, \tag{11.13}$$

Emden's equation (11.2) assumes the form

$$\frac{d}{dr}\left(r^2\rho^{-2/3}\frac{d\rho}{dr}\right) + \frac{3\pi\rho r^2}{\kappa} = 0\,, \tag{11.14}$$

and the Jacobi equation (11.3) assumes the form

$$\frac{d}{dr}\left(\frac{\rho^{-2/3}}{r^2}\frac{dz}{dr}\right) + \frac{3\pi z}{\kappa r^2} = 0\,. \tag{11.15}$$

In this case Emden's equation (11.14) has no simple analytic solution. Nevertheless, even though we cannot express ρ as a simple function of r, it is easy to see that the Jacobi equation (11.15) will have a solution which can be written in the form

$$z = \text{constant } r^3\rho\,, \tag{11.16}$$

since, by substituting (11.16) into (11.15) and performing the indicated operations, it is found that (11.15) then reduces to (11.14). We note that (11.16) would give one zero of z at the center where r is zero, and its next zero at the boundary of the distribution where ρ drops to zero, which, in accordance with Emden's numerical quadrature of (11.14), takes place at a finite distance r_b from the center. Hence, in this critical case, the conjugate point to the center lies just on the boundary of the distribution, and the Jacobi test for a minimum just fails, in agreement with the known circumstance that spheres of fluid for which $\gamma = 4/3$ are in *neutral* equilibrium with respect to "uniform" expansion or contraction.

Case $\gamma = 6/5$, n = 5 (*unstable equilibrium*):

With

$$\gamma = \tfrac{6}{5}\,, \tag{11.17}$$

Emden's equation (11.2) has the known physically interesting solution

$$\rho = C(1 + Br^2)^{-5/2} \qquad \text{with } B = \frac{2\pi C^{4/5}}{9\kappa}, \tag{11.18}$$

where C is the central density of the fluid and the distribution extends to $r_b = \infty$. Substituting (11.17) and (11.18), the Jacobi equation (11.3) then assumes the form

$$\frac{d}{dr}\left\{ \frac{C^{-4/5}(1 + Br^2)^2}{r^2} \frac{dz}{dr} \right\} + \frac{10\pi}{3\kappa r^2} z = 0, \tag{11.19}$$

which has a general solution of the form

$$z = C_1 z_1 + C_2 z_1 \int z_1^{-2} \frac{r^2}{(1 + Br^2)^2} dr, \tag{11.20}$$

where

$$z_1 = \frac{r^3 \left(1 - \frac{Br^2}{5}\right)}{(1 + Br^2)^{5/2}} \tag{11.21}$$

and C_1 and C_2 are arbitrary constants. Choosing C_2 equal to zero, so as to make $z = 0$ at the center, we see in the present case that z will again return to that value at

$$r = \sqrt{\frac{5}{B}}. \tag{11.22}$$

Hence, since the distribution itself extends to infinity, we have a conjugate point to the center lying inside the boundary and hence have a case of *unstable* equilibrium. The example is not typical of all cases of unstable equilibrium, since it is not necessary therefor that the distribution should be one which extends to infinity.

Cases $\gamma < 4/3$, n > 3 (*singular solutions; unstable*):

With

$$\gamma < \tfrac{4}{3} \tag{11.23}$$

there is known to be a class of singular solutions of the Emden equation of the form

$$\rho = \frac{\left[\frac{\kappa\gamma}{2\pi}\frac{4-3\gamma}{(\gamma-2)^2}\right]^{1/(2-\gamma)}}{r^{2/(2-\gamma)}}, \tag{11.24}$$

where, with $\gamma < 4/3$, the density ρ of the fluid would drop from an infinite value at the center to the value zero at $r = \infty$, and the total mass of fluid would be infinite. With a finite total amount of material such a solution might describe the distribution of one kind of fluid out to a certain distance from the center, and a different solution might describe the distribution of some other kind of fluid from there to the boundary. Substituting (11.23) and (11.24), the Jacobi equation (11.3) assumes the form

$$\frac{d^2z}{dr^2} + \frac{\beta^2 z}{r^2} = 0 \qquad \text{with } \beta^2 = \frac{2(4-3\gamma)}{(\gamma-2)^2}. \tag{11.25}$$

This has a general solution which can be conveniently written in the exponential form

$$z = r^{1/2}\left\{C_1 r^{(\frac{1}{4}-\beta^2)^{1/2}} + C_2 r^{-(\frac{1}{4}-\beta^2)^{1/2}}\right\} \tag{11.26}$$

when $\beta^2 < 1/4$, or in the trigonometric form

$$z = r^{1/2}\{D_1 \cos[(\beta^2 - \tfrac{1}{4})^{1/2}\log r] + D_2 \sin[(\beta^2 - \tfrac{1}{4})^{1/2}\log r]\} \tag{11.27}$$

when $\beta^2 > 1/4$. In either case it will be seen that the arbitrary constants C_1 and C_2, or D_1 and D_2, could be chosen so as to make $z = 0$ at any desired radius r. Hence, since we should have $z = 0$ in any case at the center, we see that a point conjugate to the center could be taken as occurring just as close thereto as we desire. The singular distributions may hence be regarded as *highly unstable.*

We may now summarize the foregoing results of applying the Jacobi test for a minimum to the potential energies of Emden spheres of fluid having different specified values of γ and arbitrary values of κ. With $\gamma = \infty$ we have a sphere of incompressible fluid with its boundary located at a radius r_b, which is determined by the total

amount of fluid available; and the Jacobi test is satisfied, since there is no point conjugate to the center appearing at any distance r. With $\gamma = 2$ we have a sphere of compressible fluid with its boundary located at $r_b = \pi\sqrt{\kappa/2\pi}$; and the Jacobi test is again satisfied, since the first point conjugate to the center appears outside the boundary at $r = 4.493\sqrt{\kappa/2\pi}$. With $\gamma = 4/3$ we have a sphere of compressible fluid with its boundary located—in accordance with the numerical quadrature of Emden—at $r_b = 6.90\ \rho_c^{-1/3}\sqrt{\kappa/\pi}$, where ρ_c is the central density; and the Jacobi test just fails, since the first point conjugate to the center also appears just at the boundary. With $\gamma = 6/5$, still keeping ρ finite and $d\rho/dr$ zero at the center, we have dropped to the highest value of γ for which the boundary of the sphere goes to infinity; and the Jacobi test fails, since the first point conjugate to the center appears at the finite radius $r = \rho_c^{-2/5}\sqrt{45\kappa/2\pi}$. Finally, for the class of singular solutions with $\gamma < 4/3$, we have spheres with infinite density at the center and with infinite radius; and the Jacobi test fails completely, since any point at an arbitrary radius r is found to be conjugate to the center.

In accordance with these results, for the somewhat limited number of cases in which we can obtain a simple analytical solution of the Jacobi equation, we see that no point conjugate to the center appears within the boundary of an Emden sphere when $\gamma > 4/3$, a point conjugate to the center appears just at the boundary when $\gamma = 4/3$, and a point conjugate to the center appears definitely within the boundary when $\gamma < 4/3$. It will be noted that this character of the results is partly determined by the circumstance that the boundary radius of Emden spheres tends to infinity as γ is decreased.

Assuming that the limited number of cases treated has been sufficient to give a valid expectation as to the qualitative nature of the results which would be obtained with intermediate values of γ, we are now led to the general conclusion that the Jacobi test would be satisfied whenever $\gamma > 4/3$ and would fail whenever $\gamma < 4/3$. Thus, in any Emden sphere of simple mechanical fluid we can expect that the potential energy will be at a minimum and the distribution will be in stable equilibrium when $\gamma > 4/3$, and can expect that the potential energy will not be at a minimum and the distribution will be in unstable equilibrium when $\gamma < 4/3$. The conclusion that we have

stable equilibrium when $\gamma > 4/3$ is in agreement with the finding in section 10 that the potential energy would exhibit a minimum toward "uniform" expansion or contraction when $\gamma > 4/3$, but is not thereby proved since it takes satisfaction of all the tests considered in this article to show that we should have a minimum toward any arbitrary kind of displacement. The conclusion that we have unstable equilibrium when $\gamma < 4/3$ is in agreement with the finding in section 10 that the potential energy would exhibit a maximum toward "uniform" expansion or contraction when $\gamma < 4/3$, and is also thereby proved since it takes only a single case where the potential energy decreases with displacement from equilibrium to demonstrate instability.

12. *Conclusion.*—It has been the task of the foregoing article to try to elucidate the principles which govern the stability of spheres of fluid held together by gravitational attraction. In making a first attack on this problem, we have assumed Newtonian forces of gravitation as an appropriate approximation and have confined our attention to simple mechanical fluids where the pressure would be a function of density alone. This has made it possible to take the presence of a minimum in the potential energy of the fluid toward small displacements from the equilibrium distribution as the condition for mechanical stability. The most important result has been to show that any equilibrium distribution of fluid would in general automatically satisfy all tests for a minimum of potential energy, and hence for stability, with the exception of the Jacobi test, where special investigation must be made in each case to see whether conjugate points would lie within the range of the distribution. In a general way it can be said that the factors which lead to failure of the Jacobi test are high central density, high central pressure, and high compressibility; and in the special case of Emden spheres it can be said that failure of the Jacobi test occurs whenever $\gamma < 4/3$. When the Jacobi test fails, it is then to be noted that the potential energy is neither a true minimum nor maximum at equilibrium and that the degree of instability may be regarded as correlated with the proximity of the conjugate points.

As an extension of the investigation, it would be natural to try to apply similar methods to spheres of fluid of sufficient density and

mass so that it would be essential to use relativistic, rather than Newtonian, gravitational theory. Such an extension, however, might involve considerable alteration in point of view and would at the least be made difficult by computational complications.

As another extension, it would be natural to try to apply similar methods in studying the stability of stellar models. The problem is then altered by the change to a system which is in a steady, rather than in an equilibrium, state; and it becomes necessary to consider non-mechanical, as well as mechanical, factors affecting stability. Nevertheless, it will be shown in a following article that the methods of the present article can be modified so as to contribute to the theory of stellar stability.

In concluding, the writer wishes to express thanks to his colleague, Professor J. R. Oppenheimer, who has been kind enough to read the manuscript of this article and to make suggestions, and to Dr. C. P. Brady, who has given expert counsel as to the methods of the calculus of variations.

NORMAN BRIDGE LABORATORY OF PHYSICS
CALIFORNIA INSTITUTE OF TECHNOLOGY
June 1939

ON THE STABILITY OF STELLAR MODELS, WITH REMARKS ON THE ORIGIN OF NOVAE

RICHARD C. TOLMAN

ABSTRACT

A brief review is first given of the results previously obtained by various investigators concerning the secular stability of stars, the stability of pulsating stars, and the relative stability of the processes of radiative and of convective thermal transfer in the interior of stars. The present article then considers, as a further aspect of the general problem, the stability of stars toward infinitesimal, instantaneous fluctuations in the distribution of stellar fluid. The necessary and sufficient criterion for such stability is that the available potential energy of the stellar model shall be a minimum toward reversible, adiabatic variations in the distribution of fluid. Setting up the integral which expresses the available potential energy, and applying the calculus of variations, it is found that this integral in general automatically satisfies all tests for a minimum, except that of Jacobi as to the location of conjugate points, where special investigation must be made in each separate case. Carrying out such investigations of the Jacobi test as are readily feasible, it is found that there is no reason to expect instability of the kind under consideration in the case of simple stellar models having radiative (or convective) thermal transfer throughout. It is also found, however, that the presence of a central convective zone or of a convective zone just under the surface of a star, otherwise having radiative thermal transfer, can introduce factors tending toward failure of the Jacobi test. Further investigation would be necessary to determine whether instability arising in such a manner could actually play an important role in stellar behavior. The article closes with remarks as to various explanations for stellar novae which have been proposed, including the tentative new suggestion that their origin might be due to instability arising from failure of the integral of available potential energy to satisfy the Jacobi test for a minimum.

1. *Introduction.*—Theoretical studies of the stability of stellar models must play an important role in our attempts to explain the behavior of actual stars. With the help of such studies we may ultimately hope to understand the existence of the great majority of stars in steady states that persist with little change over periods presumably at least of the order of 10^9 to 10^{10} years, the existence of limited classes of stars in pulsating states that produce regular or irregular variations in luminosity, and the existence of some—perhaps nearly all—stars in states that can lead to the occasional formation of novae.

As is commonly the case in investigating the stability of complicated physical systems, our studies of the stability of stellar models must consist of a series of treatments of different aspects of stability corresponding to different mechanisms by which the continued ex-

istence of a state might be disturbed. Before proceeding to the discussion of the particular aspect of stability that will concern us in the present article, it will be useful to devote the next few paragraphs to a brief—and hence also rather incomplete—summary of the present status of the theoretical investigations of stellar stability which have already been made.[1] This will make it easier to appreciate the character of our new investigation and the contribution which it may make to our total picture of stellar stability.

The *secular stability* of ordinary stars against a slow over-all contraction or expansion has been considered by Russell[2] and by Eddington.[3] Their considerations are based on the accepted dependence of the luminosity of a star on its mass and radius, in accordance with which the rate of energy escape in the form of radiation from a typical stellar model would be expected to increase if the model were contracted and to decrease if the model were expanded. From this circumstance they are led to the important conclusion that the actual long-time stability of a star, such as that of the sun over a period of 10^9 to 10^{10} years, could only be obtained provided the rate of *internal* energy generation within the material of the star depends on density and temperature in such a manner as to increase with contraction and decrease with expansion. Without such a dependence of internal energy generation on density and temperature, there would be no mechanism to prevent a star from contracting, in a period of the order of 10^7 years, in the manner described by the original Kelvin-Helmholtz theory, the gravitational energy made available by contraction being dissipated by the increased rate of energy escape; and there would be no mechanism to prevent the star from expanding at a similar rate, the gravitational energy needed for the expansion being provided by the decreased rate of energy escape. On the other hand, with the suggested dependence of energy generation on density and temperature, the increase in radiation pressure on contraction

[1] For a more complete account of previous investigations of stability, and in general for an exceedingly satisfactory account of the present status of the theory of stellar interiors, see B. Strömgren, *Ergebnisse der exakten Naturwissenschaften*, **16**, 465, 1937.

[2] See Russell, Dugan, and Stewart, *Astronomy*, **2**, 906–908, Boston, 1938.

[3] *The Internal Constitution of Stars*, § 211, Cambridge, 1926.

and its decrease on expansion could provide the necessary mechanisms for the preservation of a steady state; and a moderate increase with density and temperature would be sufficient for this purpose, since the rate of energy escape might be expected, in accordance with accepted theory, to vary approximately only as the inverse half-power of the radius.

The *stability of pulsating stars*, especially of the regular Cepheid variables, has been considered by a large number of investigators, including Eddington, Jeans, Vogt, Milne, Rosseland, and Cowling.[4] Their treatments are based on the consideration that stable pulsation might be maintained by a balance between the competing actions, of increase in the rate of internal energy generation with the compression of any element of fluid in the star as a mechanism which would promote the amplitude of pulsation, and of increase in the rate of energy dissipation with rise in the temperature of any such element as a mechanism which would dampen the amplitude of pulsation. In the earlier treatments of this problem the conclusion was drawn that a surprisingly small increase in the rate of energy generation with rise in temperature would be more than sufficient to balance the damping effects and thus to make the pulsation become unstable. The later work of Cowling,[5] however, by paying due attention to the circumstances, on the one hand, that the locus of energy generation would be concentrated toward the center of a star if the dependence on temperature were large and, on the other hand, that the amplitude of an actual oscillation would increase with distance from the center, has shown that the damping effect of the outer regions of a star would be sufficient to prevent instability even with a rate of energy generation proportional to the twentieth power of the temperature. This is a very satisfactory conclusion.

The *relative stability* of *radiative* and *convective processes* as the mechanisms of heat transfer within the body of a star have also been considered by a large number of investigators, including Schwarzschild, Eddington, Rosseland, Siedentopf, Unsöld, Biermann, and

[4] For detailed accounts and references see Eddington, *ibid.*, chap. viii; Milne, "Theory of Pulsating Stars," *Handb. d. Ap.*, **3**, Part II, 804 ff., Berlin, 1930; and Strömgren, "Die Pulsationstheorie," *ibid.*, **7**, 192 ff., Berlin, 1936.

[5] *M.N.*, **94**, 768, 1934; **96**, 42, 1935.

Cowling.[6] The general principle involved is that a steady state of radiative transfer would be unstable toward the onset of thermal convection in any zone of a star where a change to convective transfer would lead to a lowering of the temperature gradient. This condition for convection—in the case of homogeneous stellar material—can also be expressed in the useful form that the increase in pressure with density accompanying adiabatic compression of the stellar material at any point of interest must be less than the actual increase of pressure with density as we proceed inward in the star at that point, if the onset of convection is to take place. Since the increase in pressure with density accompanying the adiabatic compression of stellar material would be diminished by the presence of radiation and by the recombination of ionized electrons, high relative radiation pressure and the presence of partially ionized electron shells are factors which can promote the incidence of convection. And since high intensity of energy flow and high opacity would increase the radiative temperature gradient, a concentration of energy sources toward the center and a not too great decrease of opacity with depth are factors which would promote the incidence of convection in the neighborhood of the center. The standard Eddington stellar model proves to be stable toward radiative, rather than convective, transfer throughout the whole of its interior. Models, however, which presumably give a more appropriate representation of actual stars by having a high concentration of energy generation toward the center, tend to have a convection zone near the center (Rosseland,[7] Biermann,[8] and Cowling[9]). And one or more convection zones also tend to occur in the outer regions of stars at a temperature where some constituent atom has a partially ionized electron shell (Unsöld[10] and Biermann[11]). In the event of convection it is to be noted that the process tends to be of the turbulent variety and that the temperature gradient tends to approach quite closely to the limiting adiabatic gradi-

[6] For detailed accounts and references see Eddington, *op. cit.*, pp. 9, 97 ff.; and Strömgren, *Handb. d. Ap.*, **7**, 171 ff., Berlin, 1936.

[7] *Zs. f. Ap.*, **4**, 255, 1932.

[8] *Zs. f. Ap.*, **5**, 117, 1932.

[9] *M.N.*, **94**, 768, 1934; **96**, 42, 1935; *A.N.*, **258**, 133, 1936.

[10] *Zs. f. Ap.*, **1**, 138, 1930.

[11] *A.N.*, **259**, 221, 1936.

ent (Biermann[8] and Cowling[9]). It should be remarked, in connection with the possibility for convective zones to form, that there is no reason to expect any delay in the onset of convection in any zone where that becomes possible, in view of the violent stirring which must in any case be taking place inside a star, and hence also that there is no reason to expect sudden changes in a star as a whole to be produced by the initiation of convection.

This completes our brief account of the previous kinds of investigation of stellar stability that have been made. The investigation of secular stability has shown that a suspected possibility for ordinary stars to leave their actual steady states, by a slow over-all contraction or expansion, would be counteracted by change in radiation pressure, provided there is at least a moderate increase in rate of internal energy generation with density or temperature. The investigation of pulsating stability has shown that a suspected possibility for pulsating stars to oscillate more and more violently, if the rate of energy generation increases with temperature, would be counteracted by damping action in the outer portions of the star, provided that the rate of energy generation does not increase faster than the twentieth power of the temperature. The investigation of the relative stability of different mechanisms of heat transfer has shown that purely radiative transfer would be unstable toward convective transfer in any zone of a star where that process would lead to a decreased temperature gradient, but that there is no reason to expect any delay in the onset of convection if conditions change in such a way as to make that possible. Hence the general result may be summarized by the statement that these previous studies have not led to the discovery of any source of instability which would make a star depart from the steady behavior characterizing an exceedingly slow evolutionary development. Thus, in particular, these studies have provided no explanation for the sudden appearance of novae.

The general consideration that a reasonably complete picture of stellar stability can be obtained only by the successive examination of different mechanisms by which a steady state might be disturbed, together with the just-mentioned circumstance that no explanation for the sudden appearance of novae has as yet been provided, now make it natural to investigate further possible sources of instability

in stellar models. This furnishes the motivation for the present article, which attempts to examine the stability of stars toward small fluctuations in the distribution of stellar fluid that might transform available potential energy into kinetic energy which could increase the extent of the fluctuation. Since the methods to be used in the present investigation are similar to those developed in a previous article on the less difficult problem of the stability of spheres of simple mechanical fluid, it will be advantageous to begin by describing the general character of those methods and the changes that must be made in adapting them to our present purposes.

2. *General nature of the method.*—In the preceding article[12] a study was made of the factors which control the stability of equilibrium in spheres of simple mechanical fluid held together by Newtonian forces of gravitation. Taking the occurrence of a minimum in potential energy at equilibrium as the condition for stability, it was shown in accordance with the calculus of variations that an equilibrium distribution of such fluid would in general automatically satisfy all tests for a minimum in the potential energy, and hence for stability, except that of Jacobi, where a special examination has to be made in each particular case to determine whether points conjugate to each other are included within the range over which the integral of potential energy extends. It is the intent of the present article to examine the possibility of applying similar considerations to certain aspects of the stability of stellar models. The alteration in the nature of the problem, when we thus turn our attention to the physically more interesting behavior of models which attempt the representation of actual stars, is quite far-reaching. Instead of considering the stability of a sphere composed of a single idealized mechanical fluid in a static state of equilibrium, it now becomes necessary to consider the stability of a sphere composed of one or more fluids having approximately actual physical properties in a steady state which involves outward thermal flow.

As an immediate consequence of this alteration, it will no longer be possible to take the pressure of the fluid as a unique function of its density, since the nature and temperature of the fluid will depend on position in the sphere. Indeed, as we shall see, it will now become

[12] Tolman, this *Journal*, p. 541.

essential to distinguish clearly between changes of pressure with density, as a result of the adiabatic compression of a given element of fluid, and changes of pressure with density, as a result of changing to a different depth in the sphere.

As a further consequence of the alteration in problem, which is even more fundamental from the point of view of trying to apply methods similar to those of the previous article, it will evidently no longer be possible to take the simple mechanical idea of minimum potential energy as the criterion for stability, since the potential energy of a fluid loses its unambiguous significance when the work accompanying changes in density can depend on the rate at which the expansion or contraction is carried out and on the control of heat flow during the process. Nevertheless, we still desire to determine whether energy would be set free by any small fluctuation which might suddenly occur in the density of distribution of the fluid. Hence, to meet our present needs, it will now be appropriate to introduce the idea of "available" potential energy, so defined as to correspond to the internal and gravitational energy that could be delivered in the form of work by infinitesimal, instantaneous—*and hence reversible, adiabatic*—fluctuations in the distribution of the fluid. The presence of a minimum value for this quantity can then be taken as at least one of the necessary criteria for stability, since otherwise the work delivered would provide the kinetic energy needed to increase the extent of the fluctuation.

Finally, moreover, as a consequence of the alteration to a more complicated type of system, it will be appreciated that our proposed, appropriately altered method can no longer be expected to give a complete understanding of all the factors now affecting the stability of our models. A general reason, for the less complete character of the new considerations, lies in the circumstance that it now also becomes necessary to consider the results which follow from other kinds of initial process which do not have reversible, adiabatic character even at the start, as illustrated by the types of stability investigation described in the preceding section of this article. A more special reason for the decreased efficacy of our method, when applied to the changed problem, lies in the circumstance that it would no longer be correct to regard the further changes which might follow from an in-

finitesimal, instantaneous fluctuation as continuing to have reversible, adiabatic character; and additional investigation would be needed to determine the outcome of a change which was initiated in that manner. The situation may perhaps be described with some accuracy as follows: The presence or absence of a minimum in the available potential energy of a stellar model may be taken as the necessary and sufficient conditions, respectively, for stability or instability of the particular kind under consideration; but the absence of such a minimum cannot of itself be taken as a sufficient description of the state of the model to give a satisfactory account of the further changes which would be initiated by an infinitesimal transformation of available potential energy into kinetic form.

With this introduction we are now ready to undertake the proposed investigation. After considering the general nature of the steady states that interest us, we shall first set up the integral which expresses the available potential energy of the fluid in a stellar model, and shall show that this integral would, in general in any such steady state, automatically satisfy all tests for a minimum provided by the calculus of variations, except that of Jacobi, where special investigation must be made in each particular case. The calculations, needed for the four tests that precede the Jacobi test, turn out to be similar but not identical with those leading in the previous article to the analogous result for spheres of mechanical fluid in a state of equilibrium. We shall next set up, for the present case of stellar models in a steady state, the appropriate form for the Jacobi equation which determines the location of conjugate points. We shall find that this equation is appreciably altered from the form obtained in the previous article, and that the change in form can be roughly described as acting sometimes in the direction of stability and probably also sometimes in the direction of instability. We shall conclude the article with some remarks as to the possible bearings of the present investigation on the occurrence of stellar novae. We may now proceed to the detailed calculations.

3. *Stellar model in a steady state.*—A typical star, which emits radiation at a sensibly constant rate, may be treated with the help of a stellar model in a steady state. Such a model may be taken as a spherically symmetrical distribution of fluid, consisting of matter

and partially entrained radiation, in a condition which does not alter appreciably with time. The fluid composing the sphere is at least roughly in hydrostatic equilibrium under the combined action of the forces of gravity and of pressure, and the radiation which ultimately escapes from the surface is being generated by some interior mechanism at a constant rate. The density and opacity of matter throughout the main body of the sphere are high, and the radiation escapes slowly enough so that thermal equilibrium may be regarded as approximately established at each point of the interior, with matter and radiation at a common temperature which decreases from the center outward. The surface temperature of the sphere is low enough so that the total pressure of gas plus radiation may be taken as having dropped substantially to zero at the boundary.

Assuming Newtonian forces of gravity and taking, for simplicity, units of mass which make the constant of gravitation equal to unity, the condition for hydrostatic equilibrium in a sphere such as described above may be written in the form

$$\frac{1}{\rho}\frac{dp}{dr} + \frac{m}{r^2} = 0\,, \tag{3.1}$$

where ρ is the density of fluid at any radius r, p is the total pressure of matter plus radiation at that radius, and m is the mass *inside* that radius.

It will be convenient to note that the *density of fluid* at any point in the sphere can evidently be expressed in terms of the increase of mass with radius by the equation

$$\rho = \frac{1}{4\pi r^2}\frac{dm}{dr} = \frac{m'}{4\pi r^2}\,, \tag{3.2}$$

where we use an accent ($'$) to denote differentiation with respect to r.

4. *The integral of available potential energy.*—In treating stellar models by the methods that now concern us, it is convenient to choose the zero of available potential energy as corresponding to a condition which could be reached by dividing the fluid in the sphere into small elements without change in composition, separating these elements to such a distance that their gravitational interaction becomes negligible, and then expanding each element to a state where the pressure and density are substantially zero and the temperature

and internal condition are such as would result if the expansion were reversible and adiabatic.[13] The available potential energy of the model can then be taken as the sum of the amounts of work which would have to be done against the forces of pressure and against the forces of Newtonian attraction to return the fluid, by reversible and adiabatic processes, back to the condition which it has in the model. The first of the two terms in the sum may be called the "mechanical part" of the available potential energy and will be positive; the second of the two terms may be called the "gravitational part" and will be negative.

With the foregoing definition it will be seen that any decrease in the available potential energy, accompanying an infinitesimal and instantaneous—and thus reversible and adiabatic—fluctuation in the density of distribution in the model, would make available the necessary kinetic energy to increase the extent of the fluctuation. Hence we can take the presence of a minimum in the available potential energy as a necessary criterion for stability.

To calculate the *mechanical part* of the available potential energy, it is convenient to begin by considering the available potential energy *u per unit mass* of the fluid at any density of interest. For this we can write

$$u = -\int_0^\rho p d\left(\frac{1}{\rho}\right) = \int_0^\rho \frac{p}{\rho^2}\, d\rho\,, \tag{4.1}$$

where we integrate the work done, against the pressure p, in the reversible adiabatic compression of unit mass of the fluid from the density zero in the above-described zero state to the density ρ of interest. For the total mechanical part of the available potential energy we can then write, with the help of equation (3.2),

$$U_{\text{mech}} = 4\pi \int_0^{r_b} u\rho r^2 dr = \int_0^{r_b} um'dr\,, \tag{4.2}$$

where we integrate over all the fluid in the sphere from the center $r = 0$ to the boundary $r = r_b$, which may be taken as reached when the pressure and density have dropped substantially to zero.

[13] In regions where heat transfer is taking place by turbulent thermal convection, the fluid may be regarded as divided into elements large enough so that they can be characterized by the average values of such quantities as density, pressure, and temperature.

In making later use of this expression, we shall need to consider the dependence of the available potential energy per unit mass of fluid u on the variables, radius r, mass m inside that radius, and rate of change of mass with radius m', by which we shall describe the distribution of fluid in the model. In accordance with (4.1), it is evident that u for any element of fluid in the sphere will be determined by its composition and temperature in the zero state and by the density to which it is compressed. On the one hand, since we shall consider variations in the distribution which would alter the radius r of any given fluid element of interest but which would not change the mass m lying inside that element, it will be appropriate to regard the latter quantity as permanently labeling the different elements, and hence take the composition and temperature in the zero state as a function of m. On the other hand, the density ρ to which an element of fluid is compressed is given, in accordance with (3.2), in terms of the variables that concern us by $m'/4\pi r^2$. Hence, we can now re-write (4.1) in the form

$$u = \int_{\rho=0}^{\rho=m'/4\pi r^2} \frac{p(m,\rho)}{\rho^2}\, d\rho\,, \tag{4.3}$$

as giving a full expression for the dependence of u on the variables r, m, and m' pertaining to the distribution.

For our later use, it will be necessary to have expressions for first and second partial derivatives of u with respect to m and m'. Making renewed use of (3.2), it will be seen that these can be written in the forms

$$\left.\begin{aligned}
\frac{\partial u}{\partial m} &= \int_{\rho=0}^{\rho=m'/4\pi r^2} \frac{1}{\rho^2}\frac{\partial p}{\partial m}\, d\rho\,,\\
\frac{\partial u}{\partial m'} &= \frac{p}{4\pi r^2\rho^2}\,,\\
\frac{\partial^2 u}{\partial m^2} &= \int_{\rho=0}^{\rho=m'/4\pi r^2} \frac{1}{\rho^2}\frac{\partial^2 p}{\partial m^2}\, d\rho\,,\\
\frac{\partial^2 u}{\partial m\,\partial m'} &= \frac{1}{4\pi r^2\rho^2}\frac{\partial p}{\partial m}\,,\\
\frac{\partial^2 u}{\partial m'^2} &= \frac{1}{4\pi r^2}\left(\frac{1}{\rho^2}\frac{\partial p}{\partial \rho} - \frac{2p}{\rho^3}\right)\frac{\partial \rho}{\partial m'}\\
&= \frac{1}{16\pi^2 r^4\rho^2}\left(\frac{\partial p}{\partial \rho} - \frac{2p}{\rho}\right).
\end{aligned}\right\} \tag{4.4}$$

It will also be necessary to have the following expressions for a total and for a partial derivative with respect to r:

$$\frac{du}{dr} = \frac{p}{\rho^2}\frac{d\rho}{dr} + \frac{\partial u}{\partial m}\frac{dm}{dr} \tag{4.5}$$

and

$$\frac{\partial}{\partial r}\frac{\partial u}{\partial m} = -\frac{2m'}{4\pi r^3\rho^2}\frac{\partial p}{\partial m} = -\frac{2}{r\rho}\frac{\partial p}{\partial m}. \tag{4.6}$$

In the foregoing expressions it will be appreciated, from the form of (4.3), that $(\partial p/\partial \rho)$ denotes the rate at which the pressure p for a given element of fluid would change with the density ρ in a reversible adiabatic compression without change in composition, and that $(\partial p/\partial m)$ denotes the rate at which the pressure p would change with the variable m, which labels the different elements of fluid, maintaining constant density with the help of a reversible adiabatic adjustment of volume. Thus we may write

$$\frac{\partial p}{\partial \rho} \equiv \left(\frac{dp}{d\rho}\right)_{s,c}, \tag{4.7}$$

where the subscripts indicate the constancy of entropy and composition. And from the total dependence of pressure on radius

$$\frac{dp}{dr} = \frac{\partial p}{\partial \rho}\frac{d\rho}{dr} + \frac{\partial p}{\partial m}\frac{dm}{dr}$$

we may write, with the help of (3.2),

$$\frac{\partial p}{\partial m} \equiv \frac{1}{4\pi r^2\rho}\left(\frac{dp}{dr} - \frac{\partial p}{\partial \rho}\frac{d\rho}{dr}\right). \tag{4.8}$$

We may now turn to the *gravitational part* of the available potential energy of the model. To calculate this quantity it is convenient to consider the work against gravitational forces which would be needed to remove the material in the sphere, layer by layer to infinity. In this way we readily obtain the desired expression

$$U_{\text{grav}} = -4\pi\int_0^{r_b}\frac{m}{r}\rho r^2 dr = -\int_0^{r_b}\frac{mm'}{r}dr, \tag{4.9}$$

where we again integrate over the whole sphere from $r = 0$ to $r = r_b$.

Adding (4.2) and (4.9), we now obtain the desired expression for the *total available potential energy.*

$$U = \int_0^{r_b} \left(um' - \frac{mm'}{r} \right) dr \,. \tag{4.10}$$

This integral, which for stability must be a minimum toward small fluctuations in the distribution of fluid, has just the same form as that obtained in the preceding article[12] for the case of a sphere of simple mechanical fluid. The quantity u, however, now has a more complicated dependence on the variables r, m, and m'.

The integrand, in the expression which is to be a minimum,

$$f = um' - \frac{mm'}{r} \,, \tag{4.11}$$

is seen to be a function of the independent variable r and the dependent variable m and its derivative m'. With respect to these latter quantities it has partial derivatives, which can be written with the help of (3.2) and (4.4) in the forms

$$f_m = \frac{\partial f}{\partial m} = m' \frac{\partial u}{\partial m} - \frac{m'}{r} \,, \tag{4.12}$$

$$f_{m'} = \frac{\partial f}{\partial m'} = m' \frac{\partial u}{\partial m'} + u - \frac{m}{r} = \frac{p}{\rho} + u - \frac{m}{r} \,, \tag{4.13}$$

$$f_{mm} = \frac{\partial^2 f}{\partial m^2} = m' \frac{\partial^2 u}{\partial m^2} \,, \tag{4.14}$$

$$f_{mm'} = \frac{\partial^2 f}{\partial m \partial m'} = m' \frac{\partial^2 u}{\partial m \partial m'} + \frac{\partial u}{\partial m} - \frac{1}{r} = \frac{1}{\rho} \frac{\partial p}{\partial m} + \frac{\partial u}{\partial m} - \frac{1}{r} \,, \tag{4.15}$$

$$f_{m'm'} = \frac{\partial^2 f}{\partial m'^2} = m' \frac{\partial^2 u}{\partial m'^2} + 2 \frac{\partial u}{\partial m'} = \frac{1}{4\pi r^2 \rho} \frac{\partial p}{\partial \rho} \,. \tag{4.16}$$

We are now ready to determine the conditions under which the available potential energy of a stellar model in a steady state would be a minimum toward small fluctuations in the distribution of fluid. For this purpose it will be sufficient to consider fluctuations which

preserve spherical symmetry, and hence to apply the known tests for a minimum, provided by the calculus of variations, to the integral (4.10), taking m and m' as subject to variation. In carrying this out, we shall give a somewhat abbreviated treatment, since the work parallels that of the preceding article,[12] where a more complete statement of the nature and significance of the various tests will be found.

5. *The Euler test.*—The Euler test, in the present example, requires the validity of the equation

$$\frac{d}{dr}\frac{\partial f}{\partial m'} - \frac{\partial f}{\partial m} = 0 . \tag{5.1}$$

Substituting (4.12) and (4.13) and making use of (4.5) to cancel certain terms, it will be found that this becomes

$$\left.\begin{aligned} &\frac{d}{dr}\left(\frac{p}{\rho} + u - \frac{m}{r}\right) - m'\frac{\partial u}{\partial m} + \frac{m'}{r} \\ &\quad = \frac{1}{\rho}\frac{dp}{dr} - \frac{p}{\rho^2}\frac{d\rho}{dr} + \frac{du}{dr} + \frac{m}{r^2} - \frac{m'}{r} - m'\frac{\partial u}{\partial m} + \frac{m'}{r} \\ &\quad = \frac{1}{\rho}\frac{dp}{dr} + \frac{m}{r^2} + \frac{du}{dr} - \frac{p}{\rho^2}\frac{d\rho}{dr} - \frac{\partial u}{\partial m}\frac{dm}{dr} \\ &\quad = \frac{1}{\rho}\frac{dp}{dr} + \frac{m}{\rho^2} = 0 , \end{aligned}\right\} \tag{5.2}$$

which is seen to be valid from (3.1) since the distribution in a steady state is in hydrostatic equilibrium.

6. *The Legendre test.*—The Legendre test, in the present example, requires the validity of the expression

$$f_{m'm'}(r, m, m') \geqq 0 , \tag{6.1}$$

where we consider the value of this second derivative at any point in the distribution as a function of the values of r and m and of the slope m' at that point. This is readily seen to be valid, however, in the stronger of the two forms with the sign of inequality, since in accordance with (4.16) it is equivalent to

$$\frac{1}{4\pi r^2 \rho}\frac{\partial p}{\partial \rho} \geqq 0 , \tag{6.2}$$

where ρ is the density of the fluid and $(\partial p/\partial \rho)$ is the rate of change of pressure with density for an adiabatic compression of the fluid, at the point in question.

7. *The Weierstrass test.*—The Weierstrass test, in the present example, then requires the validity of the expression

$$f_{m'm'}[r, m, m' + \theta(M' - m')] \geqq 0 , \tag{7.1}$$

where we now consider values of this second derivative at any point in the distribution as a function of the actual values of r and m at that point and of the altered slope $m' + \theta(M' - m')$, where M' is any physically realizable value of the increase in mass with radius and θ lies between zero and one. This is seen to be valid, however, with the sign of inequality, since it reduces to the same form as (6.2):

$$\frac{1}{4\pi r^2 \rho} \frac{\partial p}{\partial \rho} \geqq 0 , \tag{7.2}$$

where ρ and $(\partial p/\partial \rho)$ are now the values of those quantities that would correspond to the altered slope.

In accordance with the foregoing satisfaction of the Euler, Legendre, and Weierstrass tests we now see that the available potential energy of our stellar models would be a minimum toward reversible adiabatic changes in the distribution, which do not change the boundary radius, provided the Jacobi test as to the location of conjugate points is also satisfied.

8. *The mobile-boundary tests.*—Up to this point we have considered the conditions for a minimum when variations are made in the distribution of fluid which do not alter the total radius of the sphere. To include the possibility of alterations in the radius r_b in our considerations, let us now examine the available potential energy

$$U = \int_{r=0}^{r=r_b} f(r, m, m')dr \tag{8.1}$$

as a function of the limit of integration r_b, when we consider neighboring distributions of fluid subject to the condition that the various distributions should in each case satisfy the Euler test for an extre-

mum and should be reached from one another by reversible adiabatic processes, and also subject to the further condition that the connection between mass and radius at the boundary must necessarily satisfy the equation

$$\tilde{m} = \text{constant}\,, \tag{8.2}$$

since we have a definite amount of fluid available.

Differentiating (8.1) with respect to r_b, taking r_b as a parameter which determines the form of f, and making use of the circumstance that the forms under consideration are to satisfy the Euler test for an extremum and be attainable by reversible, adiabatic processes, we then obtain an expression of the known form

$$\frac{dU}{dr_b} = f(r, m, m') + (\tilde{m}' - m')f_{m'}\,, \tag{8.3}$$

where the values of the terms are to be taken at the boundary $r = r_b$. Since $\tilde{m}'$ is seen from (8.2) to be identically equal to zero, and since $f_{m'}$ is to be given the value corresponding to reversible adiabatic changes, the foregoing result reduces with the help of (4.11) and (4.13) to the form

$$\frac{dU}{dr_b} = um' - \frac{mm'}{r} - m'\left(m'\frac{\partial u}{\partial m'} + u - \frac{m}{r}\right) = -m'^2\frac{\partial u}{\partial m'}\,. \tag{8.4}$$

Making use of (3.2) and (4.4), and remembering that we are to take the value of the right-hand side at the boundary, this then gives us

$$\frac{dU}{dr_b} = -\,4\pi r_b^2 p_b\,, \tag{8.5}$$

where r_b and p_b are the values of the radius and pressure at the boundary of the distribution.

In the first place, this expression now shows us that the first derivative of the available potential energy with respect to the boundary radius will be equal to zero, in the case of any stellar model that we wish to test, since the value of the pressure p_b at the boundary

will be equal to zero. The so-called "transversality test" for a minimum is thus immediately satisfied. In the second place, the foregoing expression also shows us that we can usually expect the available potential energy actually to increase when we change, under the conditions mentioned above, to a neighboring distribution of different boundary radius, since, on physical grounds, we can then usually expect an increase in p_b with decrease in r_b. Hence, applying similar arguments to those of section 7 in the preceding article,[12] we are led to the desired conclusion, that the Jacobi test—supplemented by special treatment when conjugate points fall just at the limits of integration—will remain, in typical cases, as a necessary and sufficient condition for minimum, available potential energy, also when changes in the boundary radius are permitted.

9. *The Jacobi test.*—The foregoing has shown that the available potential energy for a stellar model in a steady state would, in general, automatically satisfy all tests for a minimum, except for the requirement of Jacobi that no pair of conjugate points should fall within the range of integration. The location of successive conjugate points, in the present example, would be given by the location of successive possible zeros for the quantity z, defined as a function of r by the differential equation

$$\frac{d}{dr}\left(f_{m'm'}\frac{dz}{dr}\right)+\frac{df_{mm'}}{dr}z-f_{mm}z=0\,. \tag{9.1}$$

Substituting the values given by (4.14), (4.15), and (4.16), this can be written in the form

$$\left.\begin{aligned}&\frac{d}{dr}\left(\frac{1}{4\pi r^2\rho}\frac{\partial p}{\partial \rho}\frac{dz}{dr}\right)\\&\qquad+\frac{d}{dr}\left(m'\frac{\partial^2 u}{\partial m\partial m'}+\frac{\partial u}{\partial m}-\frac{1}{r}\right)z-m'\frac{\partial^2 u}{\partial m^2}z=0\,.\end{aligned}\right\} \tag{9.2}$$

Making use of (3.2), (4.4), and (4.6), it can then be re-expressed, after some rearrangement, in the form

$$\frac{d}{dr}\left(\frac{1}{4\pi r^2\rho}\frac{\partial p}{\partial \rho}\frac{dz}{dr}\right)+\frac{1}{\rho}\frac{d}{dr}\left(\frac{\partial p}{\partial m}\right)z+\frac{z}{r^2}=0\,. \tag{9.3}$$

And, introducing the expression for $(\partial p/\partial m)$ given by (4.8), it can also be written in the form

$$\frac{d}{dr}\left(\frac{1}{4\pi r^2\rho}\frac{\partial p}{\partial \rho}\frac{dz}{dr}\right)+\frac{1}{4\pi\rho}\frac{d}{dr}\left\{\frac{1}{r^2\rho}\left(\frac{dp}{dr}-\frac{\partial p}{\partial \rho}\frac{d\rho}{dr}\right)\right\}z+\frac{z}{r^2}=0. \quad (9.4)$$

It will be noted, by comparing (9.4) with (8.2) in the preceding article,[12] that our present more general form of Jacobi equation differs from the earlier form by the appearance of the partial derivative $(\partial p/\partial \rho)$ at constant entropy and composition in place of the total derivative $(dp/d\rho)$ previously present, and by the appearance of the additional second term on the left-hand side of (9.4). Hence, it will be seen that our present Jacobi equation reduces to the previous one when applied to a simple mechanical fluid where $(\partial p/\partial \rho)$ and $(dp/d\rho)$ become identical.

In order to consider the application of the Jacobi equation (9.4) to our present problems, it may be regarded as solved for z as a function of r, under the condition $z = 0$ at $r = 0$ but not identically zero for larger values of r. If a second zero for z then appears inside the boundary at $r = r_b$, we may conclude that an appropriate infinitesimal, instantaneous fluctuation in the distribution of fluid over the range between such conjugate points would be theoretically possible, which would deliver available potential energy in the form of kinetic energy in such a manner as to increase the extent of the fluctuation and thus to lead to instability. Equation (9.4) is so complicated that its actual solution must, in general, be carried out by some method of numerical quadrature. We shall content ourselves in the present article with an attempt to obtain insight into the possible consequences of the equation by the following discussion of different cases.

10. *Models with convective thermal transfer.*—The application of the Jacobi equation (9.4) would be considerably simplified in the case of a sphere of fluid with a temperature gradient maintained throughout the interior by a vigorous process of convective thermal transfer. Assuming that the convection is sufficiently vigorous, as is reasonable in view of the nature of our interests (see Biermann[8] and Cowling[9]), we could then take the adiabatic change in pressure

with density as closely equal to the actual change in pressure with density,

$$\frac{\partial p}{\partial \rho} = \frac{dp}{d\rho}, \tag{10.1}$$

and equation (9.4) would reduce to the same forn as the Jacobi equation (8.2) in the preceding article:[12]

$$\frac{d}{dr}\left(\frac{1}{4\pi r^2 \rho}\frac{dp}{d\rho}\frac{dz}{dr}\right) + \frac{z}{r^2} = 0. \tag{10.2}$$

This would then permit the same treatment of stability as already given in that article, with the general conclusion that high central pressure, high central density, and high compressibility would be the factors which tend to lead to instability, and with the specific conclusion, in case the distribution could be represented as an Emden polytropic sphere, that the exponent γ therefor would have to be less than $4/3$ in order for instability to arise.

The result thus obtained cannot be regarded as of direct importance for stellar models, since we now believe that convective heat transfer takes place in a star, if at all, only in somewhat limited zones. Nevertheless, the result is of indirect interest in indicating no immediate new tendency toward instability, since we should usually expect values of γ corresponding to the adiabatic compression of stellar material larger than $4/3$—e.g., in the case of a mixture of perfect monatomic gas and radiation dropping from $5/3$ to $4/3$ as the pressure of the radiation becomes large compared with that of the gas, and then to 1 only as the density of the radiation becomes large compared with that of the gas.

11. *Models with radiative thermal transfer:*

a) Assumed constancy of γ_A *and* γ_R.—The application of the Jacobi equation (9.4) in the case of a stellar model with a temperature gradient maintained throughout the interior by radiative thermal transfer would be less simple than in the foregoing case of convective transfer, since the adiabatic change in pressure with density $(\partial p/\partial \rho)$ would now be greater than the actual change in pressure with density $(dp/d\rho)$,

$$\frac{\partial p}{\partial \rho} > \frac{dp}{d\rho}; \tag{11.1}$$

and the second term in (9.4) would no longer vanish, except perhaps at isolated points.

To study the kinds of effect that might be expected from the inequality (11.1), it will be natural to set

$$\frac{\partial p}{\partial \rho} = \gamma_A \frac{p}{\rho} \quad \text{and} \quad \frac{dp}{d\rho} = \gamma_R \frac{p}{\rho} \tag{11.2}$$

with

$$\gamma_A > \gamma_R , \tag{11.3}$$

and to treat the newly introduced coefficients γ_A and γ_R in first approximation as constants, since their variation with r might often be expected to be small. For example, in the case of the standard Eddington model, applied to a perfect gas with negligible radiation pressure, γ_A would have the constant value $5/3$ throughout the model corresponding to the pressure-density adiabat for such a gas, and γ_R would have the constant value $4/3$ corresponding to the actual pressure-density relation maintained by radiative thermal transfer in that model.

The assumed constancy of γ_A and γ_R introduces considerable simplification, and the constancy of γ_R carries with it the special advantage that we can now take the distribution of fluid as that for an Emden sphere, with the exponent

$$\gamma = \gamma_R , \tag{11.4}$$

corresponding to the radiative mechanism by which the pressure-density relation is maintained; with the actual dependence of pressure on density given by

$$p = \kappa \rho^{\gamma} \tag{11.5}$$

where κ is a constant; and with the distribution of density in the model determined by the Emden differential equation

$$\frac{d}{dr}\left(r^2 \rho^{\gamma-2} \frac{d\rho}{dr}\right) + \frac{4\pi \rho r^2}{\kappa \gamma} = 0 . \tag{11.6}$$

b) Simplified form of Jacobi equation.—Substituting (11.2) in the general form of Jacobi equation (9.4), and making use of the assumed

constancy of γ_A and $\gamma_R = \gamma$, we can now re-write that equation for our present purposes in the form

$$\frac{d}{dr}\left(\frac{\rho^{\gamma-2}}{r^2}\frac{dz}{dr}\right) - \frac{\gamma_A - \gamma}{\gamma_A}\frac{1}{\rho}\frac{d}{dr}\left(\frac{\rho^{\gamma-2}}{r^2}\frac{d\rho}{dr}\right) z + \frac{4\pi z}{\kappa\gamma_A r^2} = 0\,; \quad (11.7)$$

and by combining with the Emden equation (11.6), this can be re-expressed, after considerable rearrangement, in the more convenient form

$$\frac{d}{dr}\left(\frac{\rho^{\gamma-2}}{r^2}\frac{dz}{dr}\right) + 4\,\frac{\gamma_A - \gamma}{\gamma_A}\,\frac{\rho^{\gamma-3}}{r^3}\frac{d\rho}{dr}\,z + \frac{4\pi z}{\kappa\gamma r^2} = 0\,. \quad (11.8)$$

This present form of Jacobi equation is now seen to differ from that previously obtained for Emden spheres of simple mechanical fluid (see eq. [11.3], preceding article[12]) only by the additional appearance of the second term on the left-hand side of (11.8). This then makes it easy to draw a conclusion as to the stability of our present class of models, since the coefficient of z in the new term will necessarily be negative, owing to the positive value of $(\gamma_A - \gamma)$ as the condition for radiative transfer and to the negative value of $(d\rho/dr)$ in all Emden spheres. Therefore, in accordance with Sturm's theory of the oscillatory properties of the solutions of such equations, the effect of the added term will always be such as to make the distance between conjugate points in any of our present stellar models greater than in the corresponding Emden sphere of simple mechanical fluid with the same values of κ and γ. Hence, in the light of our previous conclusion for such spheres of simple fluid that the first point conjugate to the center would lie outside or inside the boundary of the sphere according as γ is greater or less than $4/3$, we may now at least conclude that our present stellar models would, in any case, be stable toward infinitesimal, instantaneous fluctuations in the distribution of fluid whenever γ is greater than $4/3$.

c) *Solution of Jacobi equation for a special case.*—This finding as to the values of γ which would lead to stability can be confirmed and supplemented by information as to the values of γ_A which would lead to stability. For this purpose we note that our present form of the Jacobi equation (11.8) would have a very simple possible solution for

the special case $\gamma_A = 4/3$, without reference to the value of γ. This solution is of the form

$$z = \text{constant } r^3\rho \tag{11.9}$$

with

$$\gamma_A = \tfrac{4}{3} \quad \text{and} \quad \gamma = \text{constant} ; \tag{11.10}$$

and the correctness of this solution can be immediately verified by the substitution of (11.9) and (11.10) in (11.8), with the result that the Jacobi equation (11.8) is then found to reduce to the Emden equation (11.6), which, of course, is necessarily true.

Noting the form of (11.9), we now see for the special case $\gamma_A = 4/3$ that there would be a pair of conjugate points—one at the center of the sphere where $r = 0$, and the other at the boundary of the sphere where $\rho = 0$. Hence, since the effect of varying the value of γ_A in the second term of (11.8), with κ and γ held constant, would be to increase or decrease the distance between conjugate points according as γ_A is increased or decreased, we are now led to the conclusion that we should have stability or instability according as γ_A is greater or less than $4/3$, with neutral stability when γ_A is just equal to $4/3$.

As γ_A is in any case not less than γ, the present conclusion confirms our previous finding that we should have stability whenever γ is greater than $4/3$, but gives a more complete description of the circumstances which separate the stable and unstable cases.

In connection with our present conclusion as to the values of γ_A which characterize stable and unstable cases, it may be mentioned that methods similar to those of section 10 in the preceding article[12] can be applied to our present models to study the dependence of their total available potential energy on γ_A. The application is somewhat more complicated than the preceding one, since it now becomes necessary to use different expressions for the dependence of pressure on density—i.e., integrals of the two equations (11.2)—when we consider adiabatic changes in the volume of any element of fluid in the sphere and positional changes from one element to another. Nevertheless, it proves possible, in analogy with our previous results, to show that the total available potential energy of our present models would be negative for stable models with γ_A now, rather than γ, greater than $4/3$ and positive for unstable models with γ_A less than

4/3, and also to show that the available potential energy would be at a minimum in the case of stable models and at a maximum in the case of unstable models with respect to reversible adiabatic changes, away from the steady state, by "uniform" expansion or contraction of the model. It is of interest to note these properties of our present stable and unstable models, since such properties are not necessary consequences merely of stability and instability.

The most important result of our present conclusion as to the dependence of stability on the value of γ_A lies in the circumstance that we cannot now expect instability, of the kind under study, in any star having radiative thermal transfer, which can be appropriately represented by a model with constant values of γ_A and γ_R, since a constant value of γ_A less than 4/3 would be quite improbable for actual stellar material. The treatment of stars having radiative thermal transfer, which cannot be represented by so simple a model, may be regarded as included in the qualitative discussion given in the next section to more general models where the constancy of γ_A and γ_R will not be assumed and where the variation of these quantities might or might not be such as to lead to zones of convective, as well as of radiative, thermal transfer.

12. *Models with convective and radiative zones.*—Since no probable source of stellar instability has been uncovered in the models already discussed, it now becomes of interest to undertake the treatment of more general models. For this purpose we shall at present attempt only a qualitative discussion of the general form of the Jacobi equation (9.4). The discussion will be broad enough so as to apply to the important case where the mechanism of thermal transfer may be convective, instead of radiative, in certain zones of the star, as well as to the case where the mechanism is radiative throughout the star.

To carry out the proposed discussion let us now return to the general form of the Jacobi equation, as previously given by (9.4),

$$\frac{d}{dr}\left(\frac{1}{4\pi r^2\rho}\frac{\partial p}{\partial \rho}\frac{dz}{dr}\right)+\frac{1}{4\pi\rho}\frac{d}{dr}\left\{\frac{1}{r^2\rho}\left(\frac{dp}{dr}-\frac{\partial p}{\partial \rho}\frac{d\rho}{dr}\right)\right\}z+\frac{z}{r^2}=0\,; \quad (12.1)$$

and let us again consider the result of setting

$$\frac{\partial p}{\partial \rho}=\gamma_A\frac{p}{\rho} \quad \text{and} \quad \frac{dp}{d\rho}=\gamma\frac{p}{\rho}\,, \quad (12.2)$$

without this time assuming that γ_A and γ can be treated as constants throughout the model.

With the help of the ratio between $(\partial p/\partial \rho)$ and $(dp/d\rho)$, given by (12.2), we may begin by re-writing (12.1) in the form

$$\frac{d}{dr}\left(\frac{\gamma_A}{\gamma}\frac{1}{r^2\rho}\frac{dp}{d\rho}\frac{dz}{dr}\right)+\frac{1}{\rho}\frac{d}{dr}\left(\frac{\gamma-\gamma_A}{\gamma}\frac{1}{r^2\rho}\frac{dp}{dr}\right)z+\frac{4\pi z}{r^2}=0.$$

Making use of the equation of hydrostatic equilibrium (3.1), for the change in pressure with radius, this can be re-expressed in a more transparent manner,

$$\frac{d}{dr}\left(\frac{\gamma_A}{\gamma}\frac{m}{r^4}\frac{1}{-\frac{d\rho}{dr}}\frac{dz}{dr}\right)+\frac{1}{\rho}\frac{d}{dr}\left(\frac{\gamma_A-\gamma}{\gamma}\frac{m}{r^4}\right)z+\frac{4\pi z}{r^2}=0,$$

which indicates the essentially positive character of the various factors involved. Carrying out the differentiations of the factors involving the γ's, and rearranging, this gives us

$$\frac{\gamma_A}{\gamma}\frac{d}{dr}\left(\frac{m}{r^4}\frac{1}{-\frac{d\rho}{dr}}\frac{dz}{dr}\right)+\frac{\gamma_A-\gamma}{\gamma}\frac{1}{\rho}\frac{d}{dr}\left(\frac{m}{r^4}\right)z+\frac{4\pi z}{r^2}+\frac{m}{r^4}\left(\frac{1}{-\frac{d\rho}{dr}}\frac{dz}{dr}+\frac{z}{\rho}\right)\frac{d}{dr}\left(\frac{\gamma_A}{\gamma}\right)=0.$$

Finally, re-expressing the mass m out to any radius r in terms of the mean density $\bar{\rho}$ out to that radius, we can then re-write our general Jacobi equation in the desired form

$$\left.\begin{aligned}&\frac{\bar{\rho}}{r\frac{-d\rho}{dr}}\frac{d^2z}{dr^2}+\frac{d}{dr}\left(\frac{\bar{\rho}}{r\frac{-d\rho}{dr}}\right)\frac{dz}{dr}\\&\quad+\frac{\gamma_A-\gamma}{\gamma_A}\frac{1}{\rho}\frac{d}{dr}\left(\frac{\bar{\rho}}{r}\right)z+3\frac{\gamma}{\gamma_A}\frac{z}{r^2}\\&\quad+\left(\frac{d}{dr}\log\frac{\gamma_A}{\gamma}\right)\left(\frac{\bar{\rho}}{r\frac{-d\rho}{dr}}\frac{d\log z}{dr}+\frac{\bar{\rho}}{r\rho}\right)z=0.\end{aligned}\right\}\qquad(12.3)$$

In applying this equation to typical models, the actual density ρ can be taken as decreasing continuously from its central value at $r = 0$ to a value which is substantially zero at the boundary at $r = r_b$; the mean density $\bar{\rho}$ can be taken as decreasing from the central value to a value which still remains finite at the boundary; the decrease of density with radius $(-d\rho/dr)$ can be taken as increasing from the value zero at the center to a maximum value—say in the neighborhood of $r = r_b/7$ (Eddington model)—and then decreasing again to a value which still remains positive and finite at the boundary $r = r_b$, where the density ρ is itself substantially zero; and the quantity γ_A can be taken as equal to, or greater than, γ, according as we are in a convective or radiative zone.

We now wish to use this last form of expressing our general Jacobi equation to obtain insight into the circumstances, which might lead to instability, by making a pair of zeros for z occur within the radius of the model. For this purpose we may regard ourselves as constructing a solution of (12.3) which starts out with z increasing from zero at $r = 0$, and as then determining whether a second zero of z occurs before we reach the boundary at $r = r_b$.

Let us first consider the character of our equation when γ_A and γ are constants. The left-hand side of (12.3) will then reduce to its first four terms, since the last term depends on the rate of change of those quantities with r; and, in accordance with our previous work in section 11, the solution of this simplified form of the equation will then be such that no second zero of z will fall within the radius of the model when γ_A is greater than $4/3$. We are actually interested, however, in the possibility for a pair of zeros when γ_A does have a value larger than $4/3$ over most of the model—e.g., a value in the neighborhood of $5/3$ over those ranges where the pressure of the stellar fluid can be treated as that for a non-dissociating monatomic gas with negligible admixture of radiation.

Hence, let us now consider the character of equation (12.3) when γ_A and γ are not treated as constants, and see if their possible dependence on r might be such as to favor the appearance of a second zero for z within the range of the model. In doing so, it will be appropriate to regard the pressure p and density ρ in the model as having

some specified dependence on r which we wish to study. This then gives us a model of definite radius r_b, with γ some definite function of r, and we can fix our attention on inquiry as to the kind of dependence of γ_A on r which might lead to the appearance of a second zero for z within the radius r_b. Since the appearance of such a second zero would primarily depend on a sufficient rate of decrease of dz/dr from its originally positive values in the neighborhood of $r = 0$ to large-enough negative values as we proceed outward from the center, it is evident that the needed kind of dependence of γ_A on r would have to be such as to give increased negative values for the first term in (12.3) through increase in the positive character of later terms in that equation.

Carrying out this method of qualitative attack, we actually do find that the occurrence of a second zero for z, as we pass outward from the center, might be significantly favored by the presence of an inner convective zone around the center of the star and also by the presence of an outer convective zone just under the surface of the star, both possibilities seeming reasonable ones to consider in accordance with the remarks made in section 1. Under such circumstances the quantity γ_A in equation (12.3) would be equal to γ in the central convective zone, would increase above γ as we pass outward from that zone, and would then again decrease to γ and increase once more above that value as we pass through the convective zone just under the surface of the model. To see that this kind of behavior for γ_A would favor the appearance of a second zero for z, we must show that the dependence of γ_A on r would be such as to favor positive values for the last three terms on the left-hand side of (12.3), which depend directly on that quantity.

In the case of the third and fourth terms in (12.3), we at once note that the equality of γ_A with γ in the assumed convection zones would favor the return of z to zero, since the essentially negative coefficient in the third term will become zero when γ_A drops to γ, and the essentially positive coefficient in the fourth term will be as large as possible when γ_A drops to γ. In view, however, of our previous investigations on models with constant γ_A and γ, we cannot expect that this alone would be sufficient in cases of interest to lead to a second zero

of z before reaching the boundary, and must especially turn our attention to the fifth term in (12.3), which depends directly on the change of (γ_A/γ) with r.

In the case of the fifth term in (12.3), the coefficient of z will be equal to zero within the convective zones and also approximately equal to zero over that great range in the intermediate radiative zone where the change of (γ_A/γ) with r will be small. Hence, we must examine the coefficient in particular when we pass out of the central convective zone and into and out of the outer convective zone. As we pass out of the central convective zone, since $d \log (\gamma_A/\gamma)/dr$ will be positive and $d \log z/dr$ also presumably still positive, the coefficient of z in the fifth term of (12.3) will be positive, and indeed will be very large if the boundary of the zone is close to the center, since both r and $(-d\rho/dr)$ go to zero at $r = 0$. As we pass into the second convective zone, since $d \log (\gamma_A/\gamma)/dr$ will now be negative and $d \log z/dr$ now also presumably negative, there will be a competition between the two components into which the coefficient of z may be divided; and it will not be possible a priori to say whether the resulting value will be positive or negative. Nevertheless, since r has now become large, it may well be that both components will be small. Finally, as we emerge from the outer convective zone, since $d \log (\gamma_A/\gamma)/dr$ will now be positive and since ρ will go substantially to zero at the boundary while $(-d\rho/dr)$ remains finite, we can conclude that the value of the coefficient of z might be positive and very large if the zone in question lies close to the surface.

We thus see that the presence either of a central or of an outer convective zone in a stellar model, with the corresponding lack of constancy in (γ_A/γ), would introduce factors which might have important effects in the direction of bringing a pair of zeros for the Jacobi equation within the radius of the model. A more exact calculation, to determine whether this result would actually ever be the outcome in reasonable stellar models, would be complicated and would presumably involve a detailed knowledge as to the dependence of γ_A and γ on r. Nevertheless, since we would get a pair of zeros for the Jacobi equation within the radius of the model, with constant values for γ_A and γ, when we drop to $\gamma_A = 4/3$, it does not seem impossible that the above-discussed effects of the lack of constancy of γ_A and γ

might also sometimes lead to that same result even when γ_A has, for the most part, a value in the neighborhood of $5/3$. Hence, it would hardly be safe at the present time to assert that the available potential energy of stellar models, having convective, as well as radiative, zones of thermal transfer, would necessarily be at a minimum, so that the model would be stable against fluctuations in the distribution of stellar fluid.

13. *Brief summary of results.*—Before concluding this somewhat long article, it will first be desirable to give a brief statement of the results obtained.

The main function of the article has been to discuss the stability of stellar models toward small, instantaneous fluctuations in the distribution of the fluid composing the model. With respect to this particular aspect of the general problem of stellar stability, it was seen that the necessary condition for stability would be the requirement of a minimum value for the available potential energy of the model toward reversible, adiabatic changes in the distribution of stellar fluid. Setting up the integral that expresses the available potential energy, and applying the methods of the calculus of variations, it was then shown that the available potential energy would in general satisfy all tests for a minimum, except that of Jacobi as to the location of conjugate points, for which separate investigation must be made in each particular case.

Carrying out such investigations of the Jacobi test as were readily feasible, it was next found—as perhaps the most important result of the article—that there would be no reason to expect instability of the kind under consideration in the case of simple stellar models having radiative (or convective) thermal transfer throughout. For example, in the case of the standard Eddington model it was seen that the structure would be in a completely stable state toward small variations in the distribution of fluid; even though in an Emden sphere of simple mechanical fluid, with the same dependence of pressure and density on radius, the structure would only be in neutral equilibrium toward such variations.

Finally, in the case of more complicated models having zones of convective, as well as of radiative, transfer, it was found that the presence either of a central convective zone or of an outer convective

zone just under the surface of the star would introduce a tendency toward possible instability which must be kept in mind until more accurate treatments of the Jacobi test are available.

14. *Remarks on the origin of novae.*—Part of the original motivation for the work presented in this article was the idea that the kind of instability under consideration might provide an explanation for the occurrence of stellar novae. It will be of interest to make a few remarks in this connection.

Suggestions as to the origin of novae may be conveniently grouped into three classes. In the first class we have the suggestion that a star becomes a nova as the direct result of a collision with some other astronomical body or bodies. In the second class we have the suggestion that a star becomes a nova as the consequence of some sudden alteration in the rate of internal energy generation. In the third class we may place the suggestion that a star becomes a nova because of the presence of some kind of internal instability which can suddenly make a large amount of energy available when the appropriate internal fluctuation in the distribution of stellar fluid takes place.

The suggestion that stars become novae as a direct consequence of the kinetic energy made available on collision with another star, or perhaps with a distribution of smaller bodies, is not now regarded as a satisfactory explanation. Russell[14] calculates that the number of such collisions—at least of one star with another—would be millions of times less frequent than needed to account for the appearance even of the brighter novae. And Unsöld[15] regards the similarity between different novae, especially as illustrated by Hubble's[16] observations on the novae in Andromeda, as further evidence against the hypothesis of formation by any random kind of collisions.

The suggestion that stars become novae as a consequence of some sudden alteration in the rate of internal energy generation seems a much more probable kind of explanation. Various hypotheses concerning the initiation of this change in rate have been made.

Russell,[17] following a suggestion of Pickering, considers the possi-

[14] See Russell, Dugan, and Stewart, *op. cit.*, p. 789.

[15] *Loc. cit.*

[16] *Ap. J.*, **69**, 103, 1929.

[17] See Russell, Dugan, and Stewart, *op. cit.*, p. 789.

bility that the change in rate of energy generation might itself be initiated by a collision of the star with some wandering body of small dimensions, perhaps no larger than an asteroid. The penetration of such a small body into the interior of the star might produce a "hot pocket" where the rate of energy generation was temporarily increased, by rise in temperature, to a sufficient extent to account for the energy outburst of the nova. The occurrence of such minor collisions, which do not directly provide sufficient kinetic energy to produce a nova, might well be frequent enough to account for the frequency of novae. The hypothesis might meet difficulties in explaining the degree of similarity between different novae.

Milne[18] has considered the possibility that the matter in the central region of a star might suddenly change into the degenerate condition of matter in a white dwarf and liberate a large amount of energy by gravitational contraction. Baade and Zwicky[19] have made a similar suggestion for the special case of supernovae, where the matter in the star is taken as changing into a neutron gas, which ultimately results in a very dense neutron core. Vogt[20] has, in addition, pointed out that a change of matter into the degenerate condition, as in a white dwarf, would lower the opacity and thus permit the escape of entrained radiation; and Zwicky[21] has pointed out the similar situation in connection with the change into neutron gas. The main difficulty encountered by such hypotheses lies in the assumed suddenness of the change for which no appropriate mechanism seems available. In addition, it might be difficult with the help of such hypotheses to account for the recurrent appearance of nova outbursts as in T Pyxidis.

Another kind of hypothesis as to the mechanism by which the rate of energy generation in a star might be changed lies in the possibility that some material involved in the nuclear reactions producing the energy might become largely exhausted in the central region of the star, where a steady rate of energy generation has been going on. This might then be followed by a sudden increase in rate of energy

[18] *M.N.*, **91**, 4, 1930; *Observatory*, **54**, 140, 1931.

[19] *Phys. Rev.*, **45**, 138, 1934; **46**, 76, 1934; *Proc. Nat. Acad. Sci.*, **20**, 259, 1934.

[20] *A.N.*, **263**, 1, 1937.

[21] *Phys. Rev.*, **55**, 726, 1939. See I (2).

generation in one or the other of two ways. In the first place, the material in question might be a primary constituent of the "stellar fuel"; and its exhaustion at the center of the star, with a consequent decrease in temperature and pressure, might be followed by a collapse suddenly bringing new fuel into a region of high-enough temperature, so as to lead to a sudden increase in the rate of energy generation. In the second place, the material in question might be somewhat less simply involved in a chain of nuclear reactions, in such a way that its exhaustion removes an inhibiting action on the rate of the main energy-producing steps. Hypotheses such as these must, of course, be regarded as tentative in the absence of detailed mechanisms. The main difficulties might lie in devising an internal mechanism of sufficient suddenness and in showing that the sudden change at the center of a star would be reflected in a sudden outburst at the far-distant boundary, which is the only region available to our observation when a nova occurs.[22]

We must now turn to the third class of suggestions, that the formation of novae is due to the presence of internal instability. In this case we have in mind some mechanical or thermal-mechanical kind of instability connected with the distribution of the stellar fluid, which can lead to a sudden tranformation within the star away from a previously steady state when an appropriate fluctuation in the distribution of the fluid accidentally takes place.

The first suggestion of such a possibility appears to have been made by Unsöld.[23] On the basis of his own calculations of the effect of changing degree of ionization on the properties of stellar fluid under adiabatic compression, and also on the basis of known observations of the character of the sun's surface, he was led to the conclusion that the presence of a convective zone just under the surface of

[22] Since the enormous store of radiant energy entrained within the interior of a main-sequence star would act as a reservoir, it does not appear plausible to assume that a sudden increase in the rate of energy generation at the center would of itself lead to a sudden increase in the rate of arrival of radiant energy at the surface. Sudden mechanical changes at the center, however, accompanying either a sudden increase or decrease in the rate of energy generation, might produce sudden mechanical changes with attendant thermal consequences at the surface.

[23] *Loc. cit.*

a star would be possible. This then led to the suggestion that the sudden formation of such a convective zone from a previously present unstable condition of radiative thermal transfer would furnish the necessary energy for nova formation. The suggestion was supported by estimates as to the amount of energy that might thus be made available and as to the velocity of expansion of the photosphere that might thereby result. The suggestion also has the attractive feature that the whole process takes place near the surface of the star, so that the suddenness of the original change would certainly be reflected in the suddenness of the observed phenomenon. Nevertheless, the suggestion would seem to encounter the serious difficulty, in view of the violent stirring presumably present in the interior of stars, that there appears to be no reason to assume any delay in the initiation of thermal convection when the conditions within a star make this possible, and no reason to assume that an extensive zone in an unstable state of radiative transfer could be built up which would then suddenly change into the stable state of convective transfer.

Finally, as a further suggestion, which might connect the origin of novae with the presence of internal instability, we come to the possibility, of special concern for the present article, that the distribution of fluid in a star might not be such as to secure a minimum value of the available potential energy, owing to a failure of the distribution to meet the requirements formally expressed by the Jacobi test for a minimum; and that this would provide a source of kinetic energy which could be released when an appropriate fluctuation in the distribution of stellar fluid accidentally took place. This suggestion would have the attractive feature, since the accidental fluctuation would have to be of an appropriate character over the whole range between Jacobi's conjugate points, that the release of kinetic energy would be delayed until such a fluctuation did take place and that the process would then develop suddenly. The suggestion would also have the attractive feature, with the outermost conjugate point in the neighborhood of the surface, that energy would be suddenly set free at the surface of the star in agreement with observation. Nevertheless, in view of the further complicated calculations that would be necessary, to ascertain the conditions under which actual failures of

the Jacobi test might be expected, to determine the probable time interval needed for the appropriate fluctuation to occur, and to describe the resulting behavior of the star when the instability is released, it would not be proper at this time to assert that the origin of novae is to be explained in the suggested manner.

In conclusion, the writer wishes to express his thanks to his colleagues, Professors J. R. Oppenheimer and I. S. Bowen, with whom he has had helpful discussions and from whom he has received valuable suggestions as to the matters treated in this article.

Norman Bridge Laboratory of Physics
California Institute of Technology
June 1939

PHYSICAL PROCESSES IN GASEOUS NEBULAE

VIII. THE ULTRAVIOLET RADIATION FIELD AND ELECTRON TEMPERATURE OF AN OPTICALLY THICK NEBULA

LAWRENCE H. ALLER,[1] JAMES G. BAKER,[1] AND DONALD H. MENZEL

ABSTRACT

The theory of the transfer of radiation in the Lyman continuum that was developed in papers VI and VII of this series is applied to a numerical example. A central star radiating as a black body at a temperature of 80,000° C. is assumed to illuminate a nebular shell whose optical thickness at the Lyman series limit is 3.0. The numerical methods of solution are discussed in detail. The redistribution of electron velocities by collisions and free-free transitions is shown to have considerable effect upon the character of the radiation field. Near the series limit more radiation gets through the nebula than would otherwise be expected. The electron temperature at the inner boundary is almost that of an optically thin nebular shell, and at the outer boundary it approaches that of the central star.

In the preceding paper of this series[2] we have derived the differential equations of transfer for radiation in the Lyman continuum for optically thick nebulae. In order to study the variation of the radiation field and electron temperature throughout a given nebula we found it necessary to consider the transfer of radiation in each element of the continuum rather than to treat the continuum as a single level. A term was introduced to take into account the interlocking between the elements of the continuum. The equation of transfer (VII, 25) is

$$\frac{d^2\mathfrak{J}_\nu}{d\tau_\nu^2} = \lambda_\nu^2\mathfrak{J}_\nu - 3p_\nu e^{-\tau_\nu} - 3\mathfrak{R}_\nu\,, \qquad (1)$$

where $\lambda_\nu^2 = 3(1 - p_\nu)$ and $\mathfrak{J}_\nu$ is the intensity of the diffuse radiation. The expression for $\mathfrak{R}_\nu$ is

$$\mathfrak{R}_\nu = \frac{(e^{y_1} - 1)}{G_{T_e}}\, e^{T_1(y_1-y)/T_e} \int_{y_1}^{\infty} (\mathfrak{J}_\nu + e^{-\tau_\nu})\, \frac{dy}{y(e^y - 1)} - p_\nu(\mathfrak{J}_\nu + e^{-\tau_\nu})\,. \qquad (2)$$

[1] Society of Fellows, Harvard University.

[2] (Part I) *Ap. J.*, **85**, 330, 1937; (II) **86**, 70, 1937; (III) **88**, 52, 1938; (IV) **88**, 313, 1938; (V) **88**, 422, 1938; (VI) **89**, 587, 1939; (VII) **90**, 271, 1939. The papers of this series are referred to in the text as (I), (II), (III), etc.

An alternate form of the equation of transfer, as given in (VII, 30), is

$$\frac{\partial^2 \mathfrak{J}_\nu}{\partial \tau_{\nu_1}^2}\left(\frac{y}{y_1}\right)^6 = 3\mathfrak{J}_\nu - \frac{3(e^y-1)}{G_{T_\epsilon}} e^{T_1(y_1-y)/T_\epsilon} \int_{y_1}^{\infty} (\mathfrak{J}_\nu + e^{-\tau_\nu}) \frac{dy}{y(e^y-1)}, \quad (2a)$$

where the g-factor has been neglected. For the numerical calculation we found it preferable to deal with equation (1), in which we have taken the Gaunt factor into account. The optical depth at any frequency is given, then, by

$$\frac{\tau_{\nu_1}}{\tau_\nu} = \frac{\alpha_1}{\alpha_\nu} = \left(\frac{\nu}{\nu_1}\right)^3 \frac{g_{\nu_1}}{g_\nu}. \quad (3)$$

In the solution of (1) we must remember that the variables employed are not strictly independent. The relation (3) must always be kept in mind when we manipulate (1).

Except for the term in $\mathfrak{R}_\nu$, (1) is of the same form as the equation of transfer given by Ambarzumian and Chandrasekhar. This "correction term" is a measure, for any frequency, of the effect of the interlocking between the various levels of the continuum. $\mathfrak{R}_\nu$ can scarcely be regarded, however, as a mere correction, because it often proves to be as large as, or larger than, the other terms on the right-hand side of (1). To neglect it would be to consider the continuum as a manifold of levels interacting only with discrete levels and not with each other. We could avoid some of the difficulty by treating the continuum as a single level, in which case $\mathfrak{R}_\nu$ would vanish; but we should encounter the new difficulty of choosing a proper mean value of p_ν, which would certainly vary throughout the nebula along with the variation of the radiation field and T_ϵ.

The trouble arises from the fact that $\mathfrak{R}_\nu$ contains the unknown $\mathfrak{J}_\nu$ integrated over all frequencies, whereas (1) is valid for only one particular frequency. Note also that $\mathfrak{R}_\nu$ contains the electron temperature both explicitly and implicitly through G_{T_ϵ}. No rigorous solution of the differential integral equation (2a), in terms of elementary functions, appears to exist. One is therefore compelled to seek a solution by a method of successive approximations. As a working basis, we found it expedient to start our approximation by setting $\mathfrak{R}_\nu = 0$.

By so doing, we have adopted a preliminary set of values of $\mathfrak{J}_\nu$ for which the interlocking between the elements of the continuum has been neglected. The resultant solution of (1) is well known and may be written as[3]

$$\mathfrak{J}_0 = A_0 e^{\lambda\tau} + B_0 e^{-\lambda\tau} + \frac{3p}{\lambda^2 - 1} e^{-\tau}, \tag{4}$$

where

$$A_0 = B_0 + \frac{3p}{\lambda(\lambda^2 - 1)},$$

$$B_0 = \frac{-3p}{\lambda(\lambda^2 - 1)} \frac{(1 + \frac{2}{3}\lambda)e^{\lambda\tau_0} + \frac{1}{3}\lambda e^{-\tau_0}}{(1 + \frac{2}{3}\lambda)e^{\lambda\tau_0} + (1 - \frac{2}{3}\lambda)e^{-\lambda\tau_0}}. \tag{5}$$

These values of $\mathfrak{J}_0$ lead immediately to the determination of a preliminary set of values of $W_{1\kappa}$ by the relation

$$W_{1\kappa} = \mathfrak{J}_\nu + e^{-\tau_\nu}. \tag{6}$$

With this approximate value of $W_{1\kappa}$ one can compute first the electron temperature T_e by the method outlined in (V), and then $\mathfrak{R}_\nu$ by (2). This procedure completes the first step. For the purposes of the next approximation, $\mathfrak{R}_\nu$ can be taken as constant with optical depth, although its functional dependence on frequency is retained. The resultant solution of (1) is of the form

$$\mathfrak{J}_\nu = A'_\nu e^{\lambda_\nu\tau_\nu} + B'_\nu e^{-\lambda_\nu\tau_\nu} + \frac{3p_\nu e^{-\tau_\nu}}{\lambda_\nu^2 - 1} - \frac{3\mathfrak{R}_\nu}{\lambda_\nu^2}, \tag{7}$$

where the new constants of integration, A' and B', are related to the old by simple additive terms:

$$A' = A_0 + \Delta' A\ ; \qquad B' = B_0 + \Delta' B,$$

where

$$\Delta' A = \Delta' B = -\frac{3\mathfrak{R}_\nu}{\lambda^2\{(1 - \frac{2}{3}\lambda)e^{-\lambda\tau_0} + (1 + \frac{2}{3}\lambda)e^{\lambda\tau_0}\}}. \tag{8}$$

With these improved values of the $\mathfrak{J}$'s, double-entry tables of $W_{1\kappa}$ and $\mathfrak{R}_\nu$ as functions of optical depth are computed. The dependence

[3] Cf. Rosseland, *Theoretical Astrophysics*, p. 328.

of T_ϵ on the optical depth is, of course, obtained as an intermediate step in passing from $W_{1\kappa}$ to $\mathfrak{R}_\nu$. With these values of $\mathfrak{R}_\nu$ we now proceed to a third approximation.

For the third and succeeding approximations we have found that, to a high order of accuracy, $\mathfrak{R}_\nu$ may be taken as a linear function of the optical depth.[4] Therefore, we adopt[5]

$$\mathfrak{R} = a_0 + a_1\tau\,, \tag{9}$$

whence

$$\mathfrak{J} = Ae^{\lambda\tau} + Be^{-\lambda\tau} + \frac{3pe^{-\tau}}{\lambda^2 - 1} + a_0 + a_1\tau\,, \tag{10}$$

where

$$a_0 = \frac{3a_0}{\lambda^2}\,; \qquad a_1 = \frac{3a_1}{\lambda^2}\,. \tag{11}$$

Then

$$\Delta B = \frac{e^{\lambda\tau_0}(1 + \frac{2}{3}\lambda)\frac{a_1}{\lambda} - (a_0 + \frac{2}{3}a_1) - a_1\tau_0}{\{(1 + \frac{2}{3}\lambda)e^{\lambda\tau_0} + (1 - \frac{2}{3}\lambda)e^{-\lambda\tau_0}\}} \tag{12}$$

and

$$\Delta A = \Delta B - \frac{a_1}{\lambda} \tag{13}$$

and

$$A = A_0 + \Delta A\,; \qquad B = B_0 + \Delta B\,. \tag{14}$$

These expressions for the constants of integration are taken as final.

[4] It might be supposed on first sight that $\mathfrak{R}_\nu$ should be expanded as a power series in the optical depth. In assuming a series expansion, however, we encounter a rather unusual mathematical difficulty. The coefficients of the higher-order terms in the expansion of $\mathfrak{R}_\nu$ turn out to be large numerically. The contribution of each term to $\mathfrak{R}_\nu$ is small because the optical depth raised to a high power is small. If we assume that $\mathfrak{R}_\nu$ is a power series, it is clear that the coefficients in this series must be related to the coefficients in a corresponding power series in $\mathfrak{J}$. From the nature of the boundary conditions it turns out that the rth coefficient in the expansion for $\mathfrak{R}_\nu$ and also the $(r + 2)$, $(r + 4)$, $(r + 6)$, etc., coefficients occur with factors only of the order of unity. As a result, the uncertain and numerically large coefficients overpower the significant coefficients a_0 and a_1 and render the resultant $\mathfrak{J}$ meaningless.

[5] All the quantities in these equations are functions of ν. The subscript ν is dropped as superfluous.

For a numerical application of the present theory we have adopted a gaseous nebula of optical depth 3.0 at the Lyman limit surrounding a hot central star which is assumed to radiate as a black body at a temperature of 80,000°. The procedure outlined above was followed closely in the numerical calculations. For each of the steps, double-entry tables of the various functions needed in the calculation were prepared. The independent variables were taken to be ν/ν_1 and τ_{ν_1} (e.g., see Table 1).

TABLE 1

ν/ν_1	$\tau_{0\nu}$	g_ν/g_{ν_1}	S_ν
1.001	2.991	1.000	1.0665
1.01	2.937	1.010	1.0724
1.03	2.775	1.010	1.0877
1.06	2.568	1.020	1.1079
1.10	2.340	1.035	1.1331
1.20	1.836	1.060	1.1802
1.40	1.200	1.100	1.2244
1.60	0.831	1.135	1.2077
2.00	0.444	1.186	1.0542
2.50	0.234	1.220	0.7589
3.00	0.138	1.235	0.4892
6.00	0.015	1.250	0.1085

First of all, tables of τ_ν, g, and S_ν were computed. With these fundamental starting data, A_0 and B_0 were computed with the aid of (5), and $\mathfrak{J}_0$ from (4). For the calculation of the electron temperature by the method of (V) we were required to find the integrals

$$\int W_{1\kappa} \frac{dy}{e^y - 1} \quad \text{and} \quad \int W_{1\kappa} \frac{dy}{y(e^y - 1)},$$

where

$$W_{1\kappa} = \mathfrak{J}_0 + e^{-\tau}.$$

By the methods described in (V), values of T_e have been computed for the four values of $\tau_{\nu_1} = 0$, 1, 2, and 3. For the purpose of the second approximation, values of $\mathfrak{R}_\nu$ and T_e were adopted corresponding to an optical depth τ_{ν_1} of about 1.5. For this second approximation the dependence of $\mathfrak{R}_\nu$ on frequency was retained, of course, and formulas (7) and (8) were applied. For the third and higher approxi-

mations a linear variation of $\mathfrak{K}_\nu$ with τ_ν was adopted, and from the $\mathfrak{J}$-values of the second approximation it was possible to compute $\mathfrak{K}_\nu$ for the four optical depths corresponding to $\tau_{\nu_1} = 0, 1, 2$, and 3 and to evaluate the coefficients a_0 and a_1 in (9). By means of equations (11), (12), (13), and (14), $\mathfrak{J}$ was now calculated, $\mathfrak{K}_\nu$ was derived from (2), and the procedure was repeated for the fourth approximation. The character of $W_{1\kappa}$ on the basis of the third and fourth approximations is exhibited in Figure 1, computed for $\tau = 0$, where a comparison with the Ambarzumian value (first approximation) is shown.

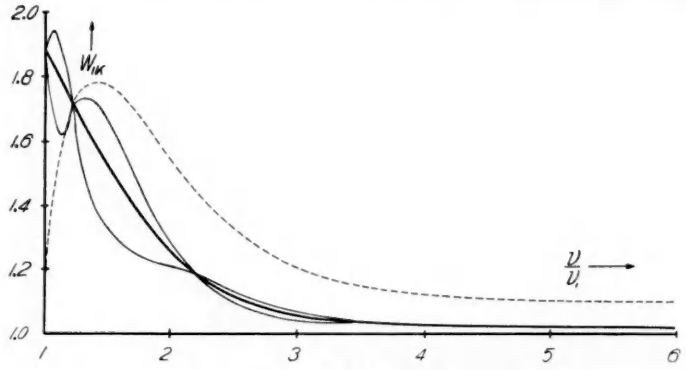

FIG. 1.—$W_{1\kappa}$ at the inner boundary

The successive approximations yield curves that pass through nodal points, analogously to the way in which a Fourier series approximates a given function. These nodal points must also lie on the final curve, and, indeed, one would obtain a very excellent approximation to the final curve merely by evaluating these nodal points. In future calculations involving nebulae of various total optical depths the position of the nodal points should be determined first. Then the functions can be evaluated for these special points. The calculations will be considerably shortened if this procedure is followed. Having noted the character of the approximations, we found it expedient to guess at the final form of the function $W_{1\kappa}$ and thereby to arrive immediately at an approximation of a high order. If successive approximations were carried through blindly, the slow convergence would render the computations of hopeless length. A mean curve was drawn through the nodal points given by the inter-

section of the third and fourth approximations to $W_{1\kappa}$. The Ambarzumian curve passes through the second nodal point, which lies at the frequency for which $\mathfrak{R}_\nu = 0$. The frequencies of the various nodal points are nearly independent of optical depth, at least within the errors of the calculation. This new curve was treated as the fifth approximation, and one more numerical solution of the equations was effected. There were, thus, six approximations in all.

The comparison of the final values of $\mathfrak{J}$ with those obtained in the first approximation (i.e., the $\mathfrak{J}_0$ values derived from the Chandrasek-

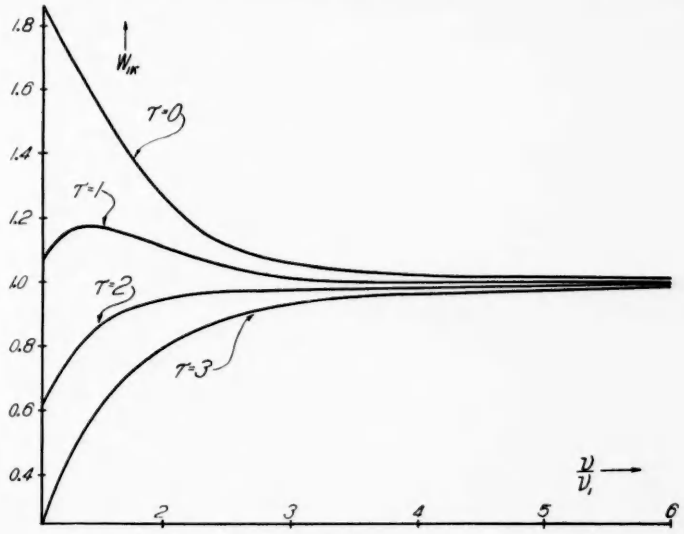

FIG. 2

har modification of the Ambarzumian equations) exhibits strikingly the effect of the interlocking between the various states of the continuum. Much energy is degraded to the lower frequencies by collisions and free-free emissions. The heavy full curve in Figure 1 is the function $W_{1\kappa}$ that satisfies the differential equation of transfer (2) and also (2*a*). The dashed curve represents the Ambarzumian values, and the full light-curves represent the third and fourth approximations. These are the curves for the inner boundary, but they are typical of the other three sets of curves for $\tau_{\nu_1} = 1$, 2, and 3. Figure 2 gives $W_{1\kappa}$ as a function of frequency for the optical depths $\tau_{\nu_1} = 0$, 1, 2, and 3. Figure 3 gives $\mathfrak{R}_\nu$ as a function of frequency at the inner

and outer boundaries of the nebula. Since it was possible to take $\mathfrak{R}_\nu$ as a linear function of τ_ν, values of $\mathfrak{R}_\nu$ for the inner points of the nebula are intermediate between the two curves drawn.

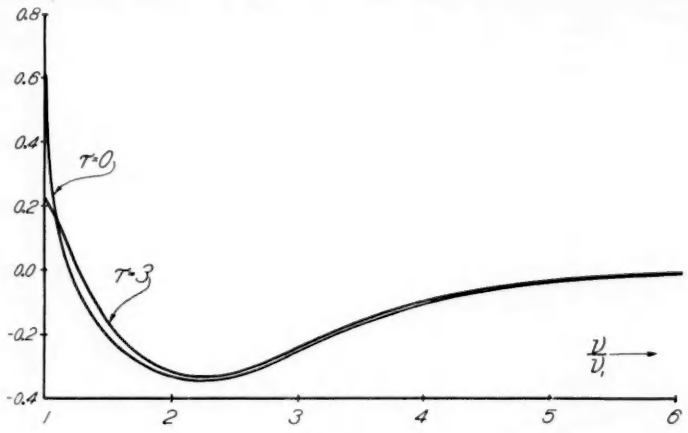

FIG. 3

It thus appears that the dependence of $\mathfrak{R}_\nu$ on frequency is rather insensitive to the position in the nebula. Equation (VII, 3) requires that

$$\int_{\nu_1}^{\infty} \eta d\nu = \int_{\nu_1}^{\infty} \frac{R_\nu N_1 a_\nu}{p_\nu h\nu}\, d\nu = 0 . \tag{15}$$

After canceling out all terms independent of the frequency, we find that (15) reduces to

$$\int_1^{\infty} \frac{R_\nu \dfrac{\tau_{0\nu}}{\tau_{0\nu_1}}}{p_\nu \left(\dfrac{\nu}{\nu_1}\right)} d\left(\frac{\nu}{\nu_1}\right) = 0 .$$

This check was applied to the curves in (3) and was found to hold within the error of the computations.

Another point of interest is the change of the electron temperature through the nebula (this variation is shown in Fig. 4):

τ_{ν_1}	T_e
0	59,000
1	61,000
2	64,000
3	76,000

From the results of the calculations of (V) we recall that, for a thin nebular shell illuminated by a star radiating as a black body at a temperature of 80,000°, the electron temperature is 57,000°. We arrive, therefore, at the interesting conclusion that a nebula of optical thickness 3.0 at the Lyman limit will assume on its inner boundary a temperature almost corresponding to that of a thin nebular shell and that, on the outer boundary, the temperature will be close to that of the central star.

These calculations were carried out partly with the intention of providing a guide for future numerical work on nebulae of different optical thicknesses and central stars of different temperatures. The

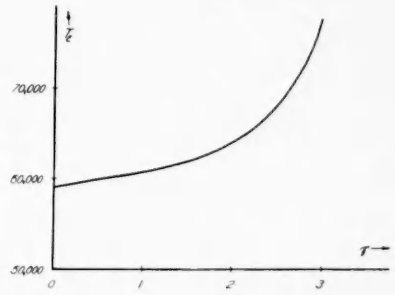

FIG. 4

slow convergence of the approximations seems very discouraging until one remembers that the initial approximation, i.e., that of no coupling between the various states of the continuum, is a poor one, as a glance at the curve for $\mathfrak{R}_\nu$ will show.

In a recent comprehensive publication[6] Y. Hagihara discusses the problem of transfer in the Lyman continuum. Hagihara takes the problem further than does Chandrasekhar or Ambarzumian in that he uses the temperature of the nuclear star as a parameter rather than mean capture-probabilities. He still considers the continuum as a single state, however, and neglects the effect of the reshuffling of electron velocities. In addition he makes the assumption that the temperature of the electron gas is constant throughout the nebula and equal to that of the nuclear star. This restriction cannot be fulfilled, as we have shown, for a pure hydrogen nebula, so that Hagihara's results do not agree too well with our final values. They

[6] *Japanese J. of Astron. and Geoph.*, **15**, 1, 1938.

correspond more closely to our first approximation, weighted according to frequency by Hagihara's method.

With this paper we shall leave, for the present, the problem of the equilibrium of a nebula consisting of pure hydrogen. The effect of collisions in populating the higher atomic levels remains still to be considered; but we shall postpone discussion of this question, although a partial analysis of the problem has been carried out. We

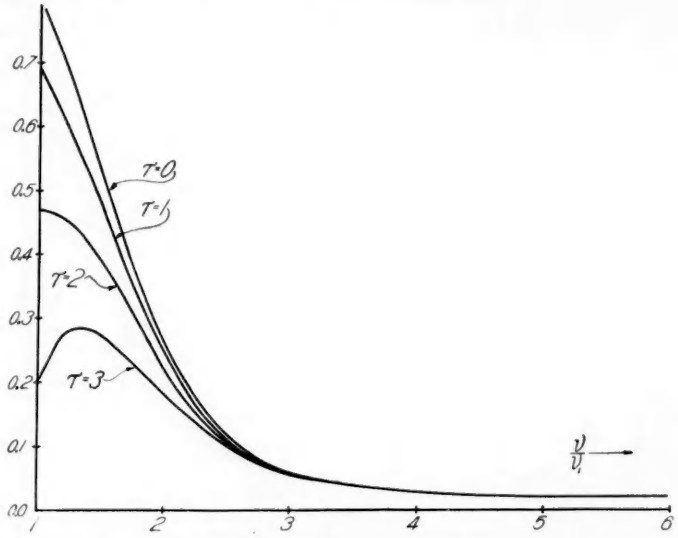

FIG. 5.—$\mathfrak{J}_\nu$ as a function of frequency and optical depth

shall also defer discussion of the problem of transfer in the hydrogen lines because of the complications introduced by expansion of the nebular shell. It is our desire to develop the theory along lines that can be directly compared with observation.

The next papers of this series will deal, accordingly, with the excitation of the lines of oxygen, helium, nitrogen, etc. The discussion will include investigation of significant atomic properties, transition probabilities, capture probabilities, and target areas for collisional excitation. The quantum mechanical calculations are essentially complete, and the relevant papers will appear shortly.

HARVARD COLLEGE OBSERVATORY
June 8, 1939

NEGATIVE IONS OF HYDROGEN AND THE OPACITY OF STELLAR ATMOSPHERES

RUPERT WILDT

ABSTRACT

Compared to the current theory of the atmospheric absorption coefficient, the photospheric level is raised considerably in all spectral types later than $F5$ by including the contribution to the opacity made by the negative ions of hydrogen. Likewise, the discontinuity at the Balmer limit is greatly reduced, so the values of this quantity observed in F stars can be represented without the assumption, advocated by Unsöld, of an abundance ratio of hydrogen to metals equal to 50:1. The abundance ratio adopted by Russell and Pannekoek ($H:M = 1000:1$) appears to be compatible with the observations of the Balmer discontinuity.

The current theory of the atmospheric absorption coefficient is beset with two difficulties: the lack of an adequate theory of the continuous absorption of metallic atoms, and the great uncertainty with respect to the relative abundance of hydrogen and the metals in the outer layers of the stars. Since these matters have been comprehensively reviewed by Unsöld and by Page,[1] there is no need for a more detailed introduction to this paper, which is to present the results of a computation of the contribution to the opacity of stellar atmospheres made by negative ions of hydrogen. An announcement of the astrophysical significance of these particles was made in a paper[2] read at a symposium held at the Yerkes Observatory in June, 1938. In a later note[3] some of the results of the present paper were anticipated, utilizing the absorption coefficients of H^- given by Jen.[4] However, Jen's data are impaired by an error, which was kindly pointed out to the writer by Professor H. S. W. Massey, of London. Then the work was repeated and amplified on the basis of new absorption coefficients of H^- derived by Professor Massey and communicated in advance of publication to the writer, who gratefully acknowledges this assistance.

Massey's absorption coefficients refer to the bound-free transi-

[1] A. Unsöld, *Physik der Sternatmosphären*, Berlin: Julius Springer, 1938; T. L. Page, *M.N.*, **99**, 385, 1939.

[2] *Ap. J.*, **89**, 295, 1939.

[3] R. Wildt, *Pub. A.A.S.*, **9**, 236, 1939.

[4] *Phys. Rev.*, **43**, 540, 1933.

tions (photoelectric ionization), the ground state of H^- being represented by Hylleraas'[5] wave function and the continuous state by a plane wave. Throughout the visual range and the near ultraviolet, Massey's and Jen's absorption coefficients are of the same order of magnitude, about $2 \cdot 10^{-17}$ cm^2 per H^- ion; but in the infrared Massey's curve drops rapidly and reaches zero at the ionization limit (λ 17400), whereas Jen's curve retains a finite value at the ionization limit. The absorption coefficients for the free-free transitions of H^- have been taken from Pannekoek's[6] Table 13*b*, which was compiled from data given by Menzel and Pekeris.[7] After adding the terms for the bound-free and the free-free transitions, the Rosseland mean of the sum was computed. Since each of these two terms is proportional to the electron pressure, only one graphical integration was needed for every temperature. Furthermore, the Rosseland mean for the sum of the absorption of H and H^- was computed. Of course, it was necessary to carry out a graphical integration for every electron pressure at a given temperature, because the relative contributions of H and H^- to the total depend on the ionization equilibrium between H^+, H, and H^-. It should be clearly understood that the electrons involved in this equilibrium are not supposed to have originated from ionization of the hydrogen atoms alone but are thought to have been released from the metals of low ionization potential present in stellar atmospheres (cf. n. 2, above). It has recently been suggested to the writer by Professor H. N. Russell that all the former investigations of the ionization equilibrium in stellar atmospheres of medium and late spectral types should have led to an ionization degree systematically too low, by inadvertently neglecting the fact that neutral hydrogen acts as an acceptor for free electrons and, therefore, tends to increase the ionization of the metals. Most fortunately, a quantitative analysis has revealed that this effect, though doubtless operating in stellar atmospheres, is entirely negligible numerically.[8]

[5] *Zs. f. Phys.*, **60**, 624, 1930, and **63**, 291, 1930.

[6] *Pub. Astronomical Institute of U. of Amsterdam*, No. 4, Addendum.

[7] *M.N.*, **96**, 77, 1935.

[8] The effect described is an instructive analogue, of opposite sign, to King's well-known experiment performed in the electric furnace, where the decrease of the ionization of a metallic vapor on addition of another metal of lower ionization potential can be

Space does not permit the publication of all the monochromatic absorption coefficients. The values of the Rosseland mean of the mass-absorption coefficient are separately given in Table 1 for atomic hydrogen alone (reproduced from Pannekoek's work,[6] Table 8*a* of Addendum), for negative ions of hydrogen alone, and finally for the sum of both, i.e., the total absorption produced by hydrogen. In the upper left corner and the lower right corner of Table 1 the contributions of the atoms and the negative ions, respectively, are predominant. At temperatures lower than 4000° the free-free transitions of H^- become more and more important, compared with the bound-free transitions, on account of the shift of the maximum flux into the infrared. Menzel and Pekeris did not extend their calculations into the infrared because of the lack of convergence of the approximations they used. Their data had to be slightly extrapolated in computing the Rosseland mean at 4852° and 4200°. At still lower temperatures the continuous absorption by molecular hydrogen, too, would gain prominence. It is of interest to note that molecular hydrogen also forms a negative ion. Eyring, Hirschfelder, and Taylor[9] have shown that H_2^- has stable electronic states. Although these cannot be reached by the collision of an electron with H_2, they might be formed through unusually favorable three-body collisions between H^-, H, and a third atom or molecule. The probability of such a process appears to be so low that it is not surprising that the ion H_2^- has not yet been observed in the mass spectrograph.[10]

---

observed directly. It is not difficult to verify the following formula, pertaining to the hydrogen effect:

$$\frac{x^2}{1-x} - \frac{x_0^2}{1-x_0} = \frac{AK_1}{p_e + K_3} - \frac{A}{B}\frac{K_1K_2}{p_e(K_2 + p_e)},$$

where x_0 is the ionization degree of a certain metal (ionization constant K_1) at the electron pressure p_e, resulting from Saha's formula $x_0/(1 - x_0) = K_1/p_e$. If now there are added another metal (ionization constant K_2) and atomic hydrogen (K_3 ionization constant of the negative ions of hydrogen), the ionization degree of the first metal assumes the value x at the electron pressure p_e. A and B denote the abundance of hydrogen in units of the first and second metal. The first term on the right-hand side of the equation represents the small increase of ionization produced by the electron affinity of hydrogen, which, however, may be masked by the presence of another metal, as indicated by the negative sign of the second term.

[9] *J. Chem. Phys.*, **4**, 479, 1936.

[10] J. W. Hiby, *Ann. d. Phys.*, **34**, 473, 1939.

In a preceding note[3] it had been pointed out how well the correction of Pannekoek's monochromatic absorption coefficients, by in-

TABLE 1

ROSSELAND MEAN OF THE ABSORPTION COEFFICIENT OF HYDROGEN

$\log_{10} \bar{k}(H)$
$\log_{10} \bar{k}(H^-)$
$\log_{10} \bar{k}(H+H^-)$

$\log_{10} P_e$ Dynes/Cm²	$5040/T$ and $T°$ K							
	0.5 10,080°	0.6 8400°	0.7 7200°	0.8 6300°	0.9 5600°	1.0 5040°	1.1 4852°	1.2 4200°
−3.0	6.03	6.42	6.71	6.94	6.73	5.67	5.01	4.94
	.....	0.29	1.99	3.58	4.73	4.97		
	.....	.....	.....	.....	.....	5.92		
−2.0	7.03	7.42	7.70	7.75	6.89	5.67	6.01	5.94
	0.43	2.29	3.98	5.39	5.89	5.98		
	.....	.....	.....	.....	6.96	6.56		
−1.0	8.03	8.42	8.63	8.10	6.91	5.67	7.01	6.94
	2.43	4.29	5.91	6.74	6.91	6.98		
	.....	.....	.....	8.18	7.45	7.25		
0.0	9.03	9.39	9.22	8.15	6.91	5.67	8.01	7.94
	4.43	6.26	7.50	7.79	7.91	7.98		
	.....	.....	9.26	8.50	8.09	.....		
+1.0	0.02	0.21	9.37	8.16	6.91	5.67	9.01	8.94
	6.42	8.08	8.65	8.80	8.91	8.98		
	.....	.....	9.57	9.07	8.93	.....		
+2.0	0.96	0.57	9.39	8.16	6.91	5.67	0.01	9.94
	8.36	9.44	9.67	9.80	9.91	9.98		
	.....	0.68	0.04	9.86	.....	.....		
+3.0	1.59	0.62	9.39	8.16	6.91	5.67	1.01	0.94
	9.99	0.49	0.67	0.80	0.91	0.98		
	1.62	1.01	0.77	0.81	.....	.....		
+4.0	1.77	0.63	9.39	8.16	6.91	5.67	2.01	1.94
	1.17	1.50	1.67	1.80	1.91	1.98		
	2.22	1.63	1.71	.....	.....	.....		

cluding the H^- absorption according to Jen's data, serves to represent theoretically the approximately gray character of the matter forming the solar atmosphere. The replacement of Jen's absorption coefficients by the improved ones of Massey has somewhat marred

the striking agreement of theory with observation, by reason of the fact that Massey's absorption-curve falls off rapidly throughout the near infrared and reaches zero at the ionization limit of H^-, whereas Jen's curve is only slightly dependent on the frequency throughout the same range. However, there is still a remarkable improvement, as will be seen on inspection of Table 2. Pannekoek's absorption coefficients k_P already contain the contribution from the free-free transitions of H^-; so C denotes the additive correction for the bound-free

TABLE 2

MONOCHROMATIC ABSORPTION COEFFICIENTS PERTAINING TO THE SOLAR ATMOSPHERE

λ	log k_P	log C	log k^*	log k_P	log C	log k^*	
7000....	8.38	9.33	9.38	9.11	0.33	0.35	
6000....	8.46	9.39	9.44	9.17	.39	.41	
5000....	8.63	9.49	9.55	9.33	.49	.51	$5040/T = 1.0$
4000....	8.94	9.53	9.63	9.64	.53	.58	$T = 5040°$ K
3500....	9.20	9.52	9.69	9.89	.52	.61	
3000....	9.58	9.47	9.83	0.27	0.47	0.68	
7000....	8.34	9.14	9.21	9.13	0.14	0.18	
6000....	8.39	9.20	9.26	9.18	.20	.24	
5000....	8.50	9.31	9.37	9.29	.31	.35	$5040/T = 0.9$
4000....	8.76	9.34	9.44	9.54	.34	.40	$T = 5600°$ K
3500....	9.02	9.33	9.50	9.76	.33	.43	
3000....	9.31	9.29	9.60	0.07	0.29	0.49	
	p_e = 10 dynes/cm²			p_e = 100 dynes/cm²			

transitions, the corrected value k^* being equal to $C + k_P$. The remaining discrepancy between theory and observation is far too great to be dismissed readily, but its origin cannot be ascertained at present.

While the energy distribution in the solar spectrum has been determined with fair accuracy, there is no consensus as to the absolute energy-curves of stellar spectra. Even differential spectrophotometric comparisons are systematically influenced, to a degree still unknown quantitatively, by the crowding of blended lines in the later spectral types. There is only one quantity which may be expected to be reasonably free from such purely observational errors, namely, the discontinuity at the Balmer limit, which in recent years

has become the subject of extensive studies by a group of French astrophysicists.[11] Their observations of the Balmer discontinuity, expressed as magnitude differences, have been plotted as a function of the spectral type in the right half of Figure 1; and Kuiper's temperature scale[12] has been added for sake of comparison with the left half of Figure 1, the abscissae of which are $5040/T$. The ordinates of the left half are the theoretical magnitude differences computed for the

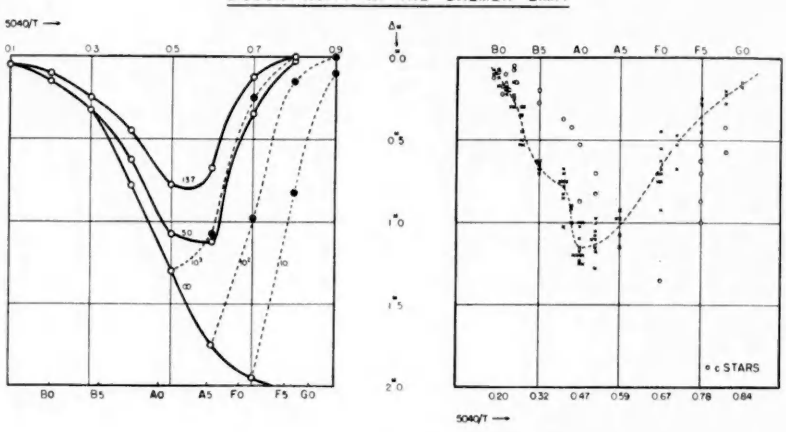

FIG. 1

Balmer discontinuity by means of Burkhardt's table,[13] which gives the monochromatic radiation flux as function of $h\nu/kT$ and $\bar{k}/k_\nu$, on the assumption that the latter quantity does not vary with the optical depth. Three heavy lines are practically coincident with those of Figure 53*a* of Unsöld's book.[1] They refer to an average atmospheric electron pressure of 100 dynes/cm², assumed to be constant along the spectral sequence, and to three different compositions of the atmospheric matter (ratio of number of hydrogen atoms to number of metallic atoms equals 13.7:1, 50:1, ∞:1, respectively). These values have been taken from Burkhardt's paper, so they do not in-

[11] A. Arnulf, D. Barbier, D. Chalonge, *et al.*, *Annales d'astrophysique*, **1**, 293 and 402, 1938.

[12] *Ap. J.*, **88**, 429, 1938. [13] *Zs. f. Ap.*, **13**, 56, 1936.

clude the opacity resulting from the negative ions of hydrogen. Under these circumstances the Balmer discontinuity increases steadily with falling temperature, in an atmosphere of vanishing content of metals; and only by adding a sufficient amount of metals can the theoretical curve be made to represent the observed relation between Balmer discontinuity and spectral type. From the theoretical curve fitting best the observational data then available, Unsöld deduced, with certain reservations, the most probable abundance ratio of hydrogen to metals to be about 50:1. In fact, this appears to be Unsöld's main argument against the abundance ratio $H:M = 1000:1$ found by Russell from his analysis of the solar atmosphere and also adopted by Pannekoek.

Furthermore, Figure 1 contains three broken curves corresponding to the absorption exerted by atoms and negative ions of hydrogen at electron pressures of 10, 100, and 1000 dynes/cm², respectively, all metallic absorption being excluded. All the three broken curves end on the heavy curve representing pure atomic hydrogen, as it should be, since the negative ions will finally be destroyed by raising the temperature. Now it becomes evident that the correction for the presence of H^- produces the same effect as the addition to the atomic hydrogen of a considerable amount of metals. Indeed, the broken curve marked $p_e = 100$ dynes/cm² runs so closely below Unsöld's curve 50:1 that it would need the addition of only an extremely small amount of metals to make the former coincide with the latter. Consequently, the existence of the negative ions of hydrogen in stellar atmospheres appears to refute Unsöld's contention that the atmospheric abundance of the metals must be as high as 1/50 of that of hydrogen. This view has always loomed, in the writer's mind, disturbingly contradictory to Russell's[14] conclusion from the great strength of the hydride spectra both in the sun and in the stars, that the atmospheric abundance ratio $H:M$ is of the order of 1000:1. With this ratio being upheld, as well representing the average stellar atmosphere, it is of interest to correct Pannekoek's table of the Rosseland mean as function of temperature and electron pressure, for the presence of negative ions of hydrogen in the Russell mixture

[14] *Ap. J.*, **79**, 317, 1934.

of elements. This has been done in Table 3 in a way that may suffice for purposes of illustration. Strictly, the monochromatic absorption

TABLE 3

OPACITY OF STELLAR ATMOSPHERES

$\log_{10} \bar{k}(H+M)$
$\log_{10} \bar{k}(H^-)$
$\log_{10} \bar{k}(H+H^-+M)$

$\log_{10} P_e$ Dynes/Cm²	5040/T and $T°$ K							
	0.5 10,080°	0.6 8400°	0.7 7200°	0.8 6300°	0.9 5600°	1.0 5040°	1.1 4852°	1.2 4200°
−3.0	.....	6.46	6.75	6.94	6.47	5.51	5.07	5.17
	.....	0.29	1.99	3.58	4.73	4.97	5.01	4.94
	.....	.....	.....	.....	.....	.....	5.34	5.34
−2.0	.....	7.46	7.73	7.59	6.62	5.98	6.00	6.14
	.....	2.29	3.98	5.39	5.89	5.98	6.01	5.94
	.....	.....	.....	.....	.....	6.28	6.31	6.33
−1.0	8.07	8.45	8.56	7.80	6.96	6.83	6.97	7.01
	2.43	4.29	5.91	6.74	6.91	6.98	7.01	6.94
	.....	.....	.....	.....	7.23	7.20	7.29	7.26
0.0	9.07	9.40	8.96	7.98	7.65	7.78	7.80	7.75
	4.43	6.26	7.50	7.79	7.91	7.98	8.01	7.94
	.....	.....	.....	8.17	8.06	8.17	8.19	8.14
+1.0	0.05	0.05	9.09	8.50	8.55	8.60	8.53	8.58
	6.42	8.08	8.65	8.80	8.91	8.98	9.01	8.94
	.....	.....	9.12	9.01	8.99	9.05	.....	9.02
+2.0	0.91	0.27	9.44	9.31	9.35	9.34	9.38	9.43
	8.36	9.44	9.67	9.80	9.91	9.98	0.01	9.94
	.....	.....	9.84	.....	.....	.....	.....	.....
+3.0	1.36	0.49	0.13	0.12	0.09	0.12	0.13	0.03
	9.99	0.49	0.67	0.80	0.91	0.98	1.01	0.94
	.....	0.79	.....	.....	.....	.....	.....	.....
+4.0	1.53	1.02	0.89	0.87	0.87	0.81	0.74	0.68
	1.17	1.50	1.67	1.80	1.91	1.98	2.01	1.94
	1.61	.....	.....	.....	.....	.....	.....	.....

coefficients, as given by Pannekoek and Massey, should be added, and then a graphical integration of their reciprocal values should be made, which would involve an enormous amount of labor. There-

fore, an approximate procedure suggested by Unsöld[15] was applied, which leads to the formula

$$\overline{(k_1 + k_2)} = \frac{4\bar{k}_1\bar{k}_2}{(\bar{k}_1 + \bar{k}_2)},$$

where $\bar{k}_1$ is the Rosseland mean for the Russell mixture of elements (Pannekoek, *op. cit.*, Addendum, Table 20*a*) and $\bar{k}_2$ is the Rosseland mean for the bound-free transitions of H^-. For the latter quantity there were substituted the values of $\bar{k}(H^-)$ given in Table 1, though these contain the free-free transitions of H^-, already included in Pannekoek's $\bar{k}_1$. The numerical difference is practically negligible, except, perhaps, at the lowest temperatures. In Table 3 the final values representative of each temperature and electron pressure have been italicized. They reveal a marked lifting of the photospheric level by taking into account the contribution of H^- to the general opacity. This is quite conspicuous at temperatures lower than about 7000° K (F stars); but at the highest electron pressures, of the order that may be realized in the atmospheres of white dwarfs, the same effect may even persist in the range of temperatures the A stars are credited with. Therefore, it is not improbable that the obliteration of the Balmer continuum in the white dwarfs, which now is regarded as a manifestation of the Stark effect, could partly be the result of the raising of the photospheric level by H^-.

To sum up, it is now to be regarded as fairly certain, on the basis of Massey's absorption coefficients, that the existence of negative ions of hydrogen constitutes a major factor ruling the structure of late-type stellar atmospheres. Hence, the question is in point whether the electron affinity of any other element might not cause a further important contribution to the atmospheric opacity. The abundant halogen atoms *F* and *Cl* have electron affinities of the order of 4 volts, and so have some astrophysically abundant diatomic molecules like *OH* and *CN*.[16] However, these atoms and radicals enter

[15] *Zs. f. Ap.*, **8**, 225, 1934.

[16] E. Lederle, *Zs. f. Phys. Chemie*, B, **17**, 351, 1932; J. Weiss, *Trans. Faraday Society*, **31**, 966, 1935.

numerous compounds with energies of dissociation of the same order of magnitude. For this reason it is safe to assume that their electron affinity plays a role only in that range of lower temperatures and higher pressures where the present theory of atomic and ionic opacity will fail in any case because of the overwhelming influence of the molecular constituents. A case of entirely different character is He, singly charged negative ions of which Hiby[10] claims to have observed in the mass spectrograph. If the stability of He^- could be established beyond doubt, both experimentally and theoretically, another amendment of the theory of atmospheric opacity may become necessary.

PRINCETON UNIVERSITY OBSERVATORY
June 1939

THE CYANOGEN DISCRIMINANT BETWEEN GIANT AND DWARF STARS

DORRIT HOFFLEIT

ABSTRACT

The cyanogen band, used by F. Becker as a criterion for discriminating between giant and dwarf stars, has been examined on Harvard small-dispersion (400 A per mm) spectra for 128 stars of spectral classes G and K. Comparisons of the *g* and *d* classifications thus obtained with those determined by Becker and with Mrs. Gaposchkin's classifications based on color excesses, indicate that the cyanogen criterion affords a safe discriminant between normal giant and dwarf stars but that it is subject to large uncertainties in supergiants.

The lines used at Harvard in the determination of absolute magnitudes from large-dispersion spectra (45 A/mm) are, in general, too weak to be employed as criteria on the small-dispersion (400 A/mm) spectra of faint stars. The intensities of the cyanogen bands at 416 μ and 389 μ have, however, been used successfully, notably by Lindblad and his associates,[1] in absolute-magnitude determinations from carefully standardized small-dispersion spectra.

For many problems in galactic structure it is not essential to know the actual absolute magnitudes of faint stars, whereas a discrimination between the giant and the dwarf stars is important. A distinction between these two types on the basis of the apparent intensity of the cyanogen bands was made both at Bergedorf and at Potsdam, from plates comparable with those used by Miss Cannon for the *Henry Draper Catalogue;* these investigations suggested that a similar separation might be effected rapidly from the unstandardized Harvard plates. The investigation is desirable because Becker's classifications of giants and dwarfs have never been independently checked at other observatories. His descriptions of the *g* and *d* classes are as follows: *d* = cyanogen definitely not present; *d:* = cyanogen suspected; *g:* = cyanogen certainly present; *g* = cyanogen strong. The band that Becker studied is at λλ 4144–4184 (the stronger band at λ 3888 is in a region of poor definition and cannot be used); the comparison region is at λλ 4227–4272.

[1] Cf. *Stockholm Obs. Ann.*, **11**, No. 12, 1934.

I have examined the spectra of one hundred and twenty-eight stars between magnitudes eight and ten in eleven southern Selected Areas, on plates taken with the 8-inch Bache telescope (dispersion of spectra, 400 A/mm). Table 1 gives a comparison between the present results and those obtained by Becker.[2] (His classifications were originally published in 1930, but in 1938 he reclassified the stars in the central 4 square degrees of the Selected Areas at $-60°$ and $-75°$. Wherever the old and the new classes disagreed, I have used

TABLE 1

COMPARISON OF CLASSIFICATIONS BASED ON CYANOGEN

HOFFLEIT	BECKER		
	g	*d*	Total
g	50	3	53
*m**	4	5	9
d	8	58	66
Total	62	66	128

* *m* = intermediate between *g* and *d*.

only the new; there are, however, too few stars in his new list for a significant comparison with it alone.) I attempted throughout to adhere strictly to Becker's descriptive definitions of the *g* and *d* classes and to disregard all other absolute-magnitude criteria. In a few instances, therefore, I recorded a star as a dwarf because no evidence of cyanogen could be detected, even when the appearance of the lines or the exceptional redness of the continuous spectrum indicated supergiant characteristics.

The very satisfactory agreement between my results and Becker's would seem to indicate that Becker's *g* and *d* designations are a reliable measure of one characteristic of the spectra, namely, conspicuousness of cyanogen. Whether or not that characteristic represents absolute luminosity remains to be determined.

Mrs. Gaposchkin[3] has determined color indices for many of Beck-

[2] *Potsdam Obs. Pub.*, **27**, 1930; **28**, No. 3, 1938.

[3] Cf. *Harvard Ann.*, **105**, 383, 1937; *Ap. J.* **90**, 321, 1939.

er's stars. On the basis of color excess she has classified the stars as *rg* (red giants), *g*, and *d*. A summary of a comparison between Becker's and Mrs. Gaposchkin's estimates for thirty-one stars in the four Selected Areas 194, 196, 197, and 199 is given in Table 2. As a result of this comparison we tentatively conclude that if Becker called a

TABLE 2

COMPARISON BETWEEN CYANOGEN AND COLOR DISCRIMINANTS

BECKER	C.H.P.G.		
	rg	*g*	*d*
g	1	8	0
d	6	7	9

TABLE 3

INTERCOMPARISON OF THREE CLASSIFICATIONS

NO. STARS	D.H.		
	g	*d*	*d??*
Becker:			
g	3	0	1
d	0	11	3
C.H.P.G.:			
rg	0	3	2
g	3	2	2
d	0	6	0

star a giant it apparently is a giant; but if he called it a dwarf, its character is as yet undetermined.

Of these thirty-one stars, I have been able to classify only eighteen; the others were too faint on the Harvard spectrum plates. Table 3 gives a comparison between the present results and the results obtained by Becker and by Mrs. Gaposchkin. The double question marks indicate that, on the basis of characteristics other than the prominence of the cyanogen band, I am inclined to call the star

a giant rather than a dwarf. From the intercomparison it appears that my results agree satisfactorily with both Becker's and Mrs. Gaposchkin's when we disregard the stars she has classified as *rg* and the ones I have questioned; these stars are probably real supergiants.

Sixty of the stars reclassified by Becker in 1938 are designated as giants or dwarfs on both his lists.[2] Eleven of the sixty stars reclassified he has changed from dwarf to giant, none from giant to dwarf. I had classified but three of the eleven; one I had called *g;* for another, classified as *m*, the spectrum was of poor quality; the third I had classified as *d??*, indicating a probable supergiant. Thus, Becker's new estimates appear to confirm the view that the conspicuous presence of cyanogen definitely indicates giant characteristics, whereas its apparent absence is alone not a safe criterion for absolute luminosity.

The reason why a rigid adherence to Becker's descriptive definitions gives erroneous results for red giant stars is probably to be found in the steep density gradient of the continuous spectrum of a supergiant star in the cyanogen region. A tremendous amount of cyanogen would have to be present to cause a perceptible depression in an already steep gradient. The cyanogen discriminant combined with color criteria should result in a satisfactory separation of giant from dwarf spectra on small-dispersion plates.

HARVARD COLLEGE OBSERVATORY
May 1939

NOTES

INTERSTELLAR CALCIUM AND COLOR EXCESS

It is known that the intensities of the interstellar calcium lines do not exhibit a very direct dependence on the amount of interstellar reddening. Sanford[1] has shown that considerable scatter exists in their correlation with distance as well as with color excess. A striking example of the absence of a direct dependence of the strength of the interstellar K line on either color excess or total absorption is available in the case of CD $-24^{\circ}12684$, HD 147889. The star is situated in very dense dark nebulosity south of ρ Ophiuchi; like that star, it is the illuminating source for a reflection nebula. Henyey[2] has shown that the star is inside the dark nebula and is at about the same distance from the sun as ρ Ophiuchi.

HD 147889 is 2.8 mag. fainter, visually, than ρ Ophiuchi, while its spectral type, B3, suggests that it is intrinsically brighter. There are no signs of exceptional luminosity for either star. We know that the two stars are at roughly the same distance by their ability to produce bright nebulosity. From the steep intensity gradient in the bright nebula surrounding HD 147889, Henyey has shown that the star is imbedded a short distance in the dark material. The difference in brightness, 2.8 mag., is therefore a minimum estimate of the visual absorption of HD 147889.This high absorption is confirmed by the color excess of +1.8 mag. found by Seares and Hubble.[3] The photoelectric measures by Stebbins and Whitford, kindly communicated by the authors in advance of publication, yield a color excess of +0.50 mag. on the photoelectric scale. On the basis of the usual relation between total absorption and color excess, we may assume that the star has suffered an absorption of about 4 mag. in the dark nebula. Its distance, after correction for absorption, is approximate-

[1] *Ap. J.*, **86**, 136, 1937.

[2] *Ap. J.*, **85**, 107, 1937.

[3] *Ap. J.*, **52**, 14, 1920.

ly 100 parsecs, so that we may neglect normal interstellar absorption, or interstellar gases.

If the density of the interstellar calcium varies in proportion to that of the dark material, then the spectrum of HD 147889 should exhibit very strong K-line absorption. An extrapolation of Sanford's linear relation between K-line intensity and photoelectric color excess predicts an intensity of the order of one equivalent angstrom. Three spectra have been obtained with the 500-mm camera of the Cassegrain spectrograph of the McDonald Observatory (dispersion 45 A/mm) on Agfa Super-Pan Press and Super Plenachrome Press films. They show only a trace of the K line. The spectra have been compared with those of stars for which equivalent widths of the interstellar K line are known:[4] ν Scorpii (B3n, $EW = 0.06$ A), χ Ophiuchi (B3e, $EW = 0.06$ A), and HD 162978 (Bo, $EW = 0.15$ A). The K line in HD 147889 is weaker than in any of these other stars and is certainly much weaker than the lines λ 3927 and λ 4121 of *He* I, which have equivalent widths of the order of 0.2 A in HD 147889.

Such a low intensity for the interstellar K line is of the order of that found in stars of negligible reddening, at distances of 100 to 200 parsecs. It should be remembered that a total absorption of 4 mag., found in this case, corresponds to a distance of the order of at least 2000 parsecs in normal regions of the Milky Way. The tremendous increase in space density of the absorbing and reddening material in the dark nebula is not accompanied by a corresponding increase in the number of ionized calcium atoms. To a certain extent the present case is proof of the independence of interstellar gas and dust.

Two spectrograms were obtained on Eastman Process film with small dispersion. The interstellar band at λ 4430 is almost certainly stronger than in a normal star whose distance is 100 parsecs. It is therefore possible that this band does show a direct correlation with the amount of reddening material.

JESSE L. GREENSTEIN[5]
OTTO STRUVE

McDONALD OBSERVATORY
July 1939

[4] Merrill, Sanford, Wilson, and Burwell, *Ap. J.*, **86**, 274, 1937.

[5] National Research Fellow.

NOTE ON THE ATMOSPHERIC OXIDES OF NITROGEN

The observational results embodied in Figure 1 appear to support the suggestion[1] that the recently discovered atmospheric band[2] which is lodged in the long wave-length wall of the great water band is produced by joint absorption by nitrous oxide (N_2O) and nitrogen pentoxide (N_2O_5).

The curve marked *AIR* was made with a relatively dry atmosphere, the sun serving as source and the atmosphere as absorbing medium. The curve marked *LAB* was produced by radiation from a Nernst glower, passing through 1 cm of nitrous oxide at atmospheric pressure, in combination with the short air path in the spectrometer. It should be noted that a change of scale occurs in the laboratory curve at a point just beyond the center of the water band.

Attention is directed to the nitrous oxide band at 7.77 μ, which appears to match the atmospheric band in question. Moreover, the shallow nitrous oxide band at 8.57 μ appears to be matched by a weak atmospheric band overlain on its long-wave-length side by additional absorption. Finally, the short-wave-length trough of the atmospheric 7.77 μ band is somewhat displaced and broadened as compared with the corresponding nitrous oxide absorption, a possible consequence of absorption by nitrogen pentoxide at 7.6 μ.

If the agreement between the atmospheric and laboratory 7.77 μ and 8.57 μ bands is not fortuitous, there would seem to be an N_2O "layer" comparable with the ozone "layer," namely, the equivalent of several millimeters at atmospheric pressure in extent.

ARTHUR ADEL

LOWELL OBSERVATORY

ON THE CONTINUOUS SPECTRUM OF STARS WITH EXTENDED ATMOSPHERES

For some time, considerable attention has been drawn toward the behavior of stars with extended atmospheres, especially in connection with their line spectra.[1] This note is intended to show that an

[1] Arthur Adel, *Ap. J.*, **88**, 186, 1938.

[2] A. Adel and C. O. Lampland, *Ap. J.*, **87**, 198, 1938.

[1] See, e.g., O. Struve and K. Wurm, *Ap. J.*, **88**, 84, 1938.

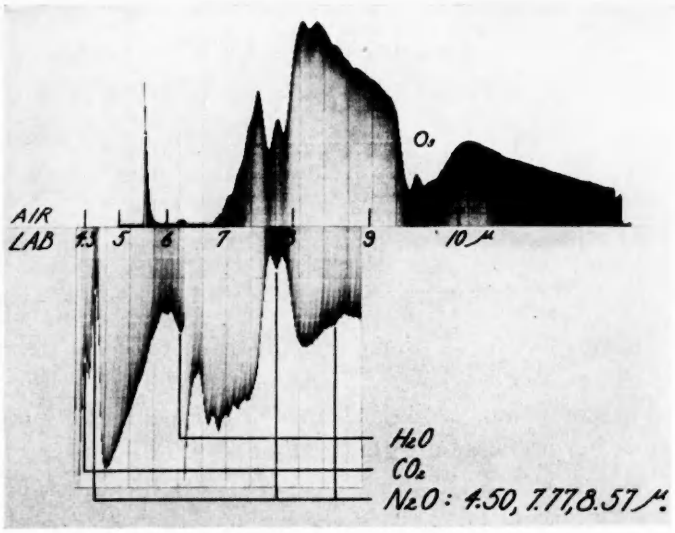

FIG. 1.—(Adel)

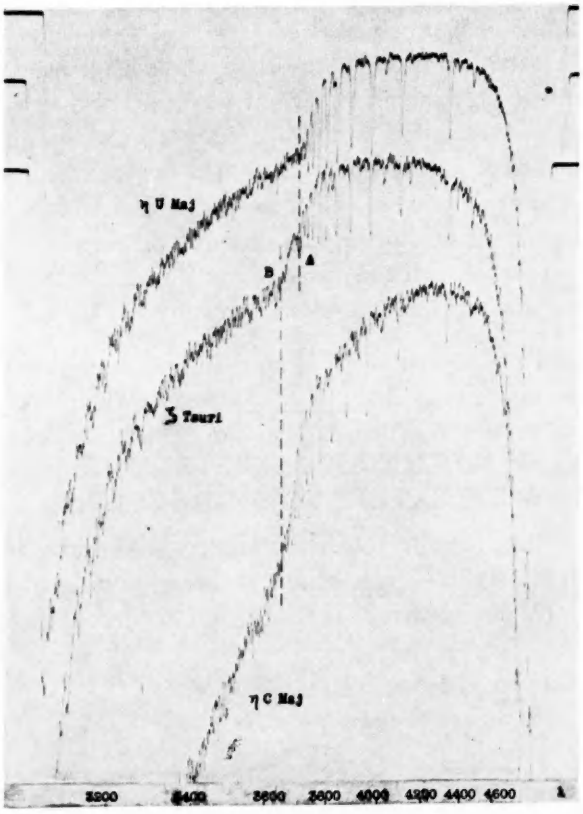

FIG. 1.—(Barbier and Chalonge)

extended envelope can also be detected in the continuous spectrum in the neighborhood of the Balmer limit.

Figure 1 reproduces a microphotometric tracing of the B3e star ζ Tauri, which is known to have an extended atmosphere, and, for sake of comparison, the tracings corresponding to a normal B3 star, η Ursae Majoris, and to a cB5 star, η Canis Majoris,[2] (with our spectrograph no cB3 star can be observed). It can easily be seen that there is, first, a step in the place marked *A* in the spectrum of ζ Tauri which is approximately at the limit of the Balmer series in η Ursae Majoris, and, second, a step at *B*, which corresponds to the limit in the c star. This shows very conspicuously the presence of hydrogen both in the photosphere and in an envelope at a very low pressure.

D. BARBIER
D. CHALONGE

INSTITUT D'ASTROPHYSIQUE
PARIS

THE COMING ECLIPSE OF ζ AURIGAE

Guthnick and his collaborators[1] give August 23.20 Greenwich Mean Time, or JD 2427672.70, as the time of the beginning of the 1934 eclipse of ζ Aurigae. They have found that the 1937 eclipse began at JD 2428644.60, and consequently there was an intervening period of 971.90 days. According to these figures, the next eclipse should begin on JD 2429616.50, or at 0^h G.C.T., December 19, 1939. Miss Swope[2] has found a period of 972.15 days from a discussion of Harvard plates extending from 1892 to 1934. Using the 1934 eclipse as a basis, this period implies that the 1939 eclipse will occur half a day later than the date predicted above. Christie and O. C. Wilson[3] have found that the duration of eclipse is 40.0 days and that of the partial phase is 1.7 days.

It may be possible to detect by photometric methods a much longer partial phase as the light from the relatively small B star passes

[2] Because of its low altitude, the last star appears much redder than the first two.

[1] *A.N.*, **262**, 430, 1937.

[2] *Harvard Circ.*, No. 399, 1935.

[3] *Ap. J.*, **81**, 438, 1935.

through the very extensive outer atmosphere of the K companion. It is therefore important to begin observations long before first contact and to continue them after fourth contact. Both C. M. Huffer[4] and K. Walter[5] have found evidence that the near-by star η Aurigae is slightly variable in brightness.

Christie has informed me by letter that he will again[6] be glad to receive any observations of ζ Aurigae. The co-operation of observers in this matter should greatly facilitate the discussion of all data.

JOHN S. HALL

AMHERST COLLEGE OBSERVATORY
August 19, 1939

NOTE ON THE INTERSTELLAR BAND AT λ 4430

1. It is sometimes true that broad, ill-defined spectral features are more easily visible on spectrograms of low dispersion than on those of higher. In particular, when high-contrast emulsions of the Process type are used and the spectra are greatly widened, some features show clearly to the eye which are visible only with difficulty on spectrograms of higher dispersion. This is the case for the interstellar band at λ 4430; on plates having a dispersion of about 225 A/mm at $H\gamma$ and obtained on Process emulsion, it is a conspicuous feature in a number of the highly reddened B stars observed by Stebbins and Huffer.

2. A list of stars having various degrees of reddening was selected from the catalogue of Stebbins and Huffer. These stars were observed for the purpose of investigating qualitatively the dependence of the intensity of the band on the amount of interstellar reddening. The band intensities were estimated on an arbitrary scale; the scale was adjusted so that intensity 1 corresponds to the weakest band that can be seen with fair certainty; bands having intensities of 3 and 4 are conspicuous to the eye. The range in intensity observed for λ 4430 is illustrated in Plate VII. The position of the band is marked by a small wedge; the highly reddened star is below, while the upper star is approximately of normal color. Stars of luminosities as

[4] *Ap. J.*, **81**, 292, 1935. [5] *Zs. f. Ap.*, **14**, 62, 1937.

[6] *Pop. Astr.*, **45**, 154, 1937; *Obs.*, **60**, 78, 1937; *J. R.A.S., Can.* **31**, 141, 1937.

PLATE VII

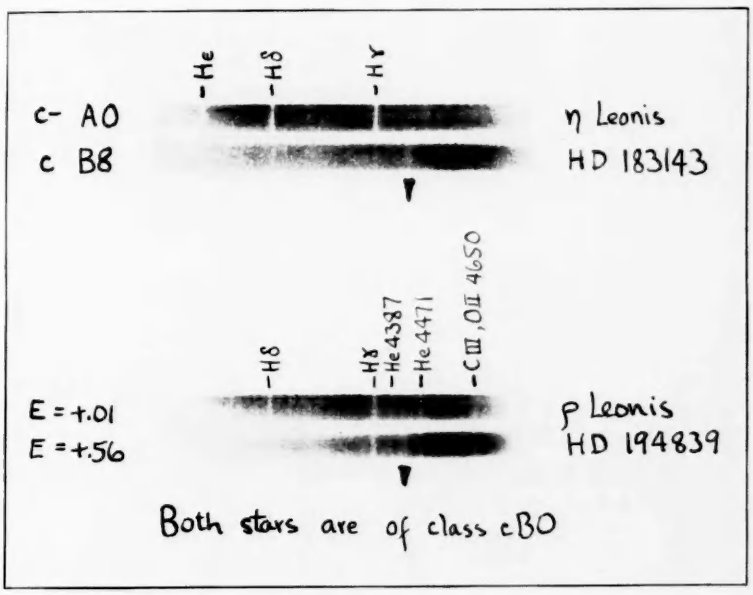

REDDENED AND UNREDDENED SUPERGIANTS SHOWING DIFFERENCES IN INTENSITY OF INTERSTELLAR BAND NEAR λ 4430

The stars η Leonis and ρ Leonis are approximately of normal color; the other two stars are greatly reddened.

UNIV. OF MICH.

similar as possible were selected for the illustration. In the case of HD 183143, the interstellar band is the most conspicuous feature in the spectrum.

3. The twenty-two stars observed are listed in Table 1. The spectral types and color excesses were taken from Stebbins' and Huffer's catalogue, with the exception of HD 194279 and HD 194839, for which types determined at the Yerkes Observatory are given. The stars are listed in order of increasing color excess.

TABLE 1

Star	Spectrum	Color Excess	Int. λ 4430
22 Cygni	B3	−0.04	0
β Cephei	B1	− .04	0
23 Cygni	B5	− .01	0
2 Cygni	B5	.00	0
ρ Leonis	Bosk	+ .01	0
HD 187879	B2k	+ .06	0
HD 188209	O8sk	+ .06	0
HD 190918	O9k+Ow5	+ .25	2
55 Cygni	B2sk	+ .25	1
HD 193183	B2sk	+ .28	2
HD 190919	B1sk	+ .29	1
HD 218342	B2	+ .30	1
HD 199216	B1sk	+ .32	0
HD 224055	B8s	+ .33	2
HD 190603	Bossk	+ .35	2
HD 200857	B2k	+ .36	1
13 Cephei	B8s	+ .39	1
HD 223960	Bo	+ .43	2
HD 183143	B8s	+ .51	4
HD 195592	Bosk	+ .52	3
HD 194279	cB2	+ .53	3
HD 194839	cBo	+0.56	3

When the errors of estimation are taken into account, the increase in intensity of λ 4430 with increasing reddening seems to be quite smooth, and the two quantities appear to be closely correlated.

4. In the early-type B stars several stellar lines are blended with the band. In the determination of its width and profile there is some advantage in using stars of types near Ao where there are no serious blends. A microphotometer tracing of a plate of the red B9 supergiant HD 193426, which had been obtained with the 82-inch telescope of the McDonald Observatory by Dr. Morgan, was measured for the wave length of the center of the band and for its width.

The original plate has a dispersion of 60 A/mm at $H\gamma$, and the interstellar band shows strongly on the tracing. The wave length obtained for the center is 4428.6 A, with an estimated uncertainty of an angstrom or two. The width was found to be about 66 A. The values found for these quantities by Beals and Blanchet are 4430.6 and 40 A, respectively. As their measures of the center depend on a number of plates, they should be given higher weight than the present determination; in the case of the width of the band, however, it is felt that the value in the present paper cannot be very far from the truth. The shape of the band in the spectrum of HD 193426 appears to be quite symmetrical.

FRANCES SHERMAN

YERKES OBSERVATORY
August 21, 1939

NOTE ON INTERSTELLAR REDDENING IN THE REGION OF γ CYGNI

1. In the course of an investigation of spectroscopic absolute magnitudes and selective absorption of stars in the region of γ Cygni,

TABLE 1

HD	m (vis)	Sp. (Yerkes)	M (Yerkes)
192422	7.10	cB1	−5.5
192660	7.72	cBo	6.0
193182	6.56	cAo	5.0
193426	8.0	cB9	5.0
194279	7.05	cB2	6.0
194839	7.45	cBo	−6.0

several early-type supergiants were found which appear not to have been known previously. The six brightest are listed in Table 1; they are all located within about $2\frac{1}{2}°$ of γ Cygni. Details of the spectra and of the determination of the luminosities will be given later; the values of the absolute magnitudes are preliminary, but it is unlikely that they are in error by more than a magnitude and a half.

2. An examination of the color excesses of the six stars as deter-

mined by a modification of the Tikhov method reveals what appears to be a marked spottedness in the absorbing material, which is roughly similar to the dark clouds observed on direct photographs. The last three stars in the table, which are all greatly reddened, are located in regions which show marked absorption on direct photographs. The first three, which are considerably bluer, are situated in the relatively transparent part of the Milky Way west of the densest obscuration. The last two stars are among the reddest B stars observed by Stebbins and Huffer. HD 193182 is probably not reddened more than one- or two-tenths of a magnitude, while HD 193426, which is less than a degree away, has the color of a giant K star.

TABLE 2

HD	m	Sp.	M	E	4430	Ca^+	Mod_1	Mod_2
194279	7.1	cB2	−6.0	+0.55	3	4.5	13.1	9.2
194839	7.5	cBo	6.0	.54	3	3.7	13.5	9.7
192422	7.1	cB1	5.5	.27	o	5.3	12.6	10.7
193322	5.8	O9	−4.5	+0.13	o	9.1	10.3	9.4

3. A region such as this is well suited to investigations of effects of distance as compared to effects of reddening. Photoelectric color indices and estimated intensities of the interstellar K line are available for three of the stars; to them has been added the near-by O9 star HD 193322, which has a very strong K line according to Plaskett and Pearce. Miss Frances Sherman has obtained spectrograms similar to those described in the preceding note for the estimation of the intensity of λ 4430. The data on the reddening, distance, and interstellar line intensities are given in Table 2. The color excesses are those of Stebbins and Huffer, and the Ca^+ intensities are by Plaskett and Pearce. The apparent distance moduli (Mod_1) have been corrected to true moduli (Mod_2) by multiplying the selective absorptions by a factor of 7.

The band at λ 4430 is exceedingly strong in the two reddest stars; it could not be seen in the spectra of the other two, and the correlation with degree of reddening seems definite. On the other

hand, there seems to be no such correlation in the case of Ca^+; it is actually weaker in the two reddest stars. We may therefore conclude that, in this particular region at least, the two features behave markedly differently; the material which absorbs λ 4430 is more directly connected with that which causes reddening than are the atoms of interstellar calcium.

W. W. MORGAN

YERKES OBSERVATORY
September 29, 1939

POSSIBLE APPLICATIONS OF SUPERNOVAE TO THE STUDY OF THE NEBULAR RED SHIFTS

Among the striking facts concerning supernovae brought to light by recent research are the following: (1) Absolute magnitudes of supernovae at maximum are very similar to the average absolute magnitude of extragalactic nebulae, namely, about -14.[1] (2) The light-curves of three supernovae have now been well determined and show a remarkable agreement in shape.[2] (3) The spectra of all supernovae thus far obtained point to the conclusion that, at similar phases, they are identical except for quite minor differences.[3] (4) The spectra of supernovae seem to terminate rather abruptly in the vicinity of λ 3900, and essentially nothing has been observed in the violet, even below λ 3300.[3] On the assumption that future observations will not seriously modify these statements, it appears that supernovae may be useful in advancing knowledge of the nebular red shift in the following ways.

a) *The nature of the red shift.*—At the present time it is not possible to decide observationally whether the red shift is a true Doppler effect, representing relative motion, or whether it is a hitherto unrecognized phenomenon of a different kind, such as, for instance, the

[1] W. Baade, *Mt. W. Contr.*, No. 600; *Ap. J.*, **88**, 285, 1938.

[2] Light-curves of the supernovae in IC 4182 and NGC 1003 have been published by Baade and Zwicky, *Mt. W. Contr.*, No. 601; *Ap. J.*, **88**, 411, 1938. The third curve referred to is for the supernova in NGC 4636, and I am indebted to Dr. Baade for information concerning it. According to Baade, none of the individual curves deviates from the mean curve by amounts in excess of 0.2 mag. for the first 150 days after maximum.

[3] R. Minkowski, *Mt. W. Contr.*, No. 602; *Ap. J.*, **89**, 156, 1939.

gradual dissipation of photonic energy. The answer to this question is, of course, important in cosmological theory. If, now, the red shift is a Doppler effect, then two events separated by a time interval Δt_0 for an observer in a nebula whose velocity of recession is V will appear to a terrestrial observer to be separated in time by an interval $\Delta t = \Delta t_0 (1 + V/c)$. Hence, the light-curve of a supernova occurring in such a nebula should appear to be expanded along the time axis in the ratio $(1 + V/c):1$ with respect to the "standard" light-curve given by relatively near-by objects.

The possibility of making observations on sufficiently distant objects to carry out this test must be considered. For the sake of argument let us take $V = 10^5$ km/sec. This velocity would slow down the apparent rate of development of a supernova to three-fourths of its normal rate and might be considered as a fairly gross effect. The velocity-magnitude relationship for clusters of nebulae has been given by Hubble,[4] and from it we deduce that a typical nebula whose $V = 10^5$ km/sec would be of about the twenty-first photographic magnitude. The average supernova in these distant systems would not, however, be even approximately as bright photographically as the nebulae themselves because the red shift would move the great gap in the violet into the ordinary photographic region. Hence, unless the supernova spectrum contains extremely strong radiations in the λλ 2300–2900 region, it is probable that supernovae could not even be detected in twenty-first magnitude nebulae on blue-sensitive emulsions. The work would therefore have to be carried on in the red, but with modern photographic material this fact should offer no serious difficulty. The number of faint nebulae available for observation is enormous; and since exceptional supernovae, such as the one in IC 4182, are known to be at least two magnitudes brighter at maximum than the average nebula, one may tentatively conclude that the foregoing test, while undoubtedly difficult, is within the bounds of possibility.

b) *Extension of the velocity-distance relation beyond the range spectroscopically observable.*—The peculiar character of the supernova spectrum suggests that the relative brightnesses of these objects in

[4] *Mt. W. Contr.*, No. 549; *Ap. J.*, **84**, 270, 1936.

properly selected regions in the red and in the blue should be a rather sensitive measure of the red shift to which the spectrum is subjected. Thus, color determinations of supernovae at known phases might be used to extend the distance-velocity relation, at least approximately, to distances so great that direct spectrographic determinations are impossible.

O. C. WILSON

CARNEGIE INSTITUTION OF WASHINGTON
MOUNT WILSON OBSERVATORY
August 31, 1939

REVIEWS

Transactions of the International Astronomical Union, Vol. VI: *Sixth General Assembly Held at Stockholm, August 3 to August 10, 1938.* Edited by J. H. OORT, General Secretary. Cambridge University Press, 1939. Pp. viii+518. $7.00

The International Astronomical Union, together with several other unions, was founded by the International Research Council at the Constitutive Assembly held at Brussels in July, 1919—less than one year after the end of the first world war. During the twenty years which have elapsed between 1919 and the recent outbreak of hostilities in Europe the I.A.U. has held six meetings: at Rome in 1922; at Cambridge, England, in 1925; at Leiden, Holland, in 1928; at Cambridge, Massachusetts, in 1932; at Paris in 1935; and at Stockholm in 1938. The proceedings of these meetings have been published in six important volumes edited by the general secretaries of the Union: Volumes I and II by Professor A. Fowler; Volumes III, IV, and V by Professor F. J. M. Stratton; and Volume VI by Dr. J. H. Oort.

The latest volume consists of six parts. Part I contains the reports of the executive committee and of thirty-one standing commissions of the I.A.U. These reports are intended to describe the progress in various branches of astronomy during the three-year period since the Paris meeting, and they furnish a valuable summary of the present activities of astronomers in many countries. From the beginning of the Union's activities these reports have included valuable tables of international importance, such as the "Table of Standard Wave-Lengths in the Infrared Solar Spectrum (7569–9899 A)" on pages 90–99 of the present volume. Special attention should be called to the list of notations recommended by Commission No. 3 under the chairmanship of Professor E. Strömgren. This list was prepared after careful discussions with many astronomers and should, whenever possible, be adopted by the authors of astronomical articles and books.

The progress reports are interspersed by numerous quotations from statements received by the chairmen from members of the various commissions. For example, Commission No. 23 (Carte du ciel) circulated a questionnaire covering the future of this co-operative undertaking. The answers of a number of leading astronomers are printed in the report.

Astronomers will welcome the list of "One Hundred Important Variable Stars" by Leon Campbell, the report on the classification of Wolf-Rayet stars by Beals, and the list of spectroscopic binaries now under observation at various observatories by Moore, Joy, and Harper. Subscribers to the astronomical telegrams from the Harvard Bureau or from the International Bureau at Copenhagen will find on pages 483–488 a description of the cipher code used for announcements of discoveries, observations, ephemerides, orbits, etc.

Part II is a report of the inaugural ceremony and of the general sessions of the Union. Part III contains the resolutions adopted by the commissions. Part IV gives the proceedings of the meetings of separate commissions. The commission on spectrophotometry (No. 36) arranged two lectures: one by A. Unsöld, on "Die Energieverteilung in den kontinuierlichen Sternspektren"; and the other by R. O. Redman, on "Sources of Error in the Measurement of Line Profiles."

A joint meeting was held by several commissions as a colloquium on "Emission Lines." The following papers, read at this meeting, are printed in the *Transactions:* H. N. Russell, "Emission Lines in Astronomical Spectra"; H. Zanstra, "Emission Lines in Nebulae and Novae"; D. H. Menzel, "Chromosphere and Corona"; P. W. Merrill, "Emission Lines in Stellar Spectra"; B. Loyt, "La Couronne et les protubérances en dehors des éclipses." The Union also held another colloquium on "Galactic Structure," which contained the following papers: B. J. Bok, "Star Counts"; H. Shapley, "Absorption Phenomena as Inferred from the Distribution of Extragalactic Nebulae"; B. Lindblad, "Spectral Types and Distribution of Special Objects." In the discussion following the presentation of these papers J. H. Oort spoke on the subject of spiral-like structure in our own galaxy; F. Becker spoke on the *Potsdam Spektral-Durchmusterung*, and K. G. Malmquist spoke on the spectrophotometry of stars in high galactic latitudes.

The I.A.U. was organized at a time when post-war emotions were strongly aroused, and it did not in the beginning have a truly international character. With the passing of hatreds engendered by the war, the Union made numerous efforts to attract the participation of all nations. But these efforts were never fully successful. Astronomers from Germany attended the Stockholm meeting and actively participated, as co-opted members of various commissions, in the work of the Union. Unfortunately, Germany, as well as several lesser countries, has never officially adhered to the Union.

A great deal may be said in criticism of the semipolitical setup of the

Union. Personal adherence of leading astronomers might have been more logical, but this would have reduced the income of the organization. On the other hand, by extending membership through co-optation to astronomers of countries not officially connected with the Union, an attempt has been made to correct the situation. Nevertheless, it is difficult to avoid the feeling that membership in the Union is more accidental than it should be. There are some striking omissions among the members of the various commissions. Most of them are probably accounted for by the fact that the persons involved are citizens of countries which do not belong to the Union, but it is doubtless harmful to the I.A.U. that it should fail to recognize such persons, especially when their entire scientific work has been carried out in countries which have always adhered to the organization. Astonishing also is the inclusion, in the commissions, of several Russian astronomers who, at the time of the Stockholm meeting, were already known to have been "purged" as being what their government describes as "enemies of the people." The U.S.S.R. officially adhered to the Union in 1935, through the medium of its Academy of Sciences, and several distinguished Russian astronomers were listed as members of various committees. In the new membership list Noumerov—believed to be dead—has been omitted from Commission 20 (Positions et mouvements des petites planètes, des comètes, et des satellites) of which he was the vice-president in 1935–38. But Gerasimovič, whose fate is unknown and whose name is pointedly omitted from the pages of all recent Russian astronomical publications, is still a member of Commissions 29 (Spectres stellaires), 27 (Etoiles variables), and 13 (Eclipses du soleil). There are other similar cases. The inconsistency between the recognition accorded the "purged" astronomers by the I.A.U. and the "silent treatment" verging upon an attempt to disregard or minimize their past work, which is accorded them in Russia is rather confusing.

These inconsistencies, which could easily have been amplified, strongly suggest that international scientific co-operation was already in 1938 no longer merely threatened but was actually brought to a standstill by the unpredictable and unreasonable actions of powerful anti-intellectual forces. The I.A.U. has made a valiant effort to maintain a spirit of international solidarity among astronomers the world over. It has probably been of particular benefit to astronomers of small countries or of countries in which there are few active astronomers. The war in Europe threatens to eradicate science in large parts of the world. The I.A.U. must carry on and save astronomy from destruction. In the light of political events

since the Stockholm meeting, particular significance attaches to the words of the newly elected president of the Union, Sir Arthur Eddington:

We cannot foresee what may happen before we meet again in Zürich. On the astronomical side we can make some guess. The 200-inch reflector will be completed or approaching completion. The marvelous advance in the photography of the corona and prominences, which has been so memorable a feature of this meeting, will bear fruit in advancing knowledge. And our numerous commissions will patiently extend their researches. But on the international side no one dares prophesy. But if in international politics the sky seems heavy with clouds, such a meeting as this at Stockholm is as when the sun comes forth from behind the clouds. Here we have formed and renewed bands of friendship which will resist the forces of disruption.

O. STRUVE

McDonald Observatory
September 28, 1939

ERRATUM

Page 319, Volume **90,** eighth line from the bottom, *instead of* more than *read* completed.